The effect of $Mo(CO)_6$ as a cocatalyst in the carbonylation of methanol to methyl formate catalyzed by potassium methoxide under CO, syngas and H_2 atmospheres

By

Samuel Jali

Submitted in the fulfilment of the academic

Requirements for the degree of Doctor of

Philosophy in the School of Chemistry,

University of KwaZulu-Natal, Durban

January 2010

As the candidate's supervisor, I have approved this thesis for submission

*Signed*_____ *Date*_____

Prof. Holger B. Friedrich (Supervisor)

Abstract

In patents describing the low temperature production of methanol from syngas catalysed by the $Ni(CO)_4/KOCH_3$ system, $Mo(CO)_6$ was claimed to enhance the catalytic activity of the system. However, there has been no clarity on the effect of $Mo(CO)_6$ and $KOCH_3$ in the activation of the catalyst. Work reported in this thesis showed that most of the methyl formate is produced *via* a normal $KOCH_3$ catalyzed process under a CO atm. When the $KOCH_3$ system is compared with the $Mo(CO)_6/KOCH_3$ catalyzed system, it is noted that the amount of methyl formate increases very slightly due to the addition of molybdenum hexacarbonyl. The experiments were also performed under H_2 and synags (1:1) atm in different solvents. In all cases dimethyl ether was produced with methyl formate. Preliminary carbonylation studies performed at a syngas ratio of 1:2 showed an increase in the amount of methanol produced. Increasing the amount of $Mo(CO)_6$ in the $Mo(CO)_6/KOCH_3$ reaction under syngas (1:1) increases the production of methyl formate.

High Pressure infrared (HPIR) studies for $Mo(CO)_6/KOCH_3$ were carried out under H_2, CO, syngas (1:1) and N_2 atmospheres. The alkoxycarbonyl complex ($Mo(CO)_5(COOCH_3)^-$) was observed as an intermediate in all reactions involving $Mo(CO)_6$ and $KOCH_3$. Under a hydrogen atmosphere, the metalloester ($Mo(CO)_5(COOCH_3)^-$) intermediate diminished to form a bridged molybdenum hydride (μ-$HMo_2(CO)_{10}^-$) species as a stable intermediate. In contrast, under syngas atmosphere, the metallloester diminished in concentration to form the bridged hydride (μ-$HMo_2(CO)_{10}^-$), which also disappeared to form the molybdenum alkoxide complex ($Mo(CO)_5OCH_3^-$). The role of methanol in the formation of methyl formate is also discussed.

Based on the HPIR studies, different types of metalloesters (alkoxycarbonyl complexes) were synthesized by nucleophilic reactions of alkoxides with $Mo(CO)_6$. Reactions of potassium alkoxides (KOR, R = $-CH_3$, $-C(CH_3)_3$, $-C(CH_3)_2CH_2CH_3$) with $Mo(CO)_6$ in THF produced water soluble alkoxycarbonyl complexes ($K[Mo(CO)_5(COOR)]$). The reaction of $KOCPh_3$ with $Mo(CO)_6$ yielded what is believed to be the metalloester as an insoluble compound. Attempts to improve the solubility of the formed alkoxycarbonyl complexes, $K[Mo(CO)_5(COOR)]$, by metathesis with bulkier counter ions (PPNCl, Et_4NCl and *n*-Bu_4NI) was not successful. The reaction of $K[Mo(CO)_5(COOCH_3)]$ with 18-crown-6 ether produced $[K(18\text{-crown-6})][Mo(CO)_5(COOCH_3)]$ which was more soluble in organic solvents. The reactions of $[PPN][OCH_3]$ and [*n*-Bu_4N][OCH_3] with $Mo(CO)_6$ produced $[PPN][Mo(CO)_5(COOCH_3)]$ and [*n*-Bu_4N][$Mo(CO)_5(COOCH_3)$], respectively.

The reactions of [K(18-crown-6)][OCH_3] and [K(15-crown-$5)_2$][OCH_3] with $Mo(CO)_6$ under reflux gave the [K(18-crown-6)][$Mo(CO)_5(COOCH_3)$] and [K(15-crown-$5)_2$][$Mo(CO)_5(COOCH_3)$] complexes. Reactions of $Ph_3PMo(CO)_5$ with $KOCH_3$ and [PPN][OCH_3] yielded K[$Ph_3PMo(CO)_4(COOCH_3)$] and [PPN][$Ph_3PMo(CO)_4(COOCH_3)$].

Other alkoxycarbonyl complexes were synthesized by an alternative approach using alcohols as solvent. For example, [PPN][$Mo(CO)_5(COOCH_2CH_3)$] was synthesized by refluxing [PPN][OEt] with $Mo(CO)_6$ in ethanol. The isopropyl derivative [PPN][$Mo(CO)_5(COOCH(CH_3)_2)$] was synthesized by refluxing [PPN][$OCH(CH_3)_2$] with $Mo(CO)_6$ in isopropanol. Two methyl derivatives were also synthesized in methanol as Et_4N and PPN derivatives. A crystal structure of the $[PPN]_2[Mo_6O_{19}]$ oxo cluster, obtained from the decomposition of [PPN][$Mo(CO)_5(COOCH(CH_3)_2)$] in acetonitrile was solved. The crystal crystallized in the monoclinic form with a space group of P-1. Another oxo cluster, $[Et_4N]_2[Mo_4O_{13}]$, formed from the decomposition of the [Et_4N][$Mo(CO)_5(COOCH_3)$] derivative. The structure was solved in the monoclinic form with a space group of P 2_1/n.

The alkoxycarbonyl complex, [PPN][$Mo(CO)_5(COOCH_3)$], was tested for catalytic behaviour under hydrogen and syngas to determine its role in the production of methyl formate. No methyl formate was produced under hydrogen, but methyl formate was produced under syngas (1:1). HPIR studies of [PPN][$Mo(CO)_5(COOCH_3)$] under syngas (1:1) showed that methyl formate is formed *via* the decomposition of [PPN][$Mo(CO)_5(COOCH_3)$] to $Mo(CO)_6$.

Interesting results for the reaction of $Mo(CO)_6$ with $KOCH_3$ under syngas (1:1) were obtained in triglyme. Here longer carbon chain alcohols were produced and identified by GC and GC-MS. These alcohols include ethanol, 2-propanol, 2-butanol, 3-methyl-2-butanol, 3-pentanol, 2-methyl-3-pentanol and 2,4-dimethyl-3-pentanol.

Preface

The experimental work described in this thesis was carried out in the School of Chemistry, University of KwaZulu-Natal, Durban, from July 2006 to December 2009, under the supervision of Prof. Holger Bernhard Friedrich.

These studies represent the original work by the author and have not been otherwise submitted in any form for any degree or diploma to any tertiary institution. Where use has been made of the work of others it is duly acknowledged in the text.

*Signed*_____ *Date*_____

Samuel Jali

Declaration 1-plagiarism

I, ……., declare that

1. The research reported in this thesis, except where otherwise indicated, is my original research.

2. This thesis has not been submitted for any degree or examination at any other university.

3. This thesis does not contain other person's data, pictures, graphs or other information, unless specifically acknowledged as being sourced from other persons.

4. This thesis does not contain other person's writing, unless specifically acknowledged as being sourced from other researchers. Where other written sources have been quoted, then:
   a. Their words have been re-written but the general information attributed to them has been referenced
   b. Where their exact words have been used, then their writing has been placed in italics and inside quotation marks, and referenced.

5. This thesis does not contain text, graphics or tables copied and pasted from the Internet, unless specifically acknowledged, and the source being detailed in the thesis and in the References sections.

*Signed*_____ *Date*_____

Declaration Plagiarism 22/05/08 FHDR Approved

Declaration 2 – publications and conference contributions

DETAILS OF CONTRIBUTION TO PUBLICATIONS that form part and/or include research presented in this thesis (include publications in preparation, submitted, *in press* and published and give details of the contributions of each author to the experimental work and writing of each publication)

Publication 1

S. Jali, H. B. Friedrich, M. D. Bala, *Dicarbonyl (η^5-cyclopentadienyl) bis(trimethylphosphine) molybdenum(II)trifluoromethanesulfonate*. **Acta Crystallographica Section E (2008), E64, m1401**

Publication 2

S. Jali, H. B. Friedrich, M. D. Bala , *Synthesis, characterization and reactions of some short chain alkoxycarbonyl molybdenum anions $[Mo(CO)_5(COOR)]^-$ (R = Me, Et, ^{i}Pr) and $[Mo(CO)_4(COOCH(CH_3)_2)_2]^{2-}$*, **to be submitted.**

Publication 3

S. Jali, H. B. Friedrich, G. R. Julius, *The effect of $Mo(CO)_6$ as a cocatalyst in the carbonylation of methanol to methyl formate catalyzed by potassium methoxide under CO, syngas and H_2 atmospheres. HPIR observation of the methoxycarbonyl intermediate,* **to be submitted.**

Conference contributions

1. Oral presentation titled "$Mo(CO)_6$ assisted carbonylation of methanol to methyl formate *via* Mo alkoxycarbonyl complex" Samuel Jali and Holger B. Friedrich, presented at the CATSA meeting, Rawsonville, 2009.

2. Oral presentation titled "Towards the mechanistic understanding of CO hydrogenation to alcohols" Samuel Jali and Holger B. Friedrich, presented at the SACI for young scientist meeting, Durban, 2008.

3. Poster titled "Towards the mechanistic understanding of CO hydrogenation to alcohols" Samuel Jali and Holger B. Friedrich, presented at the International Symposium on Homogeneous Catalysis XVI meeting, Florence, Italy, 2008.

4. Poster titled "Towards the mechanistic understanding of CO hydrogenation to alcohols" Samuel Jali and Holger B. Friedrich, presented at the CATSA meeting, Richards bay, 2007.

5. Poster titled "Towards the mechanistic understanding of CO hydrogenation to alcohols" Samuel Jali and Holger B. Friedrich, presented at the SACI meeting, Durban, 2007.

6. Poster titled "A new approach to the homogeneous hydrogenation of carbon monoxide to alcohols" presented at the CATSA meeting, Mossel Bay, 2006.

*Signed*_____

Table of contents

Acknowledgements

I would like to extend my honest acknowledgement to Prof. Holger B. Friedrich for his kind guidance, motivation and giving me a freedom to explore throughout this study. I also wish to appreciatively thank Prof. Michael Green and Dr. Fanie Otto from Sasol Technology for their mentorship, valuable discussions and giving me a chance to use their *in situ* IR during my visit at Sasol while carrying out this work. I thank Dr. Llewellyn Damoense and Dr. Gerrit R. Julius for their kind assistance on using the high pressure infrared spectrometer and their fruitful discussions during the experiments.

I thank Dr. Manuel Fernandez from the University of Witwatersrand for collecting and solving some of the X-ray crystallographic data shown in this thesis. Dr. Kirsten Stewart from the University of KwaZulu-Natal Pietermaritzburg campus is also acknowledged for collecting some of the X-ray crystallography data. I thank Dr. Muhammad D. Bala for solving some X-ray crystallographic data shown in this thesis.

I also wish to thank the following technical staff members for teaching me to operate some of the instruments they were in charge of: Mrs Anitta Naidoo (GC-MS, LECO elementary analyzer and IR spectroscopy), Mr. Dilip Jagjivan (NMR spectroscopy). I further thank the friendliness and technical assistance of the following people: Mr. Harvey Sishi, Mr. Alton Blose, Miss Bafikile Gumede, Mr. Gregory Moodley, Mr. Thabiso Hadebe and Mr. Richard Mtolo.

I gratefully acknowledge financial support from Sasol Technology and the University of KwaZulu-Natal.

I thank my family for allowing me to further my studies although there were some challenges along the way; I thank you a lot for the support and motivation; this work is dedicated to you all.

*And to **Shembe** in which all the wisdom and blessings were accredited*

"The fruits of goodness, those who have them from you, Father, They have been given by you, oh Lord, May they also be given to me" Bongani Mthethwa

Abbreviations

Acac	=	Acetylacetanato
ATR	=	Attenuated total reflectance
BNL	=	Brookhaven National Laboratory
n-Bu_4NI	=	Tetrabutylammonium iodide
Cp	=	Cyclopentadienyl ring
CRA	=	Complex reducing agent
Et_4NCl	=	Tetraethylammonium chloride
Et	=	Ethyl group
EXAFS	=	Extended X-ray absorption fine structure
Eqn.	=	Equation
FTIR	=	Fourier Transform Infrared
GC	=	Gas Chromatography
GC-MS	=	Gas Chromatography with Mass Spectroscopy
GHSV	=	Gas Hour Space Velocity
HPIR	=	High Pressure Infrared
IR	=	Infrared
Me	=	Methyl group
MeOH	=	Methanol
MF	=	Methyl formate

NMR	=	Nuclear Magnetic Resonance
Nu	=	Nucleophile
OAc	=	Acetate
OTf	=	Trifluoromethanesulfonate (Triflate)
Ph_4AsCl	=	Tetraphenylarsonium chloride
PPNCl	=	*Bis*(triphenylphosphine)iminium chloride
^{i}Pr	=	Isopropyl group
R	=	Alkyl or Aryl group
Syngas	=	Synthesis gas
TBAB	=	Tetrabutylammonium bromide
THF	=	Tetrahydrofuran
TG	=	Triglyme
Uv/Vis	=	Ultraviolet-visible
WGSR	=	Water gas shift reaction
XAFS	=	X-ray absorption fine structure
XANES	=	X-ray absorption near edge structure
15C5	=	15-crown-5
18C6	=	18-crown-6

1. CHAPTER 1

Literature review of homogeneous catalytic activation of carbon monoxide to alcohols and formates

1.1 Introduction

The worldwide existence of extensive coal reserves has generated interest in the conversion of coal to liquid (CTL) products. Furthermore, as the price of petroleum continues to rise and its continued availability remains uncertain, the use of synthesis gas (H_2/CO) as an abundant feedstock is increasingly becoming a more viable alternative for the chemical industries.[1,2] These future predictions arise from an estimation by Schulz[2] for the world usage of coal and mineral oil, that by the 23rd century, world coal reserves will be low, while there would be no more mineral oil reserves before the year 2100 (**Figure 1.1**).

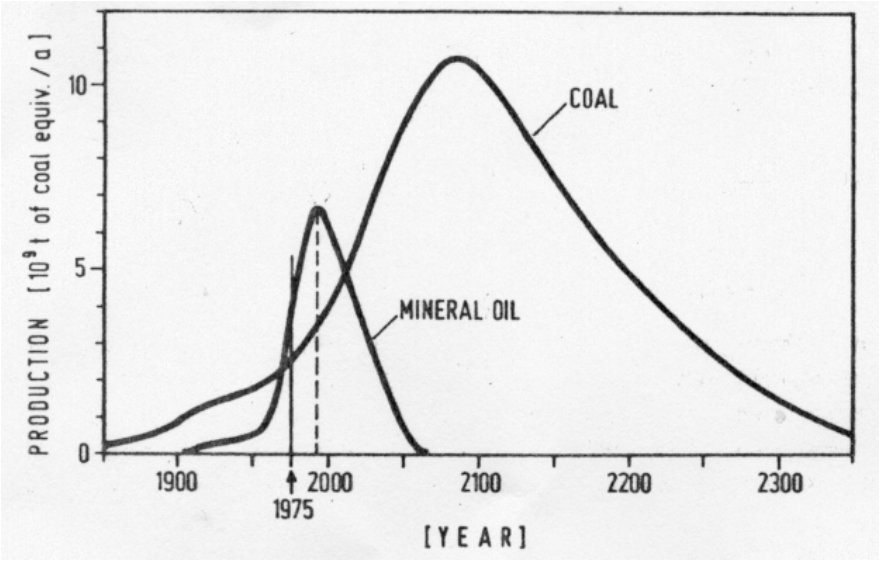

Figure 1.1: Prediction of coal usage during the 23rd century.[2]

The advantage of using synthesis gas as a feed is that it can be derived from any carbon source, e.g. coal, methane, biomass, household garbage, manure, urban and agricultural wastes.[3] Therefore, a chemical industry based on synthesis gas would be ultimately independent of the carbon source, since there are a large variety of carbon sources that can be utilised.

Syngas* plays a crucial role in chemical industries as a source of pure hydrogen and carbon monoxide. Hydrogen is utilized in large quantities in the Haber-Bosch process, in which it is reacted with atmospheric nitrogen to produce ammonia. It is also used, for example, in the production of methanol to give other important products (eqn. 1):

$$\underset{n=1}{nCO + 2nH_2} \xrightarrow{cat^*} C_nH_{2n+2}O + (n-1)\,H_2O \qquad (1)$$

Methanol, in particular, is attractive as an additive in conventional fuels, and as a versatile building block in the synthesis of organic chemicals.[4] It is also widely used as a solvent. It is commercially manufactured directly from synthesis gas using a supported Cu-ZnO heterogeneous catalyst at temperatures of 250-300 °C and pressures ranging from 5-10 MPa. However, this method shows poor thermodynamic control, which results in a gas conversion of less than 20% per pass during the reaction.[4,5] This low gas conversion is due to the exothermic nature of the reaction between carbon monoxide and hydrogen ($\Delta H_{298K} = -128.6$ kJ.mol^{-1}).

The example of the common industrial process for the conversion of syngas to hydrocarbons is the Fischer-Tropsch process,[6,7] which is mainly based on heterogeneous cobalt or iron catalysts under fairly severe conditions, *i.e*. temperatures ≥ 230 °C and pressures ≥ 400 atm. This process lacks selectivity and produces a plethora of compounds such as linear hydrocarbons which may need further conversion to obtain valuable products.

To improve the selectivity of this process to more desirable products, efforts should be directed to the development of the homogeneous catalysts, with their capability of high selectivity, reproducibility and controllability. The fact that homogeneous catalysts are easily studied and interpreted, allows for better fundamental understanding of the reaction chemistry.[8,9]

---

* *Syngas* is an abbreviation of synthesis gas, which is a trivial name for the mixture of hydrogen and carbon monoxide in different molar ratios.

1.2 Metal carbonyl clusters/monomers as homogeneous catalysts in the reduction of carbon monoxide

Previous studies on the homogeneous hydrogenation of CO required severe conditions (temperatures ≥ 230 °C and pressures ≥ 400 atm).[5] The most studied metal carbonyls for this reaction are those of cobalt[10], ruthenium[8] and rhodium[9,11,12] with different promoters, this is probably because these metals are well known in catalysis, e.g. the Fischer-Tropsh and hydroformylation processes. Cobalt catalysts (e.g. $Co(OAc)_2.4H_2O$) were found to produce methanol, polyhydric alcohols and their esters. Ruthenium complexes such as $Ru(acac)_3$ (P = 1300 atm, T = 268 °C) produced methanol and methyl formate. Addition of triphenylphosphine to the ruthenium catalyst resulted in a high selectivity to methanol over methyl formate. In contrast, an increase in CO pressures shifts the selectivity to methyl formate.[8] The dominant products for the rhodium catalyst were ethylene glycol and methanol. Formate esters of the products and other C2-C4 alcohols were also observed when a $Rh(CO)_2(acac)$ catalyst was used (P = 1973 atm, T = 230 °C).[9] Nakamura *et al*.[12] also reported that the addition of bulky trialkylphosphines such as P^iPr_3 to a Rh catalyst increased the activity of the catalyst by stabilizing the Rh mononuclear hydride carbonyl ($HRh(CO)_3P^iPr_3$). It was suggested that the formation of methanol and ethylene glycol is connected to a hydride migration to the CO; while the phosphine ligand improves the CO insertion ability to the hydroxymethyl species ($HOCH_2$-M) (**Scheme 1.1**).

Rathke and Feder[13] investigated a free radical mechanism for the cobalt-carbonyl catalysed hydrogenation of benzene in the presence of synthesis gas and serendipitously found the formation of methanol, methyl formate, ethanol, 1-propanol and ethyl formate in some of the organic products. To confirm that the methanol and methyl formate originated from the hydrogenation of CO, the experiments were repeated in heptane and *p*-dioxane at 180-200 °C respectively. The formation of C2-C3 alcohols was associated with the homologation of methanol.[14]

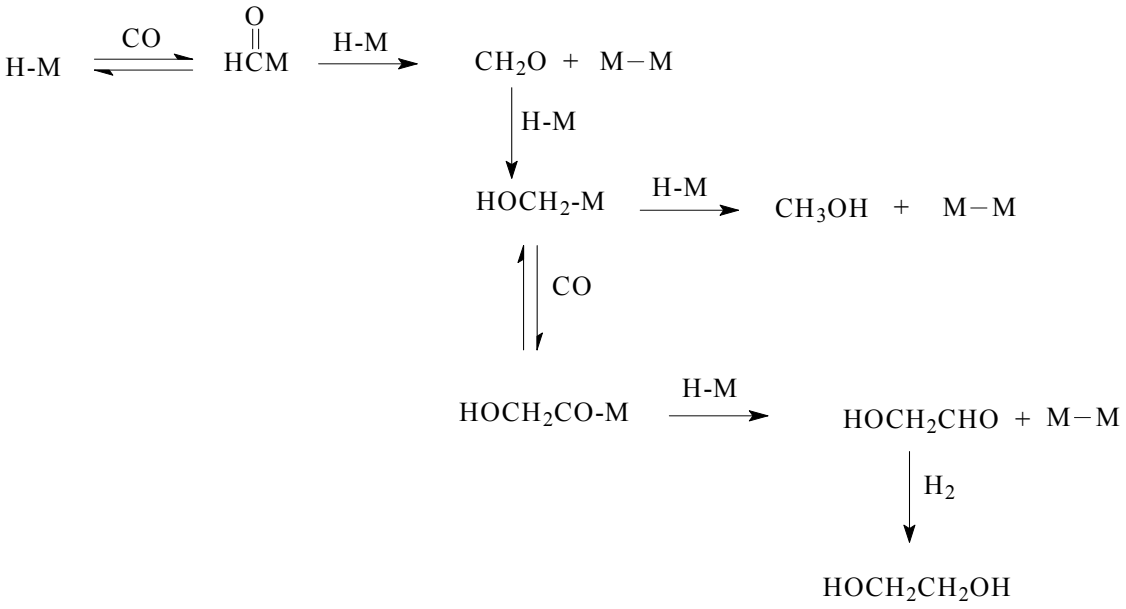

H-M =$HRh(CO)_3P^iPr_3$ or $HRh(CO)_4$

M-M= $Rh_2(CO)_6(P^iPr_3)_2$

Scheme 1.1: Mechanistic formation of formaldehyde, methanol, glycoaldehyde and ethylene glycol by the Rh catalyst ($HRh(CO)_3P^iPr_3$).[12]

Since the above three (Co, Ru and Rh) catalysts produced primarily the same products, it was presumed that a common mechanism operates. Mechanistic studies revealed that the formation of oxygenates is *via* a formaldehyde intermediate,[12,15,16] which is a thermodynamically unfavourable route, therefore requiring the use of high temperatures and pressures to shift the equilibrium to the right (eqn. 2).[3,9]

$$CO + H_2 \underset{}{\overset{K}{\rightleftharpoons}} HCHO \quad \Delta G_{(500K)} = +\ 51\ kJ/mol \qquad (2)$$

The equilibrium constant, K, for equation 2 is both temperature and pressure dependent. The use of a cobalt catalyst, at higher temperatures and pressures, increased the rate of the formation of formaldehyde, while the rhodium catalyzed reaction has been reported to be six fold faster than the cobalt catalyzed system under similar conditions.

Catalysis by metal carbonyl complexes of Mn, Fe, V, Cr, Mo, W, Re Ni, Pd, Ir, Os, and Pt has also been investigated. They showed lower activities than the Co, Ru and Rh compounds under similar conditions.[9,17,18]

In 1986 Mahajan *et al.*[19] reported a successful utilization of $Ni(CO)_4$ and its salts for the production of methanol and methyl formate from syngas under *mild conditions* (temperature 100-150 °C and pressure 6-10 atm). It is important to note that no formaldehyde was observed in the products. The utilized catalyst precusor was NaH--ROH--$Ni(OAc)_2$ (first discovered by Brunet *et al*. [20] and referred as Nic), where R= C1-C6 hydrocarbons. The authors reported a high gas conversion of 80%. However, changing the carbon chain length of R = *t*-amyl alcohol to methoxide increased the conversion to 99%.[21]

In literature, the Nic catalysts are known for their properties as complex reducing agents (CRA).[22] They are favourably compared with the best nickel hydrogenation catalysts for selective hydrogenations. They are described as heterogeneous hydrogenation catalysts at atmospheric pressure that are cheap, easily prepared, reproducible, not pyrophoric, and stable on long storage in solution. These catalysts have been used to hydrogenate alkynes to alkenes then to alkanes and exhibit good activity for carbonyl group hydrogenations at standard temperature and pressure (STP). These properties are in competition with known organic reducing agents such as $LiAlH_4$, $NaBH_4$ and Ni_2B (a black product formed from the reaction of $NaBH_4$ and $Ni(OAc)_2$).[23,24] Results from the hydrogenation studies with Nic had shown that the reactive component is a metal hydride (M-H), while an alkoxide part of Nic (*which results from the reaction of sodium hydride and an alcohol*)[25] acts as an activating agent of the catalyst.

Brunet *et al*.[20] investigated the effect of an activating agent (alkoxide) in the preparation and activity of Nic for the hydrogenation of phenylacetylene at STP. Results showed that activity increased with an increase in steric effect[26] (EtONa ≤ *i*-PrONa < *t*-BuONa > *t*-AmONa > neopentyl alkoxide) (**Table 1.1**).

Table 1.1: Influence of the nature of the activating agent on the activity of NaH-ROH-$Ni(OAc)_2$. Hydrogenation of phenylacetylene [20]

Activating agent	Preparation time (hours)	Initial rate (cm^3 of H_2/min) at STP
EtONa	24	13.3
i-PrONa	2-3	13.4
t-BuONa	2-3	19
t-AmONa	3-4	16.7
$(Me)_3CCH_2ONa$	5-6	16.7
2,5-dimethyl-2,5-hexanediol alkoxide	2-3	16.7
$Et(OCH_2CH_2)_2ONa$	2-3	20
C_6H_5ONa	8-9	6.7

Although the activity of Nic is known, its structure is still mysterious. Derivatives of Nic are prepared by the substitution of the metal salt and formulated as NaH-RONa-MX_n.[27] Those made from zinc salt are abbreviated as ZnCRA[28] and those made from cobalt acetate and ferric chloride are abbreviated as CoCRA and FeCRA respectively.[29,30] The nature of the metal also plays an important role on the reducing ability of the CRA.[27]

CoCRA catalysed the carbonylation of aryl halides to form esters; acids and benzene at atmospheric pressures (eqn. 3).[29]

$$\underset{X= Cl, Br, I}{C_6H_5X} \xrightarrow[THF,\ 63\ ^oC]{NaH\text{-}t\text{-}AmylONa\text{-}Co(OAc)_2,\ CO} \underset{R= t\text{-Amyl group}}{C_6H_5COOR} + C_6H_5COOH + C_6H_6 \qquad (3)$$

However, the nature of the active intermediate in the CoCRA catalyst is still unknown, but seems to involve cobalt carbonyl species and is abbreviated as CoCRACO. CoCRACO results from the preparation of NaH-*t*-AmylONa-$Co(OAc)_2$ in a slow stream of carbon monoxide. In addition, the

involvement of an amine (NaH-*t*-AmylONa-amine-$Co(OAc)_2$) in CoCRACO forms amides as part of the products. Important to note is that substitution of an alkoxide with an amine (NaH-amine-$Co(OAc)_2$) also forms amides as part of the product.[29] This suggests the importance of an activating agent in these catalysts.

Considering the preparation of the MCRA, NaH-RONa-MX_n, it could be reflected that reduction of metallic salts by NaH-RONa occurs, and that lower oxidation states of the metal species are present. This was confirmed by Brunet *et al.*[28] who established that the metal (Ni or Zn) in MCRA is in a zero-valent oxidation state. In addition, if MCRA is prepared in the presence of stabilizing ligands, e.g. phosphines, dienes and 2,2-bipyridine, the complex loses its reducing properties and behaves as a coupling agent.[27] If it is prepared in the presence of butadiene, oligomerisation occurs to form 1,5,9-cyclododecatriene (eqn. 4 and 5).

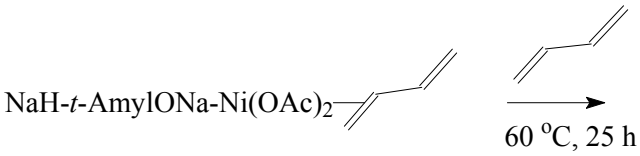

(4)

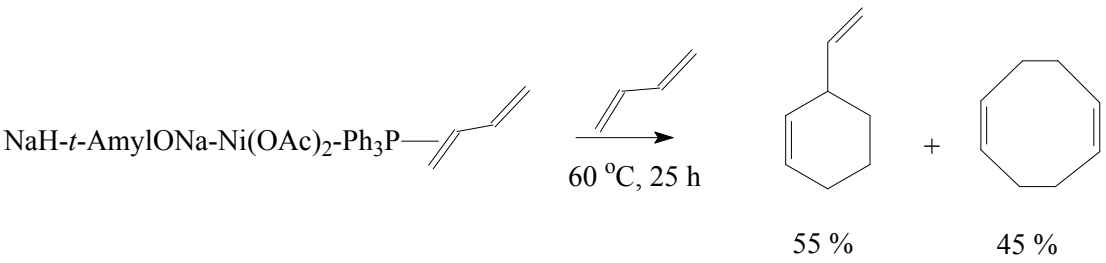

(5)

Brunet *et al.*[28] have also indicated that the active intermediates of NiCRA or ZnCRA consist of new species formed from Ni^0 (1 equiv), RONa (2 equiv), NaH (2 equiv) and sometimes with AcONa, in which all the reactants have lost their own characters. They proposed that the structure of NiCRA might involve some sandwich ionic layers which surround nickel atoms. The proposed structure is depicted in **Figure 1.2**.

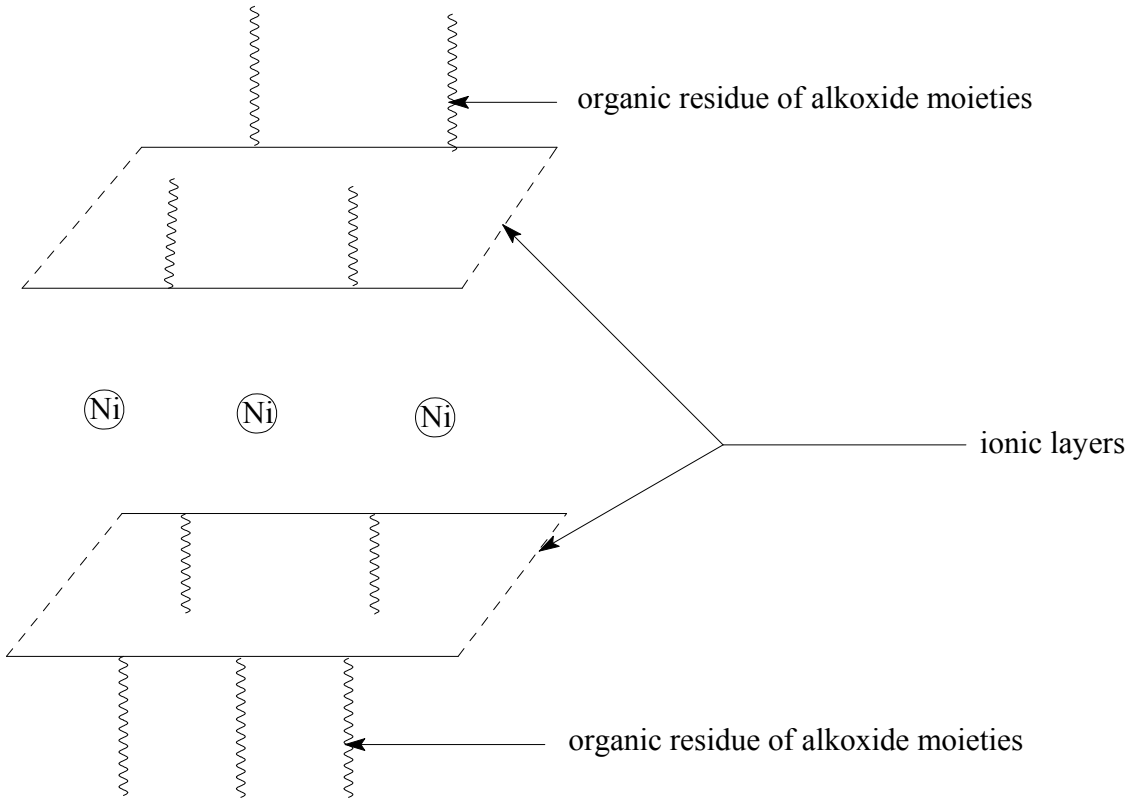

Figure 1.2: Propose structure of NiCRA.

Ohyama[25] has reproduced the work done by Mahajan *et al.*[19] and found that the catalyst (NaH-*t*-AmylOH-Ni$(OAc)_2$) forms a yellowish green slurry in solution; supporting the findings of Brunet *et al*.[20,22] in that the Nic is in a heterogeneous form. The catalyst was highly selective to form methanol from syngas as described in the above paragraph(s). The two-steps synthesis of methanol from CO and H_2 *via* methyl formate reported by Mahajan *et al*.[19] and Ohyama,[25] was first proposed by Christiansen in 1919 as a homogeneous–heterogenic system.[31] Two catalytic systems in the reaction are involved; the first step is the homogeneous carbonylation of methanol catalysed by sodium or potassium methoxide at moderate temperatures and pressures to form methyl formate (eqn. 6). The second catalytic step is conducted in the gase-phase over copper-based catalyst and involves the hydrogenolyis of methyl formate to methanol (eqn. 7).[32-34]

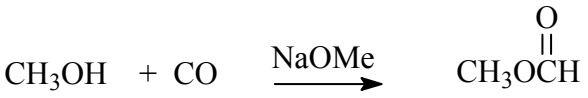

(6)

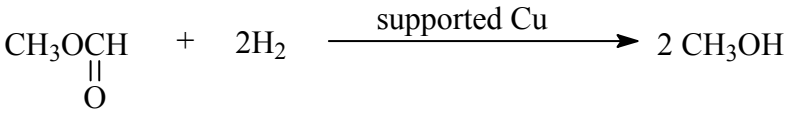

(7)

A more general synthesis of methanol from higher alcohols was reported by Christiansen[35] using the same route (eqn. 8 & 9).

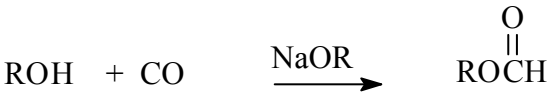

(8)

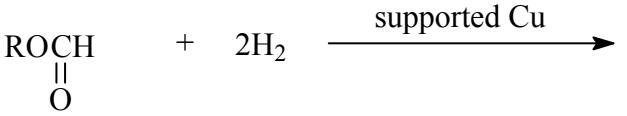

(9)

Tonner *et al.*[36] studied the base catalysed carbonylation of higher alcohols (C1-C4) to alkyl formates at 60 ^{o}C and pressures of 4000 kPa. The results showed that the rate of carbonylation increases with an increase in hydrogen substitution near the hydroxyl group, i.e. secondary and tertiary alcohols carbonylate fast as a result of an increase in substitution.

Different nickel salts ($NiCl_2$ and $NiSO_4$) were used by Ohyama *et al.*[25] to produce methanol and methyl formate; in agreement to Brunet *et al.,*[29] the results suggested that nickel salts might be converted to other forms of active species that function as the catalyst. Ohyama[37] also studied a similar reaction using XAFS (X-ray absorption fine structure), EXAFS (extended X-ray absorption fine structure) and XANES (X-ray absorption near edge structure) and found that the nickel salts are converted to nickel tetracarbonyl under syngas. $Ni(CO)_4$ therefore reacts with an alkoxide (*t*-Amyl alkoxide or methoxide) to generate an active species discussed below.

The addition of a group 6 metal carbonyls to the $Ni(CO)_4/KOCH_3$ catalyst have been reported to enhance the activity of the catalyst to yield methanol.[19] Separate studies[38] conducted with $Ni(CO)_4$, $Cr(CO)_6$, $Mo(CO)_6$ and $W(CO)_6$, to investigate their effects in the production of methanol (with and without an alkoxide) supported the conclusions of Keim *et al.*[17] and Fahey,[9] referred to above, that these metal carbonyls exhibit little activity without an alkoxide.

In the presence of an alkoxide base, all group 6 metal carbonyls produced methyl formate and dimethyl ether, while in contrast, $Ni(CO)_4$ produced methanol.[38]

In situ FTIR study revealed the formation of methyl formate when a $Ni(CO)_4/KOCH_3$ catalyst precursor was used.[39] Methyl formate may perhaps arise from the carbonylation of the initially formed methanol according to **Scheme 2**:[36,38]

$$CH_3OK \longrightarrow CH_3O^- + K^+$$

$$CH_3O^- + CO \longrightarrow CH_3OCO^-$$

$$CH_3OCO^- + CH_3OH \longrightarrow CH_3O^- + CH_3OCOH$$

Scheme 1.2: Catalytic behaviour of methoxide in the carbonylation of methanol.[36,38]

The above scheme suggests that methyl formate should dominate in every case where an alkoxide is used. However, in the presence of $Ni(CO)_4/KOCH_3$ catalyst precursor, the rate of methyl formate production decreases, while that of methanol increases with the concentration of the base (**Figure 1.3)**. This could be due to the hydrogenolysis of methyl formate to methanol by a nickel carbonyl species (eqn. 10) in addition to the simultaneous conversion of synthesis gas to methanol.[39,40]

$$HCOOCH_3 + 2H_2 \xrightarrow{[Ni]} 2\ CH_3OH \qquad (10)$$

The low temperature method for the production of methanol by the $Ni(CO)_4/KOCH_3$ catalyst[21] is reported to be superior to the conventional (alumina supported Cu-ZnO catalyst) methods, as it shows higher conversion of the feed gas and operates under *milder conditions.*

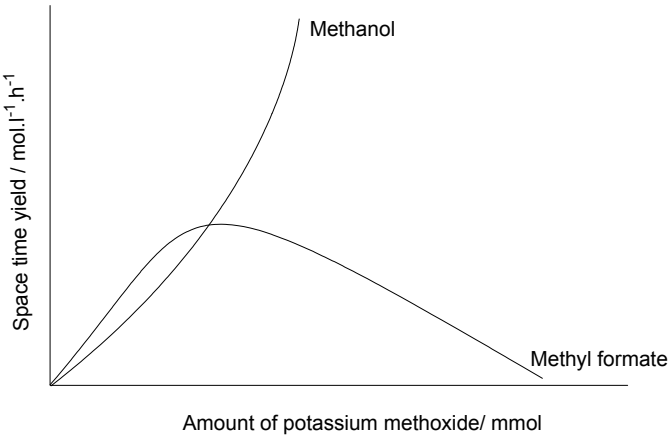

Figure 1.3: Effect of potassium methoxide and $Ni(CO)_4$ on the space time yields of methanol and methyl formate.

1.3 Nucleophlic activation of coordinated carbon monoxide

Nucleophilic attack usually occurs at the carbonyl carbon atom, which has a larger C-O bond force constant.[41] A high C-O bond force constant correlates with a more positive carbon atom, which becomes more susceptible to nucleophilic attack.[41,42] Lower values of the C-O bond force constant correlate with electrophilic addition to the oxygen atom. Many nucleophiles act as co-catalysts in reactions catalysed by metal carbonyls, including the reduction of CO, reductive carbonylation of nitroaromatics and low temperature synthesis of methanol from syngas catalysed by the $Ni(CO)_4/KOCH_3$ system. Alkoxides, amines and hydroxides are common nucleophiles which react with metal carbonyls to form alkoxycarbonyl (**1**), carbomyl (carboxamido, **2**) and/or hydroxycarbonyl (**3**) adduct anions, which are often labilised intermediate species (eqn. 11):[43-49]

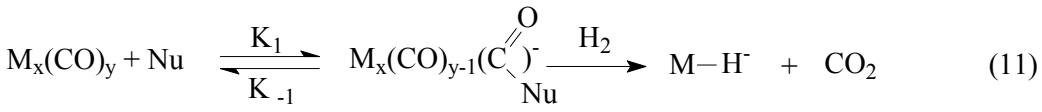

(11)

Nu = OH^-

M = Transition metals

R = Alkyl groups

adduct

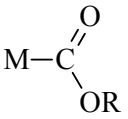

1

Alkoxycarbonyl

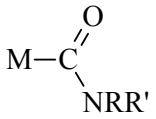

2

Carbomyl

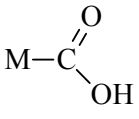

3

Hydroxycarbonyl

In the case where a nucleophile is a hydroxide anion, addition of excess hydroxide results in a subsequent decarboxylation of the hydroxycarbonyl adducts to form metal hydride ion(eqn.12).[50-52]

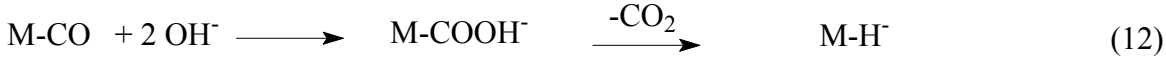

(12)

The reaction of dicobalt octacarbonyl ($Co_2(CO)_8$) with amines, hydroxides and alcohols results in the homomolecular disproportionation of the metal carbonyl. Subsequent addition of an acid produces metal hydrides (**Scheme 1.3**).[44,53] In 1972 Angelici [48] summarized these reactions as producing carboamido (carbomyl, **2**) compounds similar to the alkoxycarbonyl (**1**) or hydroxycarbonyl compounds (**3**).

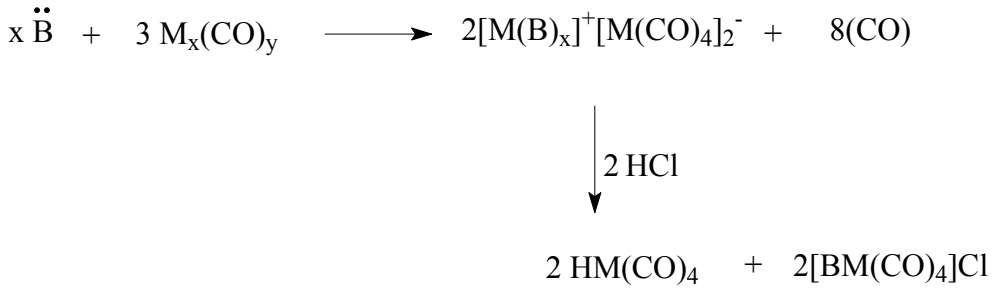

B = H_2NR, ROH, etc M= Co

Scheme 1.3: Reaction of metal carbonyls with nucleophiles.

1.4 Reaction of metal carbonyls with alkoxides, formation of alkoxycarbonyl complexes

Alkoxides react with the metal carbonyls in solution to form alkoxycarbonyl adduct (**1**) anions $M(CO)_{n-1}(CO_2R)^-$ (n = 4, M = Ni; n = 5, M = Fe, Ru, Os and n = 6, M= Cr, W and R= alkyl or aryl group).[43,47,54] In the case of $Ru_3(CO)_{12}$, addition of excess alkoxide base in aprotic solvent leads to the formation of 2:1 adducts (*i.e.* mono and *bis*(methoxycarbonyl) adducts) (eqn. 13).

$$M_x(CO)_y + 2\,OR^- \underset{K_{-1}}{\overset{K_1}{\rightleftharpoons}} \underset{\text{mono adduct}}{M_x(CO)_{y-1}(COOR)^-} + OR^- \longrightarrow \underset{\textit{bis}\text{(methoxycarbonyl) adduct}}{M_x(CO)_{y-2}(COOR)_2^{2-}} \qquad (13)$$

M = Ru
R = CH_3

There are, however, several routes for preparing alkoxycarbonyl complexes of transition metals in addition to the common nucleophilic attack of an alkoxide onto the metal coordinated carbon monoxide. These routes are reported for the group 10 (Ni, Pd and Pt) metals and include; (i) oxidative addition of haloformates (eqn. 14) to the metal complex and (ii) CO insertion into M-OR complex (eqn. 15).[48,55,56] The synthesis of alkoxycarbonyl complexes by the reaction of metal carbonyl compounds with alcohols is not common. However, some alkoxycarbonyl complexes have been synthesized by this route.[56,57] This route is only achievable when strongly activated cationic metal carbonyls are used since an alcohol is a weaker nucleophile than

its conjugate base.[49,58] The reaction also requires the presence of triethylamine as base and a CO atmosphere to shift the reaction toward the products.[59]

Some Ni and Pd alkoxycarbonyl complexes were synthesized by the oxidative addition of haloformates to the metal complexes in their zerovalent states in toluene or benzene, (eqn. 14).

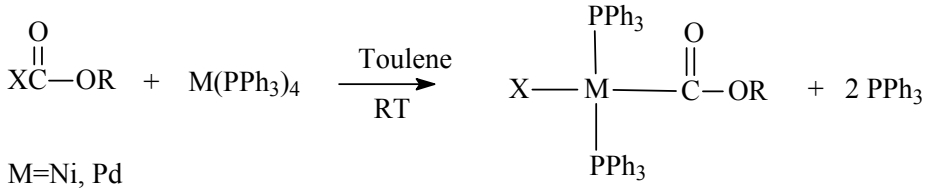

(14)

M=Ni, Pd
X= Cl, Br
R= CH_3, CH_2CH_3 and $CH_2C_6H_5$

The reaction firstly involves dissociation of PPh_3 from the $M(PPh_3)_4$ complex to give $M(PPh_3)_3$ which then eliminates a second PPh_3 and oxidatively adds the haloformate. The nickel alkoxycarbonyl complexes are reported to be very air sensitive and thermally unstable eliminating CO_2. In contrast, the syntheses of Pd alkoxycarbonyl complexes require higher temperatures compared to the nickel analogs.

The other route for the synthesis of group 10 (Ni, Pd, Pt) alkoxycarbonyl complexes involves a CO insertion into M-OR (eqn. 15) and was shown theoretically to be favourable over M-R (M= Ni, Pd, Pt) by modelling the insertion of CO into M-OR and M-R bonds.[60]

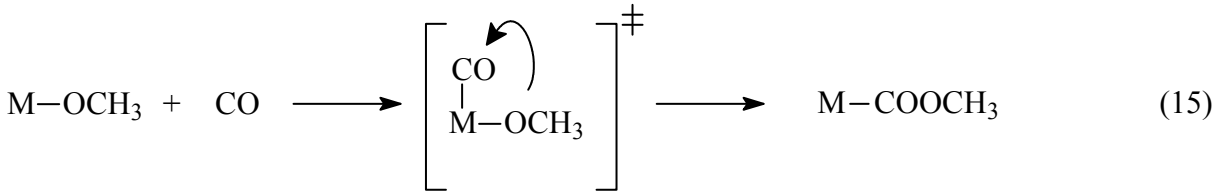

(15)

This has been demonstrated with (dppe)Pt(OCH_3)(CH_3) which reacts with CO at room temperature to give (dppe)Pt(CO_2CH_3)(CH_3). The *bis*(methoxy) platinum complex, (dppe)Pt(OCH_3)$_2$, reacts stepwise with CO to give the *bis*(methoxycarbonyl) complex, (dppe)Pt($COOCH_3$)$_2$ (eqn. 16), the same reaction is true with a palladium complex

(bipy)Pd$(OCH_3)_2$.[60] This route represents one of the basic steps in the oxidative carbonylation of methanol to form dimethyl carbonate and/or dimethyl oxalates.

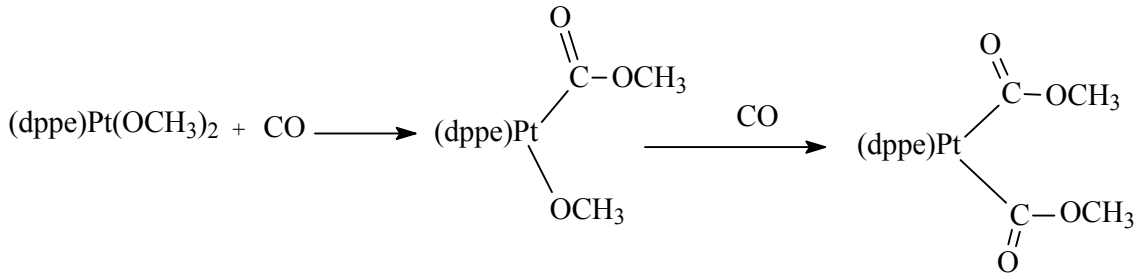

(16)

Elimination of oxalates is through a C-C coupling between two alkoxycarboxylato ligands,[61] while in the presence of an alcohol, carbonates can be generated through the nucleophilic attack of the generated alkoxide (RO^-) to the carbonyl moiety of the alkoxycarbonyl group. A similar case has been reported with palladium complexes.[61,62]

Trautman *et al*.[43] analysed the reaction of group 8 metal carbonyls with methoxide anion by IR and results indicated that it is the axial position of the trigonal bipyramidal structure (Fe, Ru and Os) which is activated by a nucleophile. This was presumed to be due to the larger C-O bond force constant of the axial CO group compared to the equatorial CO groups. This agrees with the observation by Darensbourg *et al*.[41] for the activation of group 8 metal carbonyls by nucleophiles. It also agrees with normal coordinate analyses of the IR spectra of $M(CO)_5$ (M=Fe, Ru), in which it was confirmed that the C-O bond force constant of the axial CO group is larger than that of the equatorial CO groups.[63]

IR analysis of group 8 methoxycarbonyl adducts revealed a difference in the ν_{CO} values of the terminal carbonyl bands for Na^+ and PPN^+ salts, with those of the Na^+ salts appearing at higher frequencies.[43] This is suspected to be due to the strong interaction of Na^+ with the structure B shown in **Scheme 1.4**, due to the decrease of the negative charge on the metal. The ν_{CO} bands of the group 8 methoxycarbonyl groups ($-COOCH_3$) appear at lower wavenumbers (~1600 cm^{-1}) which confirms the strong interaction of the Na^+ cation with structure B in **Scheme 1.4**.[64,65]

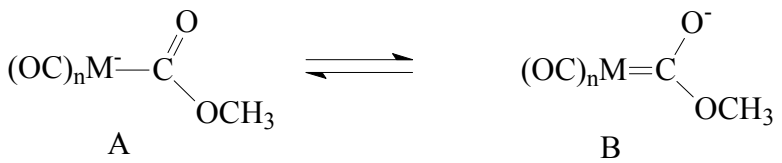

For n = 4, M = group 8 metal
n = 5, M = group 6 metal

Scheme 1.4: Resonance structures of the methoxycarbonyl adduct.

Kinetic studies of group 6 metal carbonyls with alkoxides were represented by the reaction of $W(CO)_6$ with methoxide anion in 90:10 (THF:CH_3OH) and CH_3CN solutions. The results showed a second order rate constant, which was reported to be 3 orders of magnitude lower than those, reported for group 8 methoxycarbonyl complexes under the same conditions.[66] The difference in the reactivity between the group 8 and the group 6 metal carbonyls arises from the positive charge on the carbonyls.[41] Group 8 metal carbonyls have larger C-O bond force constants than their group 6 analogues, which makes them to have a greater partial positive charge on the carbon atom of the axial CO and hence they are more reactive to nucleophiles.[41] For example, the force constant values reported for $Fe(CO)_5$ are 16.95 mdyn $Å^{-1}$ for axial C-O bond and 16.59 mdyn $Å^{-1}$ for the equitorial CO. All the CO groups of $W(CO)_6$ have the same C-O bond force constant of 16.41 mdyn $Å^{-1}$, which account for their low reactivity to nucleophiles (**Table 1.2**).[42,66] However, it has been reported that the difference in the reactivity of group 8 and 6 metal carbonyls with CH_3O^- is 2 orders of magnitude higher than expected from the difference of C-O bond force constants. There are thus other factors which also contribute to the kinetics of these reactions, e.g. solvation.

The reaction of $Fe(CO)_5$ with CH_3O^- to form the $Fe(CO)_4(COOCH_3)^-$ adduct is an example of the reactions of group 8 metal has been found to have a lower activation energy (by comparison of the results from the Erying plots) and presumed to be more solvated than the unstable $W(CO)_5(COOCH_3)^-$ adduct under similar conditions.

Table 1.2: Comparison of the rate constant per active carbonyl group with the force constant of the active carbonyl in electronically controlled reactions[42]

Compound	$F_{active\ CO}$ (mdyn/Å)	Rate of active CO x 10^{-3}
$Cr(CO)_6$	16.49	8.0
$Fe(CO)_{5\ axial}$	16.95	46
$Fe(CO)_{5\ equatorial}$	16.59	-
$W(CO)_6$	16.41	18
$(o\text{-}CH_3C_6H_4)_3PW(CO)_5$	15.45 (trans)	1.75
$(C_6H_5)_3PFe(CO)_4$	16.22 (trans)	1.84

The order of reactivity of group 8 metal carbonyl with methoxide follows the sequence, Os > Ru >Fe for the forward reaction (k_1) and the reverse reaction (k_{-1}) is of the order, Fe > Ru > Os. These observations have been rationalised in terms of lesser steric constraints, as well as higher CO force constants for the heavier metal centers.[42]

The rate of the formation of the methoxycarbonyl adduct depends on the solvent used, *i.e.* a rate study performed in 90:10 (THF: CH_3OH) showed an instant formation of an adduct when compared to a reaction performed in methanol where it took long to form. This slow rate in methanol was presumed to be due to its high polarity, because methanol tends to interact strongly with the methoxide by forming hydrogen bonds, thus reducing its reactivity.[43,67]

Group 6 and 8 alkoxycarbonyl adducts were found to be thermally stable but moisture sensitive and isolable as *bis*(triphenylphosphoranylidene)ammonium salts (PPNCl).[43,66] The reaction of $W(CO)_6$ with $NaOCH_3$ in 90:10 (THF:CH_3OH) solution was monitored by UV/Vis spectroscopy, which showed an absorbance for $[Na^+][W(CO)_5(COOCH_3)^-]$ at $\lambda = 416$ nm and by IR spectroscopy. Similar behaviour was observed for the reaction of $W(CO)_6$ with $[PPN][OCH_3]$ and the relevant IR data is shown in **Table 1.3**.

Table 1.3: Infrared spectral data for the terminal CO ligands of W complexes in 90:10 (THF: CH_3OH) solution[66]

Compound	νCO, cm^{-1}
$W(CO)_6$	1975 (s)
$[Na][W(CO)_5(COOCH_3)]$	2051(w), 1909 (s), 1876 (m)
$[PPN][W(CO)_5(COOCH_3)]$	2052 (w), 1907 (s), 1868 (m)
$[PPN][W(CO)_5OCH_3]$	2065(w), 1919(s), 1865 (m)
$[PPN][HW(CO)_5]$	2029(w), 1889(s), 1879(m)
$[PPN][\mu^2–H(W(CO)_5)_2]$	2041 (w), 1941(s), 1879 (m)

It can be noted from the above table, that the strongest ν_{CO} band (1909 cm^{-1}) for the $[Na][W(CO)_5(COOCH_3)]$ complex when the counter cation is Na^+ is shifted to 1907 cm^{-1} for PPN^+. This suggests a tighter ion pairing when the counter cation is Na^+ than PPN^+ (**Figure 1.4**).[43]

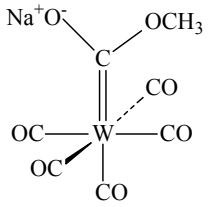

Figure 1.4: Proposed ion pairing intermediate for the addition of $NaOCH_3$ to $W(CO)_6$.

No ester ν_{CO} band was observed for the $–COOCH_3$ group in 90:10 (THF: CH_3OH) but in CH_3CN solution the ν_{CO} band for $–COOCH_3$ was observed at 1658 cm^{-1} for the Na^+ salt and 1668 cm^{-1} for the PPN^+ salt. The lower wavenumbers for an ester group observed in the Na^+ salt also indicates that a tighter ion pair is formed. However, crystallization of the $[PPN][W(CO)_5(COOCH_3)]$ compound was reported to be unsuccessful and the rapid addition of hexane gave a complex with ν_{CO} bands characteristic of the bridging hydride complex $[PPN][\mu\text{-}H(W(CO)_5)_2]$. On the other hand, slow crystallization in hexane gave $[PPN][W(CO)_5OCH_3]$ due to the loss of CO from the methoxycarbonyl adduct.[18,68]

Darensbourg *et al*.[69] have reported the synthesis of $M(CO)_5OR^-$ (M = Cr, Mo, W and R= Ph, *m*-$CH_3C_6H_4$) and found them to be unstable. The stability of these metal-alkoxide complexes followed the order W > Cr > Mo. These compounds decompose to form tetranuclear $[M_4(CO)_{12}(OR)_4]^{4-}$ species. The $Cr(CO)_5OR^-$ (R = Ph, *m*-$CH_3C_6H_4$) compounds are reported to be stable in solution for 30-45 min, if the temperature is maintained below 0 ºC, while those of Mo were not observed in solution due to their instability. Crystals of $W(CO)_5OR^-$ (R= Ph, *m*-$CH_3C_6H_4$) were grown by diffusion of hexane to THF solution at –10 ºC, as yellow-orange needles of $[Et_4N][W(CO)_5OR]$, under a CO atmosphere. The Cr and W compounds were found to be unreactive towards CO but with CO_2 they reacted to form metal coordinated carbonates. The chromium and tungsten compounds were tested for activity in the reaction with CO_2 and produced the metal pentacarbonyl phenyl carbonate. These reactions proceed readily under mild conditions (T = 0 °C, P = 1 atm). The reaction of the chromium complex with CO_2 occurred within the time of mixing, while those of tungsten took 30 min to go to completion.

The reaction of $Ni(CO)_4$ with $KOCH_3$ was studied by an *in situ* FTIR separately to elucidate the catalytic reaction for low-temperature methanol synthesis under syngas.[39] This reaction was conducted in a liquid medium at 313-333 K with an initial (CO/H_2) pressure of 3.0 MPa. Addition of $KOCH_3$ to $Ni(CO)_4$ in triglyme solution showed three bands at 1965 cm^{-1}, 1940 cm^{-1} and 1605 cm^{-1} which grew with time. The bands at 1940 cm^{-1} and 1605 cm^{-1} were assigned to the ν_{CO} bands of $[Ni(CO)_3(COOCH_3)]^-$ depicted in **Figure 1.5**.

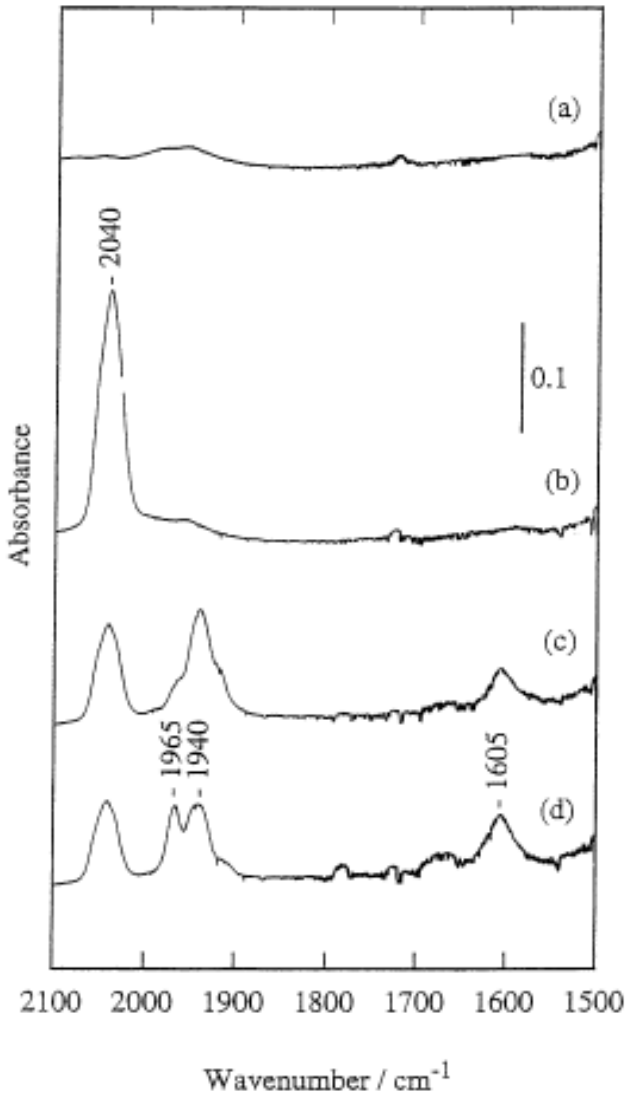

Figure 1.5: FTIR spectra of the solvent and the catalyst. (a) Triglyme; (b) $Ni(CO)_4$/trigylme; (c) $Ni(CO)_4/KOCH_3$/triglyme immediately after addition of $KOCH_3$ to (b); (d) $Ni(CO)_4/KOCH_3$/Triglyme 5 min after (c).[39]

The band at 1940 cm^{-1} was attributed to the stretching of the terminal CO bonds, whereas that at 1605 cm^{-1} was assigned to the methoxycarbonyl group ($-COOCH_3$). However, there exists a high possibility that the methoxycarbonyl anion (CH_3COO^-) contributes to the band at 1605 cm^{-1}, since it can be derived from the reaction between CH_3O^- and CO, which is one of the steps in the methyl formate process (**Scheme 1.2**).[36]

In contrast, Marchionna *et al.*[54] reported the ν_{CO} bands for the $Ni(CO)_3(COOCH_3)^-$ intermediate species to be at 2036 (w) cm^{-1}, 1939(s) cm^{-1}, 1599 (m) cm^{-1} respectively. They found that the intermediate species ($Ni(CO)_3(COOCH_3)^-$) reacts with hydrogen to generate the hydrido species $[HNi(CO)_3]^-$ (eqn. 17).

$$Ni(CO)_4 + CH_3O^- \rightleftharpoons Ni(CO)_3(COOCH_3)^- \xrightleftharpoons{H_2} HNi(CO)_3^- + HCOOCH_3 \qquad (17)$$

The reactions of $Ni(CO)_4$ and $W(CO)_6$ with $KOCH_3$ have been studied comprehensively and the conclusion has been made that they form the methoxycarbonyl complexes.[39,43,54] The catalytic study performed by Darensbourg *et al.*[18,68] for the production of methyl formate from CO and methanol catalyzed by $W(CO)_6$ and $KOCH_3$ has exposed the possible role of adding a group 6 metal carbonyl to the $Ni(CO)_4/KOCH_3$ catalytic system[19] patented by the Brookhaven National Laboratory (BNL). However, there has been no understanding of the role which may be played by $Cr(CO)_6$ and $Mo(CO)_6$ in the $Ni(CO)_4$/ $KOCH_3$ catalytic system and their reactions with alkoxides.

1.5 Summary and way forward

Previous studies have shown that metal carbonyl complexes of Co, Ru and Rh required high temperature and pressures to form methanol from syngas. This was found to be associated with the endothermic formation of the formaldehyde intermediate. The same applies to the first row, second row (group 6, group 8) and some third row (group 6, group 7 and group 8) transition metal carbonyls, as all these metal complexes produced little methanol at high temperatures and pressures. A $Rh(CO)_2(acac)$ catalyst produced formate esters of C2-C4 alcohols as well as the alcohols.

The utilization of $Ni(CO)_4$ and $KOCH_3$ for the low temperature synthesis of methanol from syngas brought some light to the process by utilizing of metal carbonyls as catalysts for CO hydrogenation. A mechanism (**Scheme 1.5**) for the formation of methanol from $Ni(CO)_4/KOCH_3$ was proposed, which involves the hydrogenation of methyl formate to form two molecules of methanol.

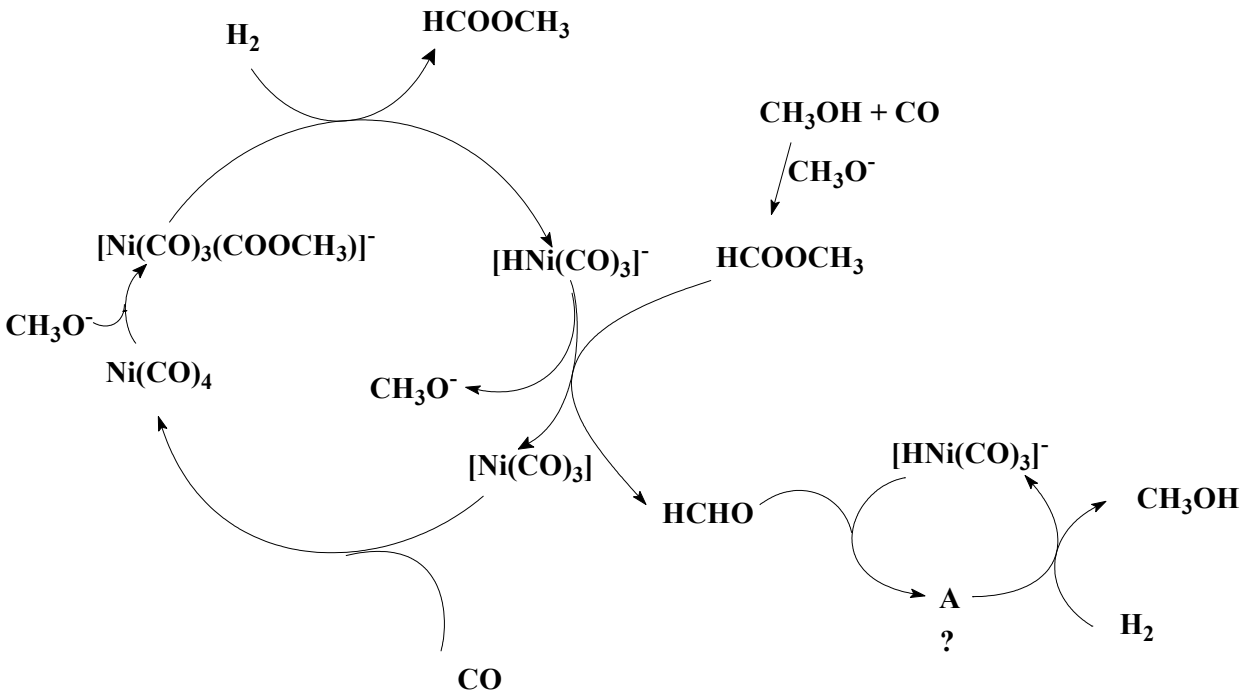

Scheme 1.5: Proposed mechanism for the synthesis of methanol from $Ni(CO)_4/KOCH_3$ system.[54]

Although this is a plausible mechanism, there are some uncertainties about its relation to the nature of the active catalytic species and some intermediates postulated. The unknown species described as A/([Ni]) by Marchiona *et al.*[54] and Mahajan *et al.*[70] add some doubt to this mechanism.

The toxicity, volatility and flammability of $Ni(CO)_4$ in this catalyic reaction makes this study difficult to be practised at an industrial scale. Therefore a less toxic metal carbonyl might be utilized. The introduction of another less toxic metal carbonyl may also result in the possibility of elongating the carbon chain lengths of the alcohols that can be produced. The $Ru_3(CO)_{12}/KOCH_3$ catalytic system set an example of the catalytic methyl formate synthesis using group 8 metal carbonyls.

The $W(CO)_6/KOCH_3$ catalytic system served as a good example of the utilization of group 6 metal carbonyls to make methyl formate. The catalyst activity exceeds that of the normal carbonylation catalyst ($KOCH_3$) by many turnovers at 125 ^oC.

In the BNL system, the role of $Cr(CO)_6$ and $Mo(CO)_6$ in the formation of methanol is not yet understood and, as a matter of fact, it still needs to be investigated, just like $W(CO)_6$ which was separately studied by Darensbourg *et al*.

There has been no explanation on how $Mo(CO)_6$ does influence the activity of the $Ni(CO)_4/KOCH_3$ catalyst and no transparency on the effect of adding potassium methoxide, CO, H_2 and syngas in the formation of methyl formate and dimethyl ether; (i) the aim is to do a fundamental study to examine the separate catalytic effect of potassium methoxide, $Mo(CO)_6$ and $Mo(CO)_6/KOCH_3$ under CO, H_2 and syngas (1:1) atmosphere on the carbonylation of methanol to methyl formate in different solvents. The results will be discussed in this thesis. A syngas ratio of 1:1 was used with an objective of elongating the carbon chain length of the possible alcoholic products, since Mahajan *et al*. and Ohyama *et al.* showed previously that a syngas ratio of 1:2 produce methanol. Alcohols are important products which can be used for many different purposes, e.g. as solvents, surfactants, octane enhancers and clean fuels, etc. (ii) Another aim is to do a fundamental study of the reaction of $Mo(CO)_6$ with $KOCH_3$ and other alkoxides (such as *t*-butoxide ($KOC(CH_3)_3$), *t*-amyloxide ($KOC(CH_3)_2CH_2CH_3$) and triphenylmethoxide ($NaOCPh_3$)) and characterize the products by IR, NMR spectroscopy and other instruments. (iii) To test the intermediate $[Mo(CO)_5(COOCH_3)]^-$ for a catalytic effect in the production of methyl formate under syngas (1:1) and hydrogen atmospheres.

Group 6 metal carbonyls are claimed by BNL to enhance the catalytic activity of the $Ni(CO)_4/KOCH_3$ system. $Mo(CO)_6$ is the preferred group 6 metal carbonyl, therefore it is important to understand its reactions with alkoxides. With an intention of propagating the carbon-chain length, it is important to understand the individual role played by each reactant in the reactions. *i.e.* the role of methoxide, hydrogen, carbon monoxide and syngas.

The interest in molybdenum has also been sparked by the finding of Friedrich and Moss **[71]** from their studies performed on nucleophilic reaction of heterodinuclear complexes at room temperature. A molybdenum center showed metalloselectivity in all cases reported. This implied that in a situation where chain propagation is important, molybdenum centered complexes can be used to elongate the carbon chain through alkyl migration. The lower toxicity of $Mo(CO)_6$ makes it easy to handle and understand the possible intermediates involved in its reactions with alkoxides.

1.6 References

[1] B. K. Warren, B. Dombek, J. Catal., 79 (1983) 334

[2] H. Schulz, Pure & Appl. Chem., 51 (1979) 2225

[3] R. A. Sheldon, Chemicals from Synthesis Gas: catalysis by metal complexes, D. Reidel Publishing Company, (1983)

[4] D. Mahajan, V. Krisdhasima, R. D. Sproull, Can. J. Chem., 79 (2001) 848

[5] P. M. Maitlis, J. Mol. Catal. A: Chemical, 204-205 (2003) 55

[6] R. B. Anderson, The Fischer-Tropsch Process, Academic press, New York (1984)

[7] B. H. Weil, J. C. Lane, The technology of the Fischer-Tropsch Process, Constable and Company Ltd, (1949)

[8] J. S.Bradley, J. Am. Chem. Soc., 101 (1979) 7419

[9] D. R. Fahey, J. Am. Chem. Soc., 103 (1981) 136

[10] W. F. Gresham, U.S. Patent 2636046 (1953)

[11] R. L. Pruett, W. E. Walker, U. S. Patent 3833634 (1974)

[12] M. Ishino, M. Tamura, T. Deguchi, S. Nakamura, J. Catal., 133 (1992) 325

[13] J. W. Rathke, H. M. Feder, J. Am. Chem. Soc., 100 (1978) 3623

[14] I. Wender, R. Levine, M. Orchin, J. Am. Chem. Soc., 71 (1949) 4160

[15] G. Henrici-Olivè, S. Olivè, Angew. Chem., Int. Ed. Engl., 15 (1976) 136

[16] M. Ishino, M. Tamura, T. Deguchi, S. Nakamura, J. Catal., 133 (1992) 332

[17] W. Keim, M. Berger, J. Schulpp,, J. Catal., 61 (1980) 359

[18] D. J. Daransbourg, R. L. Gray, C. Ovalles, J. Mol. Catal., 41 (1987) 329

[19] D. Mahajan, R. S. Sapienza, W. A. Slegier, T. E. O'Hare, U.S. Patent 4614749 (1986)

[20] J. J. Brunet, P. Gallois, P. Caubere, Tetrahedron Lett., (1977) 3955; (b) J. J. Brunet, P. Gallois, P. Caubere, J. Org. Chem., 45 (1980) 1937; (c) P. Gallois, J. J. Brunet, P. Caubere, J. Org. Chem., 45 (1980) 1946

[21] D. Mahajan, R. S. Sapienza, W. A. Slegier, T. E. O'Hare, U.S. Patent 4935395 (1990), U.S. Patent 4992480 (1991)

[22] J. J. Brunet, R. Vanderesse, P. Caubere, J. Organomet, Chem., 157 (1978) 125

[23] C. A. Brown, H. C. Brown, J. Am. Chem. Soc., 85 (1963) 1003

[24] C. A. Brown, H. C. Brown, J. Am. Chem. Soc., 85 (1963) 1005

[25] S. Ohyama, Appl. Catal. A, 180 (1999) 217

[26] C. A. Brown, J. Chem. Soc. Chem. Comm., (1974) 680

[27] B. Loubinoux, R. Vanderesse, P. Caubere, Tetrahedron Lett., (1977) 3951

[28] J. J. Brunet, D. Besozzi, A. Courtois, P. Caubere, J. Am. Chem. Soc., 104 (1982) 7130

[29] J. J. Brunet, C. Sidot, B. Loubinoux, P. Caubere, J. Org. Chem., 44 (1979) 2199

[30] J. J. Brunet, P. Caubree, Tetrahedron Lett., (1977) 3947

[31] J. Christiansen, U.S. Patent 1302011 (1919)

[32] J. W. Evans, P. S. Casey, M. S. Wainwright, D. L. Trim, N. W. Cant, Applied Catal., 7 (1983) 31

[33] R. J. Gormely, V. U. S. Rao, Y. Soong, Appl. Catal. A: General, 87 (1992) 81

[34] S. Ohyama, Top. Catal., 22 (2003) 337

[35] J. Christiansen, Chem. Soc., (1926) 413

[36] S. P. Tonner, D. L. Trimm, M. S. Wainwright, N. W. Cant, J. Mol. Catal., 18 (1983) 215

[37] S. Ohyama, Appl. Catal. A, 181 (1999) 87

[38] S. Ohyama, E. S. Lee, K. Aika, J. Mol. Catal. A, 138 (1999) 305

[39] S. Ohyama, Appl. Catal. A, 220 (2001) 235

[40] S. Vukojević, O. Trapp, J. Grunwaldt, C. Kiener, F. Schüth, Angew. Chem. Int. Ed., 44 (2005) 7978

[41] D. J. Darensbourg, M. Y. Darensbourg, Inorg. Chem., 9 (1970) 1691

[42] M. Y. Darensbourg, H. L. Condor, D. J. Darensbourg, C. Hasday, J. Am. Chem. Soc., 95 (1973) 5919

[43] (a) R. J. Trautman, D. C. Gross, P. C. Ford, J. Am. Chem. Soc., 107 (1985) 2355; (b) D. C. Gross, P. C. Ford, J. Am. Chem. Soc., 107 (1985) 585; (c) D. J. Taube, A. Rokicki, M. Anstock, P. C. Ford, Inorg. Chem., 26 (1987) 526

[44] I. Wender, H. W. Sternberg, M. Orchin, J. Am. Chem. Soc., 74 (1952) 1216

[45] K. M. Doxsee, R. H. Grubbs, J. Am. Chem. Soc., 103 (1981) 7696

[46] R. H. Crabtree, The Organometallic Chemistry of the Transtion Metals, John Wiley & Sons, (1988)

[47] T. S. Coolbaugh, B. D. Santarsiero, R. H. Grubbs, J. Am. Chem. Soc., 106 (1984) 6310

[48] R. J. Angelici, Acc. Chem. Res., 5 (1972) 335

[49] P. C. Ford, A. Rokicki, Adv. Organomet. Chem., 28 (1988) 139

[50] D. J. Darensbourg, B. J. Baldwin, J. A. Froelich, J. Am. Chem. Soc., 102 (1980) 4688

[51] D. J. Darensbourg, J. A. Froelich, J. Am. Chem. Soc., 100 (1978) 338

[52] D. J. Darensbourg, J. A. Froelich, Organometallics, 1 (1982) 1685

[53] H. W. Sternberg, I. Wender, R. A. Friedel, M. Orchin, J. Am. Chem. Soc., 75 (1953) 3148

[54] M. Marchionna, L. Basini, A. Aragno, M. Lami, F. Ancillotti, J. Mol. Catal., 75 (1992) 147

[55] S. Otsuka, A. Nakamura, T. Yoshida, M. Naruto, K. Ataka, J. Am. Chem. Soc., 95 (1973) 3180

[56] R. Bertani, G. Cavinato, L. Toniolo, G. Vasapollo, J. Mol. Catal., 84 (1993) 165

[57] A. H. Klahn, C. Manzur, Polyhedron, 9 (1990) 1131

[58] G. Cardaci, G. Bellachioma, P. F. Zanazzi, J. Chem. Soc. Dalton Trans., (1987) 473

[59] D. Carmona, J. Ferrer, J. Reyes, L. A. Oro, Organometallics, 12 (1993) 4241

[60] (a) H. E. Bryndza, Organometallics, 4, (1985) 1686; (b) G. D. Smith, B. E. Hanson, J. S. Merola, F. J. Waller, Organometallics, 12 (1993) 568; (c) S. A. Macgregor, G. W. Neave, Organometallics, 22 (2003) 4547; (d) S. A. Macgregor, G. W. Neave, Organometallics, 23 (2004) 891

[61] (a) F. Rivetti, U. Romano, J. Organomet. Chem., 154 (1978) 323; (b) F. Rivetti, U. Romano, J. Organomet. Chem., 174 (1979) 221

[62] D. M. Fenton, P. J. Steinwand, J. Org. Chem., 39 (1974) 701

[63] D. Huggins, N. Flitcroft, H. D. Kaesz, Inorg. Chem., 4 (1965) 166

[64] M. Darensbourg, B. F. Schumann, R. Lusk, S.G. Slater, Organometallics, 1 (1982) 1662

[65] K. M. Doxsee, R. H. Grubbs, J. Am. Chem. Soc., 103 (1981) 7696

[66] A. Bates, M. T. Muraoka, R. J. Tarutman, Inorg. Chem., 32 (1993) 2651

[67] P. Y. Bruice, Organic Chemistry, 2nd edition, Prentice-Hall, Inc. (1998)

[68] D. J. Daransbourg, R. L. Gray, C. Ovalles, M. Pala, J. Mol. Catal., 29 (1985) 285

[69] D. J. Darensbourg, K.M. Sanchez, J. H. Reibenspies, A. L. Rheingold, J. Am. Chem. Soc., 111 (1989) 7094

[70] D. Mahajan, Top. Catal., 32 (2005) 209

[71] H. B. Friedrich, J. R Moss, J. Chem. Soc., Dalton Trans., (1993) 2863

2. CHAPTER 2

The effect of $Mo(CO)_6$, as a cocatalyst in the carbonylation of methanol to methyl formate catalyzed by potassium methoxide under CO, syngas and H_2 atmospheres

2.1 Introduction

Early studies of carbonylation reactions date back to the time when W. Reppe, working for BASF, discovered that the reaction of CO with methanol produced acetic acid, when catalyzed by metal carbonyl compounds of Fe, Co, and Ni in the presence of iodide promoters at 210 ^{o}C and 7500 psi of CO.[1] Other reactions involving carbonylation arose from this process. Typical products of carbonylation include methyl formate, methyl acetate, acetic anhydride and acetaldehyde, etc.[2,3]

Methyl formate is among the most important industrial products, since it offers an alternative approach for the production of basic products such as acetic acid, acetaldehyde and ethanol through different processes as depicted in **Scheme 2.1**.[4-6] Other products of importance from methyl formate include formic acid, dimethyl formamides, and ethylene glycol.[7,8] It has been reported that methyl formate can also react with olefins or halogenated compounds to give esters *via* hydroesterification or alkoxycarbonylation reactions.[9,10] Therefore, a chemical industry based on methyl formate as a feed could exist, similar to the commercial Monsanto acetic acid process, particularly if carbon monoxide is available in large amounts and at low cost from a non-conventional source e.g. off-gas from the steel industry.[7,8] Although methyl formate can be produced from a variety of catalytic processes, the commercially viable process still remains the carbonylation of methanol catalysed by sodium methoxide (NaOMe) (eqn.1) at 80 ^{o}C and 45 atmosphere (675 psi) of CO, since BASF patented the process in 1925.[11]

$$CH_3OH + CO \xrightarrow[80\ ^{o}C,\ 45\ atm]{NaOCH_3} HCOOCH_3 \qquad (1)$$

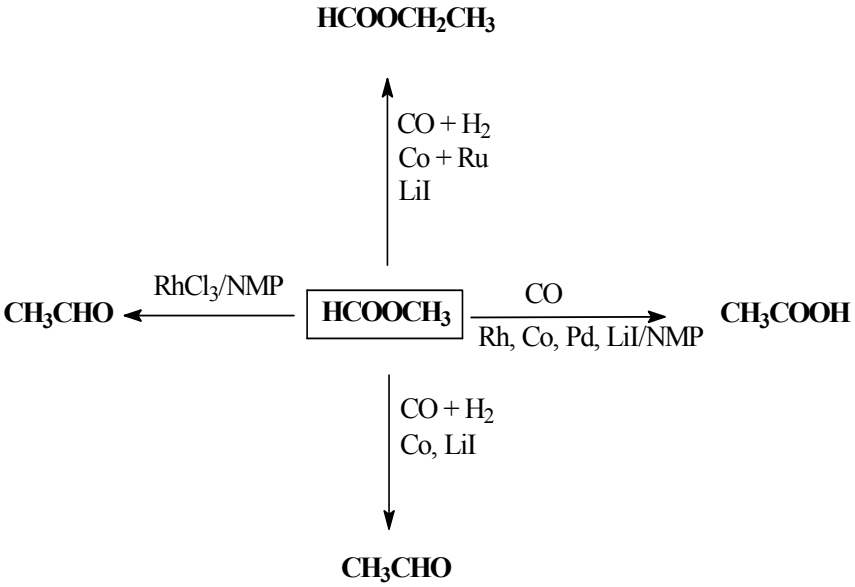

Scheme 2.1: Transformation of methyl formate to different products.[4-6]

The process involves a nucleophilic attack of the methoxide ion on carbon monoxide to form the methoxycarbonyl anion (CH_3COO^-); subsequent protonation of the methoxycarbonyl anion by a methanol molecule produces methyl formate and regenerate the methoxide catalyst. The activity of the catalyst is increased by decreasing the ionization potential of the alkali metals, *i.e.* the rate of carbonylation is slowest with lithium methoxide and fastest with potassium methoxide.[12] The weakness of this process is that it requires strictly anhydrous conditions as sodium methoxide can be hydrolysed to methanol and sodium hydroxide which inhibit the reaction. Sodium hydroxide reacts with methyl formate to form undesirable products such as sodium formate and methanol.[12] The purity of CO used is also very critical as the presence of small amounts of CO_2 results in the deactivation of the catalyst through the formation of an insoluble sodium methyl carbonate, eqn. 1.[13,14]

$$CH_3ONa + CO_2 \longrightarrow CH_3O{-}\overset{\overset{O}{\|}}{C}{-}ONa \qquad (2)$$

Therefore, a challenge still remains for the development of a new insensitive catalytic system for the carbonylation of methanol into methyl formate.[8,13] Studies from other laboratories have demonstrated that alkyl formates can be produced by the hydrogenation of carbon dioxide in the

presence of an alcohol (eqn. 2), catalyzed by metal hydrides such as $RuH_2[PPh_3]_4$,[15] $H_3Ru_4(CO)_{12}^-$, $HRu_3(CO)_{11}^-$,[16] μ-$HM_2(CO)_{10}^-$ or $HM(CO)_5^-$ and formate complexes, $HCO_2M(CO)_5^-$, [M = Cr and W].[17,18]

$$CO_2 + H_2 + ROH \xrightarrow{[M\text{-}H]^-} HCOOR + H_2O \qquad (3)$$

The process involving a group 6 metal hydride (**Scheme 2.2**) entails heterolytic bond fission of the bridged hydride (μ-$HM_2(CO)_{10}^-$) to provide a convenient monohydride, $HM(CO)_5^-$, which inserts CO_2 to form metalloformate ($HCO_2M(CO)_5^-$) complexes.[19,20] The metalloformate derivatives undergo CO ligand dissociation to provide a vacant site for the oxidative addition of dihydrogen, which is followed by the reductive elimination of formic acid. Formic acid subsequently reacts with an alcohol through a hydrocondensation process to produce methyl formate and water.[17] However, this process is inhibited by carbon monoxide as it slows down the CO dissociation.

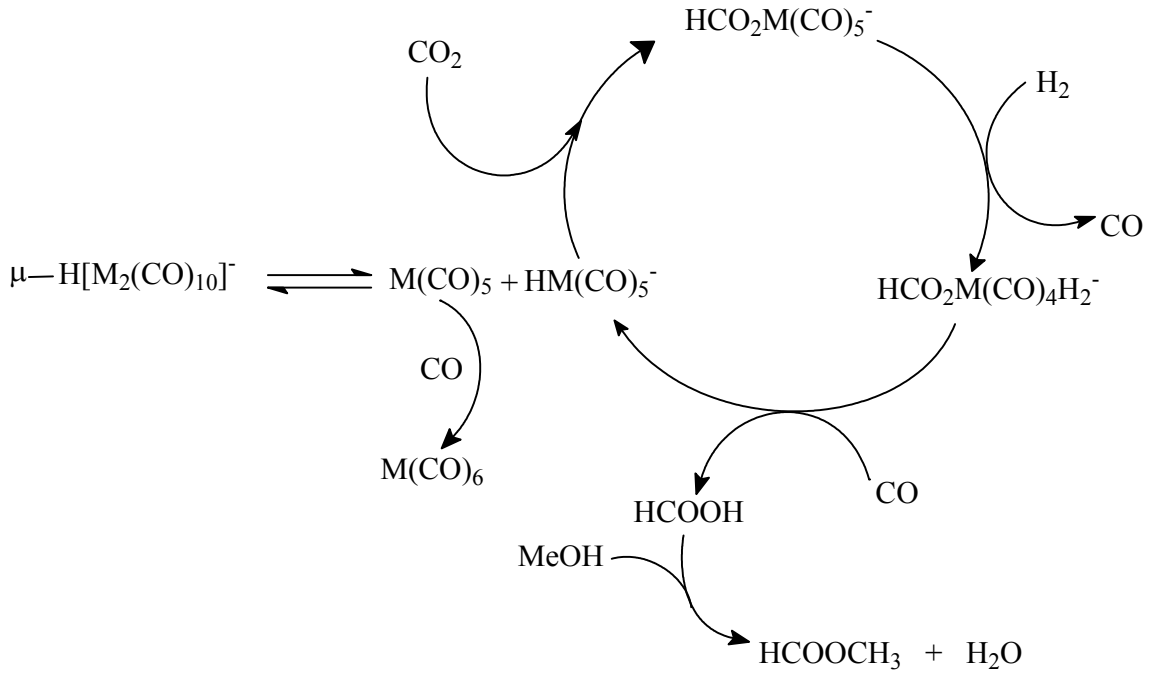

Scheme 2.2: Catalytic cycle for the synthesis of methyl formate catalyzed by the bridged hydride, μ-$HW_2(CO)_{10}^-$.[17,18]

Studies had also shown that addition of a group 6 and/or 8 metal carbonyl to the methoxide process enhances production of methyl formate and promotes the suppression of trace water impurities through a water-gas shift reaction (WGSR, eqn. 3).[7,11,21-23]

$$CO + H_2O \rightleftharpoons CO_2 + H_2 \qquad (4)$$

In the presence of a metal carbonyl, the effect of the WGSR products such as CO_2 and H_2O had been reported to have a small influence on the activity of the catalytic system as described in the above paragraphs. It has also been noted that the activity of the catalyst increased by a significant amount of turnovers compared to the catalysis with methoxide anion on its own.[7,23] This is probably because of the role played by the metal center of the metal carbonyl to provide a more electrophilic source of coordinated carbon monoxide, which is nucleophilically attacked by a methoxide, eqn. 5.[21,24-27] In this process the methoxide activates the metal coordinated CO to form a short lived alkoxycarbonyl (metallo-ester) complex (eqn.5) .

$$(CO)_{n-1}M\text{-}CO + CH_3O^- \overset{CO}{\rightleftharpoons} (CO)_{n-1}M\text{-}C(=O)OCH_3^- \qquad (5)$$

M= Ni, W, Fe, Ru, Os, Cr, Pd, Pt

At an elevated temperature ($T \geq 100\ ^oC$), the metalloester is reported to be protonated by a small amount of an alcohol in the system, to eliminate methyl formate and regenerate the methoxide. Since the rate determining step in the methoxide catalyzed reaction is the attack of the methoxide on the carbon monoxide,[7] a greater activity of the catalytic system might be expected by using a metal-coordinated CO and aprotic solvent. This agrees well with the theory which states that, nucleophilic attack occurs at the carbonyl carbon atom which has a larger C-O bond force constant.[28] In principle, a high C-O bond force constant correlates with a more positive carbon atom, which then becomes more susceptible to nucleophilic attack.[28,29] Therefore, coordinated CO is predicted to react faster than free carbon monoxide,[7,25] due to the π-back donation effect from the metal center to CO, which makes it more electrophilic.

The reactivity of the alkoxide with the metal carbonyl has been reported to be affected by the nature of the solvent used, for example, at ambient temperature the equilibrium in eqn. 5 above

had been reported to lie further to the right in tetrahydrofuran than alcohols.[24,30] This might be due to the stabilization of the methoxide by alcohols through the formation of hydrogen bonding which inhibits its nucleophilic character, eqn. 6.[31]

$$RO^- Na^+ \quad + \quad R'OH \quad \longleftrightarrow \quad [RO\text{-----}H\text{----}OR']^- Na^+ \qquad (6)$$

$R=R'= -CH_3$

Since the equilibrium in eqn. 5 has been reported to be influenced by the type of solvent used, it was anticipated that addition of tetrahydrofuran (THF) to a $W(CO)_6/KOCH_3$ mixture might result in enhanced catalytic activity of the system to produce methyl formate. Studies have indicated that the activity actually decreases with an increase in THF concentration, because of an inhibition in the step involving protonation of the metalloester intermediate.[7]

The production of methanol from CO and H_2 at temperatures and pressures (80-120 ^oC, 10-50 atm) much lower than conventional synthesis (230-300 ^oC, 50-100 atm) has been claimed in several patents.[32] The catalyst precursors involve nickel(II) salts and alkaline alcoholates (NaH-ROH mixtures). The re-investigation of these systems showed that their active core is composed of the homogeneous catalytic system, $Ni(CO)_4/KOCH_3$.[24,32,33] This system is claimed to be highly active (turnover frequency of 280 $mol.Ni^{-1}.h^{-1}$) under very mild conditions (T = 100-120 ^oC; P = 20-40 atm, CO/H_2=1/2; $Ni(CO)_4$/ $KOCH_3$ ratio 40/20; solvent = THF, diglyme and triglyme).[24,34] The selectivity to methanol is claimed to be 90-99% at a high conversion of synthesis gas. One of the patents reported that the co-existence of $M(CO)_6$, M selected from Cr, Mo, W, as the co-catalyst in conjunction with alkoxides, such as methoxide, *tert*-butoxide, *tert*-amyl alkoxide enhances the catalytic activity of $Ni(CO)_4/KOCH_3$ system in the production of methanol.[32]

Ohyama *et al.*[34] have undertaken a similar study of examining the role of group 6 metal carbonyls and $Ni(CO)_4$ in methanol production. The study was performed with and without the methoxide under syngas atmospheres with a CO/H_2 ratio of (1:2). It has been revealed that all metal carbonyls without methoxide produce little methyl formate (Cr and W) and dimethyl ether (Mo and Ni), confirming that metal carbonyls alone display little catalytic activity under the claimed conditions. The presence of methoxide enhanced the activity of these metal carbonyls

(group 6) and produced a significant amount of methyl formate and dimethyl ether, except $Ni(CO)_4$ which produced methanol. However, it was still not clear whether the results for group 6 metal carbonyls are due to the typical methoxide carbonylation mechanism, **Scheme 2.3** [11,34] or whether another mechanism involving an active intermediate such as the metalloester (eqn. 5) is dominating in this catalysis.

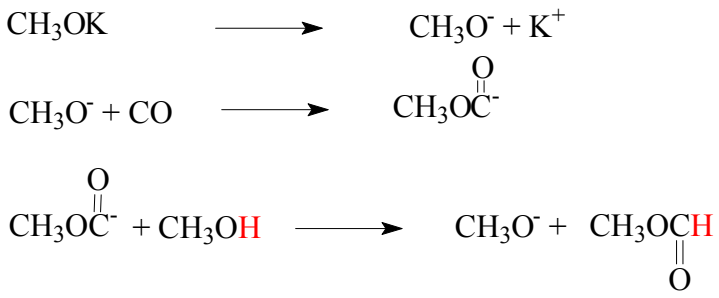

Scheme 2.3: Carbonylation of methanol catalysed by potassium methoxide.

The aim of this chapter is (i) to study the influence/role of $Mo(CO)_6$ in the carbonylation of methanol to methyl formate by comparing the amount of methyl formate produced from a $KOCH_3$ catalyzed carbonylation reaction (eqn. 1) with the amount produced by a mixture of $Mo(CO)_6/KOCH_3$ (eqn.5) under CO, syngas(1:1) and H_2 in different solvents. (ii) To study the reaction of $Mo(CO)_6$ and $KOCH_3$ using HPIR under CO, syngas(1:1), H_2 and N_2 atmospheres so as to understand the chemical influence of each gas towards the formation of methyl formate and possible intermediate species.

2.2 Results and discussions

The effect of protic and aprotic polar solvents on the reaction of $Mo(CO)_6$ and $KOCH_3$ was considered in all experiments performed. This arises since the equilibrium in eqn. 5 is reported to be highly dependent on the choice of solvent system. At room temperature, the equilibrium for the reaction between $W(CO)_6$ and $KOCH_3$ in methanol lies to the left as no characteristic formation of the metalloester was observed even in the presence of excess alkoxide.[7,35] Methanol stabilizes the methoxide ion hence making it less nucleophilic. In contrast, in pure THF the equilibrium is shifted to the product (right) even at an equivalent amount of the reactants. The same observation was made by Gross *et al.*[35] for the $Ru_3(CO)_{12}$ and CH_3O^- system.

The solvents studied were methanol, tetrahydrofuran (THF) and triethylene glycol dimethyl ether (triglyme, TG). The reactions were performed by adding individual catalytic components to different solvents. In all solvents, $Mo(CO)_6$ alone displayed no catalytic activity under CO, H_2 and syngas (1:1) atmospheres (**Table 2.1 and 2.2**). A considerable amount of methyl formate, formic acid and dimethyl ether were produced over $KOCH_3$ in all solvents under CO and syngas (1:1) atm. Dimethyl ether was associated with the dehydration of methanol,[34] while formic acid was associated to the hydrolysis of methyl formate. When the same reactions were performed over $Mo(CO)_6/KOCH_3$ (1:4) under carbon monoxide atmosphere, the amount of methyl formate produced increased very slightly compared to the $KOCH_3$ catalyst alone in all cases (**Table 2.1**). This was associated with the nucleophilic attack of $KOCH_3$ on the metal coordinated carbon monoxide (eqn. 5), which is presumed to be faster than the competing attack of $KOCH_3$ on the free carbon monoxide (eqn. 1).[7,25] The amount of methyl formate produced was higher in methanol solvent compared to the other solvents due to the regeneration of the methoxide in methanol, while in THF and triglyme the methanol from the $KOCH_3$ solution is consumed and thus the regeneration of the methoxide is inhibited, hence reducing the amount of methyl formate produced.

The results under CO atm correlate with the observation of Darensbourg *et al.,*[7,23] since the addition of $Mo(CO)_6$ enhanced the activity of $KOCH_3$ in the carbonylation of methanol to methyl formate, although the effect is not seven times that of $KOCH_3$ alone as observed for their $W(CO)_6$ system. In contrast, Ohyama *et al*.[34] demonstrated a significant increase in the production of methyl formate over $Mo(CO)_6/KOCH_3$ *vs.* $W(CO)_6/ KOCH_3$ under syngas (1:2) atm but such comparison is beyond the scope of this report. The work described here is concerned with the effect of $Mo(CO)_6$ in the $KOCH_3$ catalyzed carbonylation of methanol under CO, syngas and H_2, and characterizing the organometallic products formed from the reaction of methoxide with $Mo(CO)_6$.

A noticeable change in the amount of methyl formate produced under CO was observed for $Mo(CO)_6/KOCH_3$ and $KOCH_3$ in THF and triglyme (**Table 2.1**). This might be associated with the solubility of $Mo(CO)_6$ in these solvents which probably increases its reactivity with $KOCH_3$ and shifts the equilibrium in equation 5 to the right compared to the reaction performed in methanol.

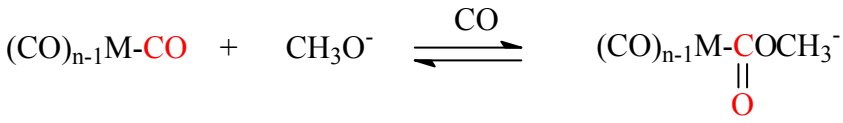

(5)

M= Ni, W, Fe, Ru, Os, Cr, Pd, Pt

The metalloester derivative might play a more important role in reactions performed in THF and triglyme than methanol. The consumption of methanol in the step involving the protonation of the metalloester to eliminate methyl formate (**Scheme 2.4**) is seen as the rate determining step in these reactions, which determines which system will produce more methyl formate.

Table 2.1: The effect of $Mo(CO)_6$ and solvent in CO carbonylation of CH_3OH, 1600 kPa CO at 125 ^oC

Catalyst	Time (hours)	Solvent	HCO_2CH_3(mmol)	TON[a] in $Mo(CO)_6$	TON in $KOCH_3$
$KOCH_3$	24	MeOH	12.40		0.35
$Mo(CO)_6/KOCH_3$	24	MeOH	13.05	1.30	0.37
$KOCH_3$	24	Triglyme	3.99		0.11
$Mo(CO)_6/KOCH_3$	24	Triglyme	5.52	0.55	0.16
$KOCH_3$	24	THF	3.56		0.10
$Mo(CO)_6/KOCH_3$	24	THF	6.22	0.62	0.02

a = TON is n(methyl formate)/n(catalyst), n is the number of moles (mmoles)

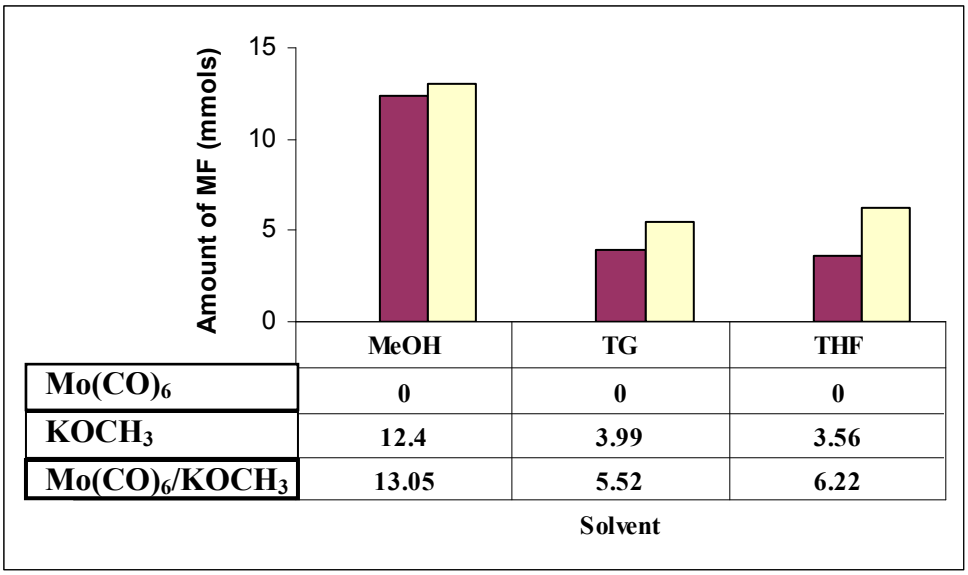

Figure 2.1: Methyl formate from $Mo(CO)_6/KOCH_3$/CO in different solvents.

Comparing the reactions performed under CO and syngas atmosphere in methanol, the results shows that more methyl formate is produced under syngas than CO in both $KOCH_3$ and $Mo(CO)_6/KOCH_3$ catalyzed experiments (**Table 2.2 and Figure 2.4**). The reaction of $Mo(CO)_6/KOCH_3$ under H_2 atm in the THF/MeOH mixture produced methyl formate in lower amounts than produced under a CO atmosphere (**Figure 2.1 & 2.2**) . This suggests that under a hydrogen atmosphere, the metalloester (eqn. 7) is hydrogenated *in situ* to form methyl formate. FTIR analysis of the organometallic product showed peaks corresponding to the formation of the metalloester[†] and methyl formate. Results also revealed that more methyl formate is produced in methanol than in THF and triglyme (**Figure 2.2**).

[†] IR bands at 2030(w), 1940(s), 1878(m), 1732 (vs, methyl formate), 1610 (s), 1602(sh) cm^{-1}.

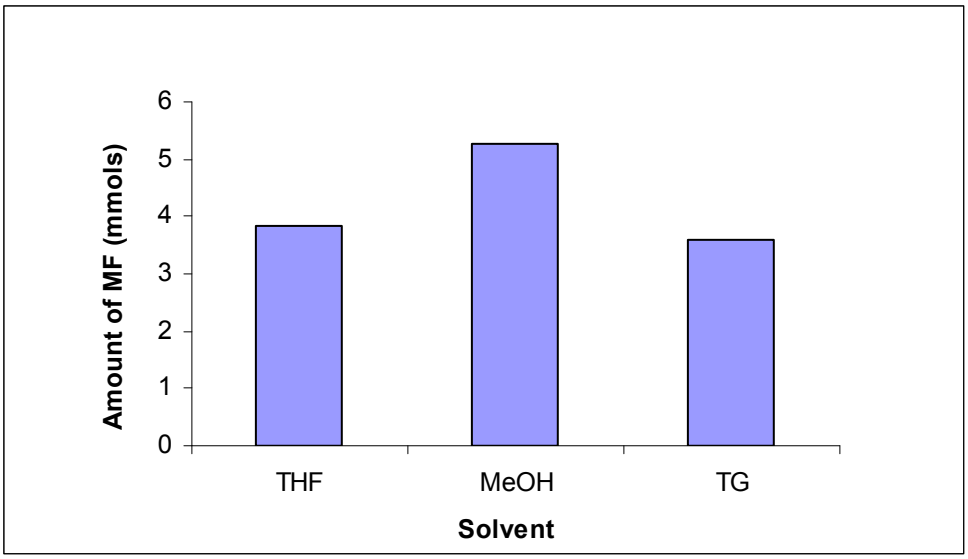

Figure 2.2: Methyl formate from $Mo(CO)_6/KOCH_3/H_2$ in different solvents.

These results under syngas atmosphere are not extraordinary based on the fact that the synthesis gas utilized here is made up of equivalent amounts of CO and H_2 (1:1). Therefore some methyl formate will be generated through the H_2 mechanism, which involves hydrogenation of the metalloester (eqn. 7). Another possibility might involve a CO mechanism (**Scheme 2.4**).

$$(CO)_5Mo{-}CO + CH_3O^- \underset{}{\overset{CO}{\rightleftharpoons}} (CO)_5Mo{-}\underset{\underset{O}{\|}}{C}{-}OCH_3^- \xrightarrow[solvent]{H_2} HCOOCH_3 + \mu\text{-}HMo_2(CO)_{10}^- \quad (7)$$

There were no characteristic peaks observed for the mono hydride ($HMo(CO)_5^-$) observed in the IR spectrum. High Pressure IR (HPIR) analysis of the same reaction showed peaks growing with the time of reaction characteristic of the stable bridged hydride (μ-$HMo_2(CO)_{10}^-$) at 2041(w) cm^{-1}, 1944(vs) $cm^{-1}$and 1881(m) cm^{-1} as the peaks characteristic of the metalloester ($Na[Mo(CO)_5(COOCH_3)]$) at 2052(w) cm^{-1}, 1912(s) cm^{-1}, 1881(m) cm^{-1} and 1678(m, br) cm^{-1} decreased. The carbonyl peak of methyl formate was observed at 1734(m, br) cm^{-1}, but also diminished as the peaks for the bridged hydride increased. The HPIR spectrum is depicted in **Figure 2.7**.

The CO mechanism involves the attack on the metal coordinated CO by a nucleophile (CH_3O^-) and protonation of the metalloester intermediate [$(CO)_5$Mo-$COOCH_3$] by an alcohol under CO atmosphere to eliminate methyl formate and $Mo(CO)_5$ intermediate as shown in **Scheme 2.4**. The $Mo(CO)_5$ intermediate reacts with CO in the system and regenerate $Mo(CO)_6$. As described in **Scheme 2.3** on page 34, there exists a possibility that some methyl formate is generated from the methoxide carbonylation of methanol. The inhibition of methyl formate production in the presence of hydrogen is not significant in this case.[7] Dimethyl ether and formic acid are probably formed through the same pathways of dehydration of methanol and hydrolysis of methyl formate.

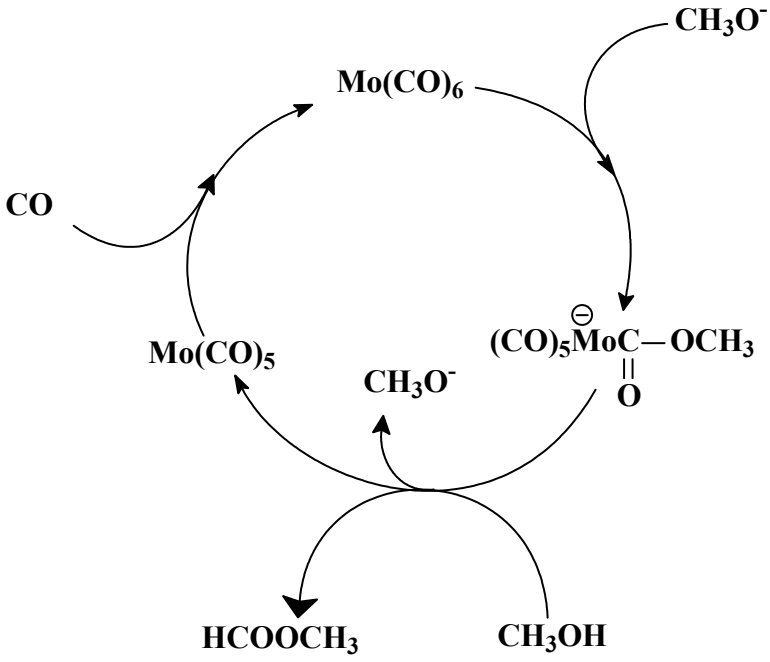

Scheme 2.4: CO mechanism for the formation of methyl formate from $Mo(CO)_6/KOCH_3$ under syngas atmosphere.

When comparing the reactions performed under CO and syngas atmosphere in THF and triglyme (**Table 2.1 & Table 2.2**), the amount of methyl formate formed under syngas is less than that produced under CO atmosphere. This can be due to the formation of other organic products which cannot form under CO atmosphere alone. Although longer chain alcohols were formed in THF solution, analysis of the organic products from $Mo(CO)_6/KOCH_3$ system under syngas in triglyme revealed the formation of longer chain alcohols (C2-C5), namely ethanol, 2-propanol, 2-butanol, 3-methyl-2-butanol, 3-pentanol, 2-methyl-3-pentanol and 2,4-dimethyl-3-pentanol in addition to methyl formate and dimethyl ether (**Figure 2.3**).

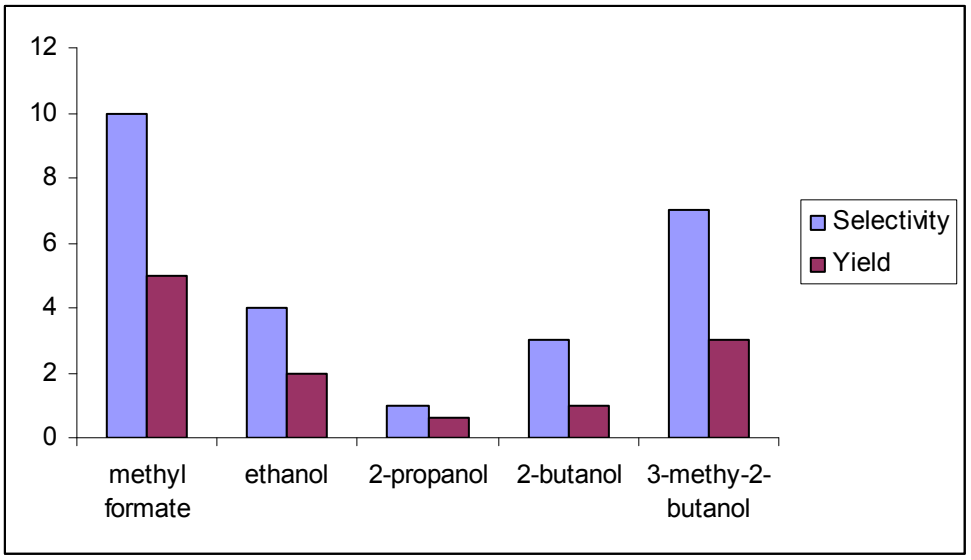

Figure 2.3: Selectivity of higher alcohols in $Mo(CO)_6/KOCH_3$/Syngas(1:1)/triglyme.

These products might be expected from the CO hydrogenation reaction catalyzed by a molybdenum catalyst since supported Mo catalysts have been used for CO hydrogenation to produce higher (C1-C6) alcohols.[36-39]

Table 2.2: The effect of $Mo(CO)_6$ and solvent in syngas carbonylation of CH_3OH, 1600 KPa CO/H_2 at 125 ^oC

Catalyst	Time (hours)	Solvent	HCO_2CH_3 (mmol)	TON[a] in $Mo(CO)_6$	TON in $KOCH_3$
$KOCH_3$	24	MeOH	22.29		0.62
$Mo(CO)_6/KOCH_3$	24	MeOH	21.00	2.10	0.60
$KOCH_3$	24	THF	3.46		0.10
$Mo(CO)_6/KOCH_3$	24	THF	4.95	0.50	0.14
$KOCH_3$	24	Triglyme	3.05		0.09
$Mo(CO)_6/KOCH_3$	24	Triglyme	5.52	0.40	0.16

a = TON is n(methyl formate)/n(catalyst), n is the number of moles (mmoles)

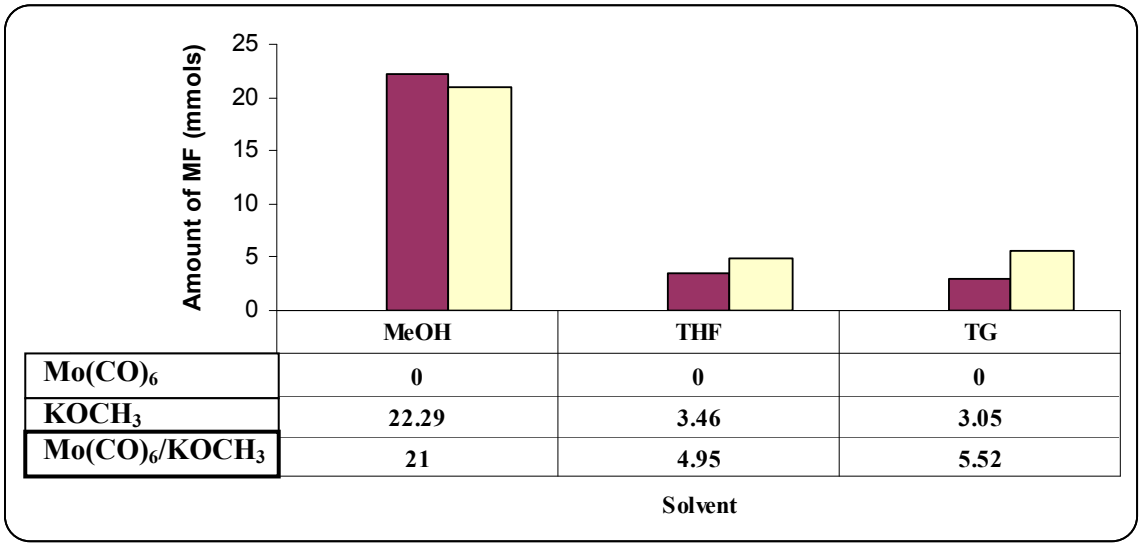

	MeOH	THF	TG
$Mo(CO)_6$	0	0	0
$KOCH_3$	22.29	3.46	3.05
$Mo(CO)_6/KOCH_3$	21	4.95	5.52

Solvent

Figure 2.4: Methyl formate from $Mo(CO)_6/KOCH_3$/syngas in different solvents.

The stoichiometric effect of $Mo(CO)_6$ in the production of methyl formate was considered only in THF under syngas (1:1), by varying its amount relative to potassium methoxide. The results reported in the above figures were performed at a stoichiometric ratio of $Mo(CO)_6$: $KOCH_3$ of 1:4. The ratios of $Mo(CO)_6/KOCH_3$ studied were 1:4, 1:2, 1:1and 2:1. The results show that the amount of methyl formate formed initially increases with the amount of $Mo(CO)_6$ added. However, a stoichiometric ratio of 1:2 gave the best results (**Figure 2.5**). This shows that $Mo(CO)_6$ does not react with water (in the WGSR) as there is no linear response to methyl formate as its amount increases.

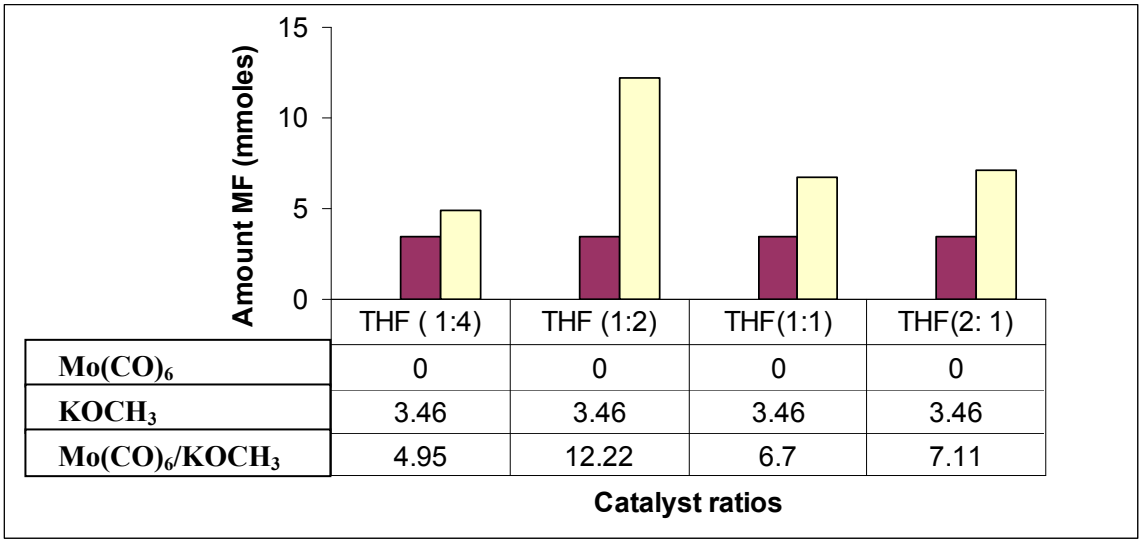

Figure 2.5: Stoichiometric effect of $Mo(CO)_6$: $KOCH_3$ under syngas (1:1) atm in THF.

The effect of each gas (CO, H_2, syngas) on the reaction of $Mo(CO)_6$ and $KOCH_3$ under pressure was then studied using a high-pressure IR reactor cell. This technique is useful, particularly for reactions involving carbon monoxide, for which transition metal carbonyl complexes are key intermediates in the catalytic mechanism. The advantage of this technique is that one is able to understand the nature of the intermediates formed under high gas pressures, which might be helpful in proposing the possible mechanistic pathways to different products.[40,41]

2.2.1 *In situ* studies on the reaction of $Mo(CO)_6$ and $KOCH_3$ under CO pressure

$Mo(CO)_6$ rapidly reacts with $KOCH_3$ under CO pressure (5 bar, 13 ^oC) to form $Mo(CO)_5(COOCH_3)^-$, which is characterized by IR stretching/vibrating peaks for CO bonds at (2054(w) cm^{-1}, 1915(s) cm^{-1}, 1882(s) cm^{-1} and 1610 (m, br)) cm^{-1}. **Figure 2.6** shows the IR spectra recorded during the reaction against temperature. The peak for $Mo(CO)_6$ (1990 cm^{-1}) decreased immediately after mixing the reactants and was not subsequently observed in the IR spectrum. The peak at 1730 cm^{-1} assigned to the 'carbonyl peak' of methyl formate grew as the reaction progressed, probably due to the reaction between CO and CH_3O^-, while the peaks of $Mo(CO)_5(COOCH_3)^-$ remained constant. Carbon monoxide stabilizes the $Mo(CO)_5(COOCH_3)^-$ species, but as the temperature was increased from room temperature to 100 ^oC, the peaks at 2054 cm^{-1}, 1915 cm^{-1}, 1882 cm^{-1} and 1610 cm^{-1} decreased, while the $Mo(CO)_6$ peak at 1990 cm^{-1} was seen again and the peak assigned for the carbonyl to methyl formate at 1730 cm^{-1} increased

(indicated by the arrows pointing up in **Figure 2.6**). At 100 ^{o}C all the peaks assigned to $[Mo(CO)_5(COOCH_3)]^-$ in the carbonyl region (2100-1800 cm^{-1}) decreased and a new species formed with peaks at 1927(m) cm^{-1} and 1882 (w) cm^{-1}. The methyl formate peak remained at 1730 cm^{-1}, while the peak at 1610 cm^{-1}(Mo-COOMe) decreased and peaks at 1617(sh) cm^{-1} and 1594 cm^{-1} were observed (**Figure 2.6**).

There was no evidence for the formation of $[Mo(CO)_5(OCH_3)]^-$ or $[Mo_3(CO)_9(OCH_3)_3]^-$. The infrared spectrum of the $[Mo(CO)_5(OCH_3)]^-$ complex has never previously been reported due to its instability by dissociating CO to form the $[Mo_3(CO)_9(OCH_3)_3]^-$ cluster(s).[42] The IR spectrum of the analogous complex $[W(CO)_5(OCH_3)]^-$ shows peaks at 2054 (w) cm^{-1}, 1901(s) cm^{-1} and 1847(m) cm^{-1}, while the IR spectrum for the cluster, $[Mo_3(CO)_9(OCH_3)_3]^-$, in CH_3CN has peaks at 1901(w) cm^{-1}, 1870(vs)cm^{-1}, 1757(s) cm^{-1} and 1732(s) cm^{-1}.[42,43] The increase in the $Mo(CO)_6$ peak intensity suggests a situation where the metalloester $[Mo(CO)_5(COOCH_3)]^-$ is protonated by methanol to eliminate methyl formate and form the reactive $Mo(CO)_5$ and CH_3O^-. $Mo(CO)_5$ then reacts with CO to regenerate $Mo(CO)_6$ (**Scheme 2.4**).

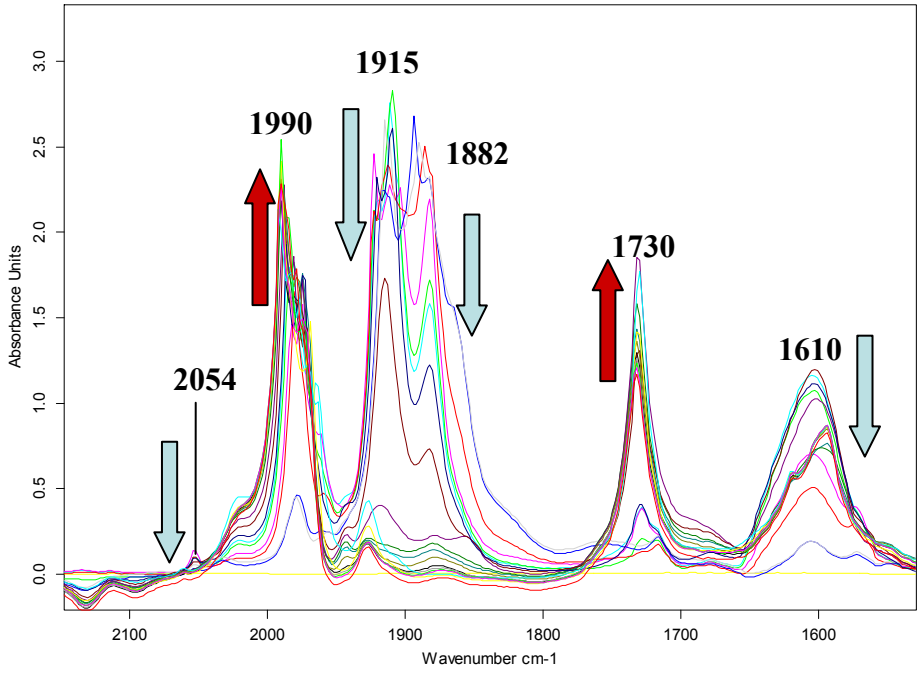

Figure 2.6: **HP-IR spectra for the reaction of $Mo(CO)_6$ with $KOCH_3$ (1:5) under CO pressure, temperature ranges from 13 ^{o}C-100 ^{o}C.**

2.2.2 *In situ* studies on the reaction of $Mo(CO)_6$ and $KOCH_3$ under H_2 pressure

The reaction of $Mo(CO)_6$ and $KOCH_3$ under H_2 pressure was performed to investigate the role of H_2 in the formation of methyl formate during the reaction. The reaction was carried out under 5 bar H_2, starting from 16 ^oC to 100 ^oC. $Mo(CO)_6$ rapidly reacted with $KOCH_3$ to produce $[Mo(CO)_5(COOCH_3)]^-$ which was characterized by CO bond stretching/vibrating peaks at 2054(w) cm^{-1}, 1914(s) cm^{-1}, 1881(m) cm^{-1} and a peak at 1570 (vw) cm^{-1} (**Figure 2.7**). As the reaction proceeded, the peaks at 1732(sh) cm^{-1} and 1680(sh) cm^{-1} increased. The peak at 1732 cm^{-1} could be assigned to carbonyl of methyl formate and the peak at 1680 cm^{-1} was assigned to the carbonyl of metal coordinated methyl ester (Mo-$COOCH_3$) group. The peaks characteristic of molybdenum pentacarbonyl (2054 cm^{-1}, 1914 cm^{-1} and 1881 cm^{-1}) decreased as the peaks for the carbonyl of methyl formate and metalloester (Mo-$COOCH_3$) grew. After 10 minutes a peak at 1600 cm^{-1} began to grow in conjunction with the peaks at 1732 cm^{-1} and 1680 cm^{-1} (**Figure 2.7**). This could indicate the possible formation of a *bis*(methoxycarbonyl) complex due to excess $KOCH_3$ in the system (eqn. 8).[44]

$$Mo(CO)_6 + 5\,CH_3OK \rightleftharpoons [Mo(CO)_5(COOCH_3)]^- \xrightarrow{CH_3O^-} [Mo(CO)_4(COOCH_3)_2]^{2-} \xrightarrow{H_2} \mu\text{-}HMo_2(CO)_{10}^- + HCOOCH_3 + \text{other products} \quad (8)$$

The peaks at 2054 cm^{-1}, 1914 cm^{-1} and 1881 cm^{-1} decreased very rapidly as the reaction proceeded to generate a new Mo carbonyl species with peaks at 2041(w) cm^{-1}, 1943 (vs) cm^{-1}, 1881(m) cm^{-1} (**Figure 2.7**), assigned to $[\mu\text{-}HMo_2(CO)_{10}]^-$. The mono hydride species ($HMo(CO)_5^-$) was observed as a shoulder in **Figure 2.7** but in **Figure 2.8** the individual peak for this species can be observed clearly.[45] It is important to note that the $Mo(CO)_6$ peak at 1978 cm^{-1} started to decrease and disappeared completely as the peak for the new species, $[\mu\text{-}HMo_2(CO)_{10}]^-$, started growing. The species could possibly be the stable bridged hydride $[\mu\text{-}HMo_2(CO)_{10}]^-$ which probably can form through a reaction of the unstable $HMo(CO)_5^-$ with $Mo(CO)_6$ (eqn. 9).[45-48]

$$HMo(CO)_5^- + Mo(CO)_6 \longrightarrow \mu\text{-}HMo_2(CO)_{10}^- + CO \quad (9)$$

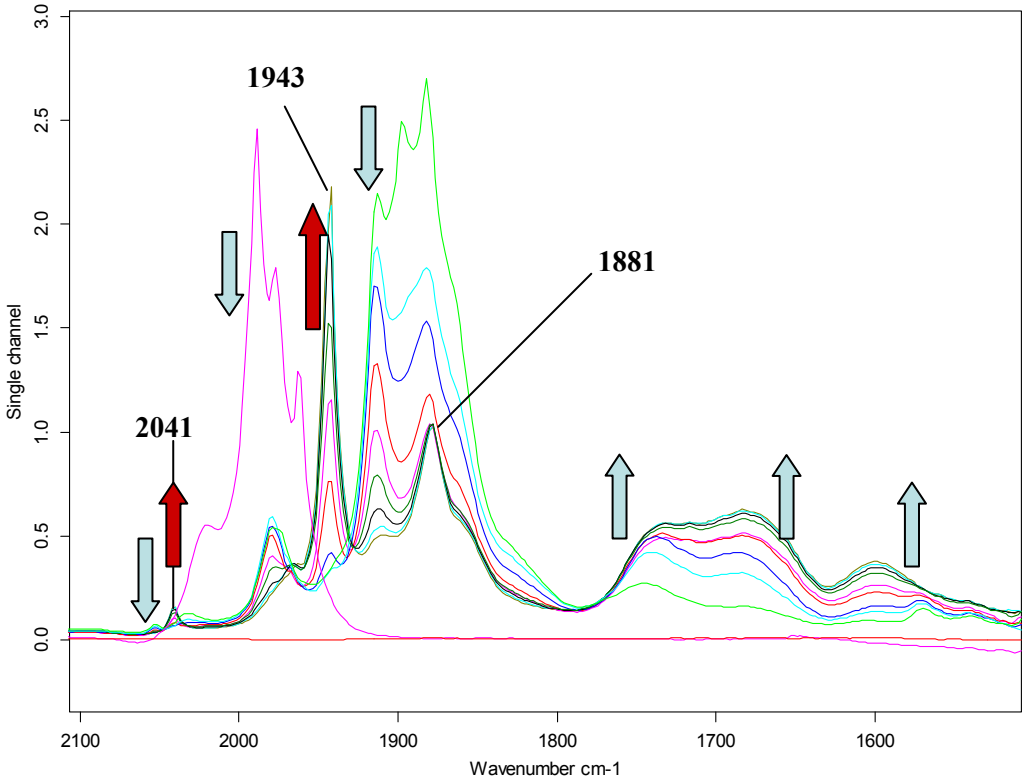

Figure 2.7: **Room temperature *in situ* HP-IR spectra for the reaction of $Mo(CO)_6$ with $KOCH_3$ (1:5) under H_2 pressure, temperature ranges from 16 ^oC-100 ^oC.**

The concentration of the first species, $[Mo(CO)_5(COOCH_3)]^-$, with carbonyl peaks at 2054 cm^{-1}, 1914 cm^{-1} and 1881 cm^{-1} decreased under H_2 pressure, until it reached an equilibrium state with the bridged hydride $[\mu\text{-}HMo_2(CO)_{10}]^-$ (the peak at 1881 cm^{-1} represented the bridged hydride peak). Upon heating, the bridged hydride is further converted to another Mo carbonyl species which has a single peak at 1860 cm^{-1} (**Figure 2.8**).

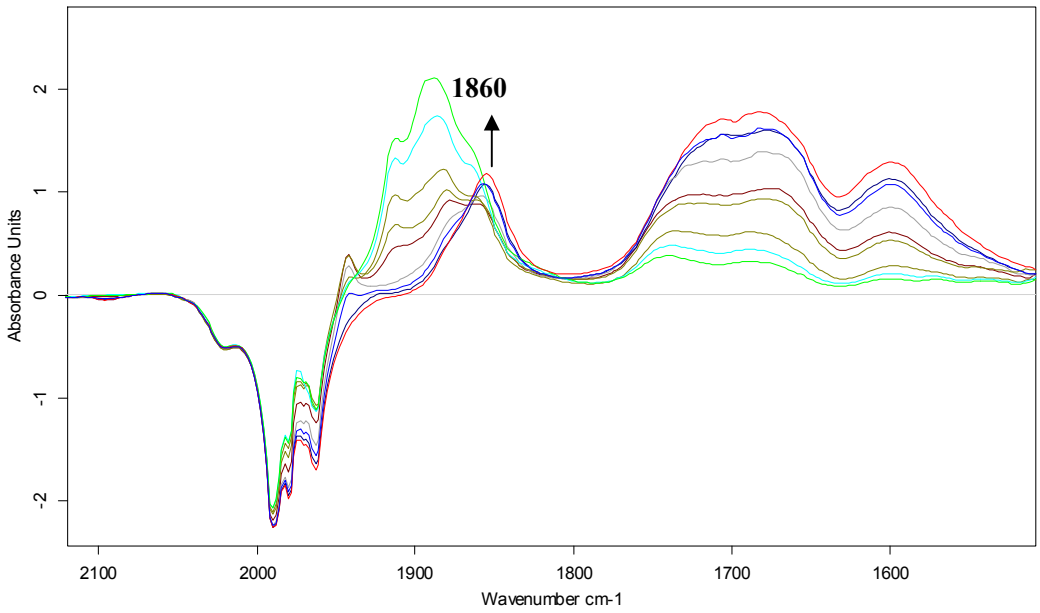

Figure 2.8: **HP-IR Spectra showing the peak representing the mono hydride species ($HMo(CO)_5^-$), temperature is 100 ^oC. Peaks pointing down show the disappearing species.**

2.2.3 *In situ* studies on the reaction of $Mo(CO)_6$ and $KOCH_3$ under syngas (1:1) pressure

The formation of methyl formate from the reaction of $Mo(CO)_6$ and $KOCH_3$ was carried out under syngas (1:1) pressure to investigate which species would be formed predominantly and determine whether it formed as a result of the CO or H_2. The first carbonyl species observed was $[Mo(CO)_5(COOCH_3)]^-$, characterized by CO bond stretching/vibrating peaks at 2053(w) cm^{-1}, 1914(s) cm^{-1}, 1881(m) cm^{-1} and 1600(m, br)) cm^{-1}. As the reaction progressed, the peak for the carbonyl of methyl formate at 1729(s) cm^{-1} began to grow, as did peaks at 2041(vw) cm^{-1} and 1943(sh) cm^{-1} characteristic of the bridged hydride species ($[\mu\text{-}HMo_2(CO)_{10}]^-$). A decreasing peak at 1675 cm^{-1} was also observed as the reaction progressed (**Figure 2.9**) as well as the peaks at 2041 cm^{-1} and 1943 cm^{-1} characteristic of the bridged hydride species ($[\mu\text{-}HMo_2(CO)_{10}]^-$).

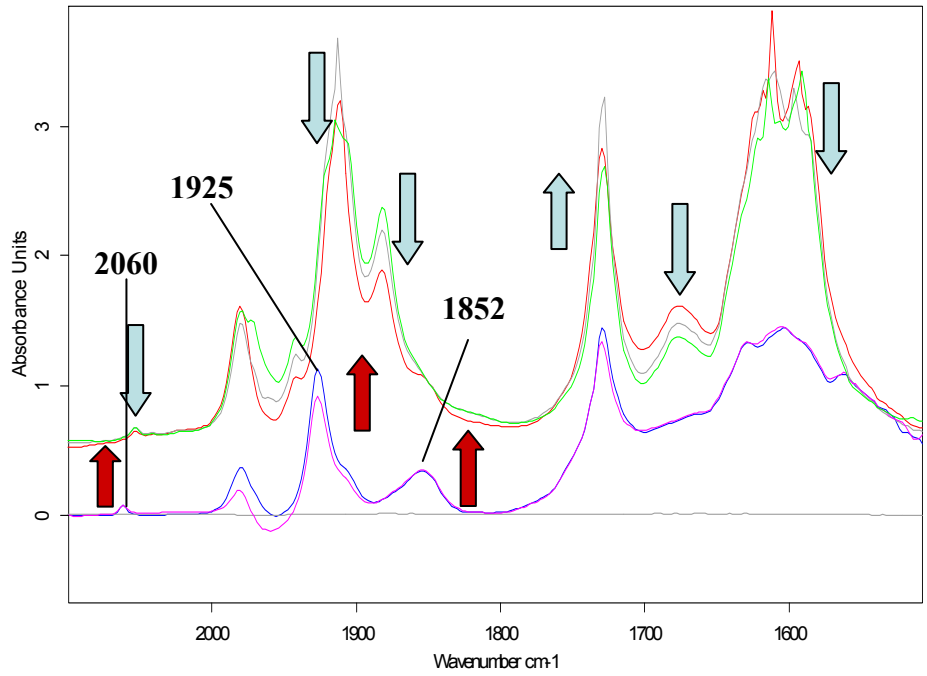

Figure 2.9: **HP-IR spectra for the reaction of $Mo(CO)_6$ with $KOCH_3$ (1:5) under syngas pressure. The arrows pointing up show growing peaks temperature ranges from 16 ^oC-100 ^oC.**

As heating began, the peaks characteristic of the $[Mo(CO)_5(COOCH_3)^-]$ at 2054 cm^{-1}, 1914 cm^{-1}, 1881 cm^{-1} and 1600 cm^{-1} decreased, while the new species $[Mo(CO)_5OCH_3^-]$ with peaks at 2060 (w) cm^{-1}, 1925 (s) cm^{-1}, 1852 (m) cm^{-1}, 1620 (sh) cm^{-1} and 1593 (m) cm^{-1} grew. The species is probably formed through a competitive reaction of the $Mo(CO)_5$ intermediate (**Scheme 2.4**) with CH_3O^- and CO in which case the reaction (eqn.10) dominates under syngas atmosphere. This dominance of equation 10 under syngas might be associated with the presence of hydrogen which inhibits the step involving the reaction of $Mo(CO)_5$ with CO, thus allowing a competitive reaction of $Mo(CO)_5$ with CH_3O^-.

$$Mo(CO)_6 + CH_3O^- \underset{\Delta}{\overset{CO}{\rightleftharpoons}} Mo(CO)_5(COOCH_3)^- + CH_3OH \xrightarrow{-HCOOCH_3} Mo(CO)_5 + CH_3O^- \xrightarrow{\Delta} Mo(CO)_5OCH_3^- \qquad (10)$$

The species was assigned based on the comparison of the peak shifts of the $[PPN][W(CO)_5O_2CCF_3]$ and $[PPN][Mo(CO)_5O_2CCF_3]$ complexes, discussed below. The peak

difference for the E band between [PPN][$W(CO)_5O_2CCF_3$] and [PPN][$Mo(CO)_5O_2CCF_3$] is 23 cm^{-1}.[49-51] The difference between the E band of [$W(CO)_5OCH_3^-$] and the compound postulated to be [$Mo(CO)_5OCH_3^-$] is 24 cm^{-1}. The final species under syngas pressure is similar to the species observed for the reaction under CO pressure, which might imply that the dominating mechanism under syngas is the CO mechanism.

2.2.4 *In situ* studies of the reaction of $Mo(CO)_6$ and $KOCH_3$ under N_2 pressure

The reaction of $Mo(CO)_6$ and $KOCH_3$ was studied under N_2 to investigate the effect of methanol from $KOCH_3$ in the formation of methyl formate. As in the previous experiments, $Mo(CO)_6$ rapidly reacted with $KOCH_3$ methanolic solution under N_2 to form the metalloester, [$Mo(CO)_5(COOCH_3)$]$^-$ (CO bond stretching/vibrating peaks at 2054(vw) cm^{-1}, 1915(s) cm^{-1}, 1881(s) cm^{-1} and a shoulder at 1680(sh) cm^{-1}) (**Figure 2.10**).

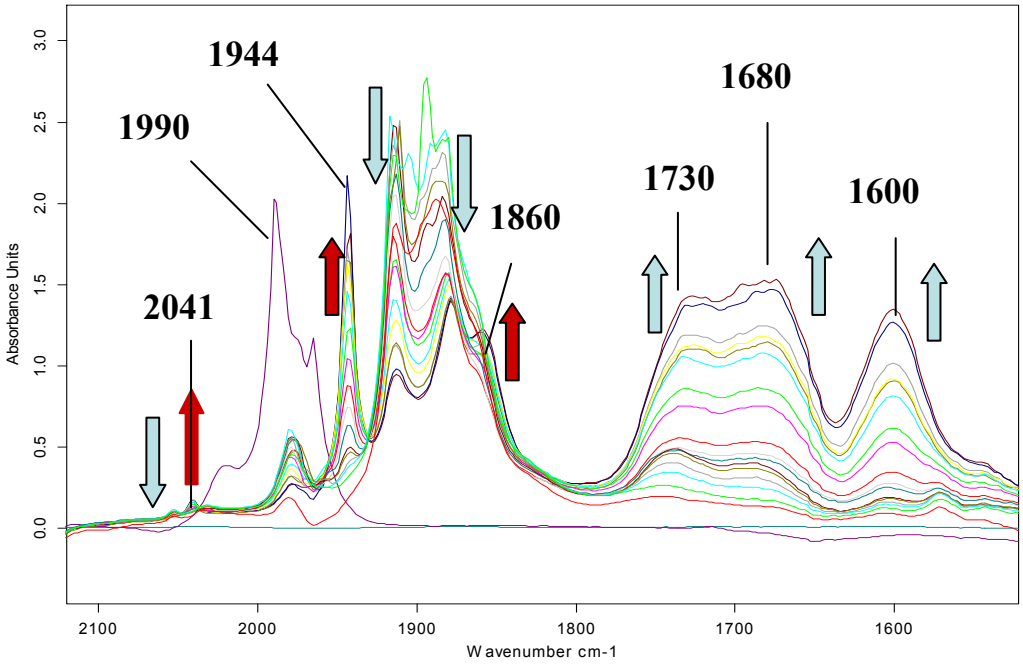

Figure 2.10: HP-IR spectra for the reaction of $Mo(CO)_6$ with $KOCH_3$ (1:5) under N_2 pressure. The arrows pointing up show growing peaks temperature ranges from 16 ^oC-100 ^oC.

As the reaction progressed, a peak at 1730 cm^{-1} grew together with the appearance of peaks at 1680 cm^{-1} and 1600 cm^{-1} characteristic of a *bis*(methoxycarbonyl) complex due to excess $KOCH_3$. At 80 ^oC, a bridged hydride species characterized by peaks at 2041(w) cm^{-1}, 1943(vs) cm^{-1} and an overlapping peak at 1881(m) cm^{-1} grew with the decrease in the metalloester species with peaks at 2054 cm^{-1}, 1915 cm^{-1} and 1881 cm^{-1}.

Similar to the experiment under H_2 pressure, the peak at 1881 cm^{-1}, assigned to the bridged hydride ($[\mu\text{-}HMo_2(CO)_{10}]^-$), did not change further. This suggests that protonation of the metalloester $[Mo(CO)_5(COOCH_3)]^-$ does occur without hydrogen being present and the effect of increasing the temperature shows that the system eliminates methyl formate at lower temperatures than 80 ^oC. This is in contrast to the $W(CO)_6/KOCH_3$ system, where Darensbourg *et al.*[23] concluded that methyl formate was eliminated at temperatures of 100 ^oC and above.

The peaks assigned to the bridged hydride ($[\mu\text{-}HMo_2(CO)_{10}]^-$) also decreased during the heating process to form a mono hydride $[HMo(CO)_5^-]$ compound with a peak at 1860 cm^{-1} (**Figure 2.8 & Figure 2.10**).

If no methanol is added to the system, $Mo(CO)_6/CH_3ONa/N_2$, it is important to note that there is no formation of the metalloester, molybdenum bridged hydride ($[\mu\text{-}HMo_2(CO)_{10}]^-$) and mono hydride species $[HMo(CO)_5^-]$, and the only peaks seen are shown in **Figure 2.11** below. However, upon addition of 1.25 ml of MeOH to this system, $Mo(CO)_6/CH_3ONa/N_2$, the above hydrides and the metalloester are formed, as is the new compound with peaks at 2061(w) cm^{-1}, 1943(s) cm^{-1}, 1881(m) cm^{-1}, 1714(s) cm^{-1} and 1640(s, br) cm^{-1} (**Figure 2.12**), which supports the importance of the solvent effect in these reactions.

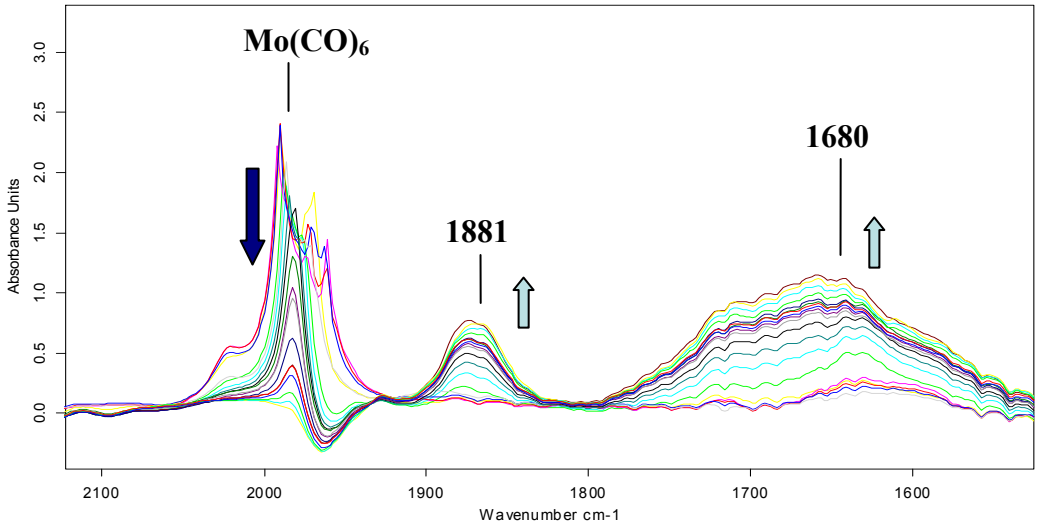

Figure 2.11: **HP-IR spectra for the reaction of $Mo(CO)_6$ with CH_3ONa (1:5) under N_2 pressure in THF only, temperature ranges from 16 ^oC-100 ^oC. The arrows pointing up show growing peaks.**

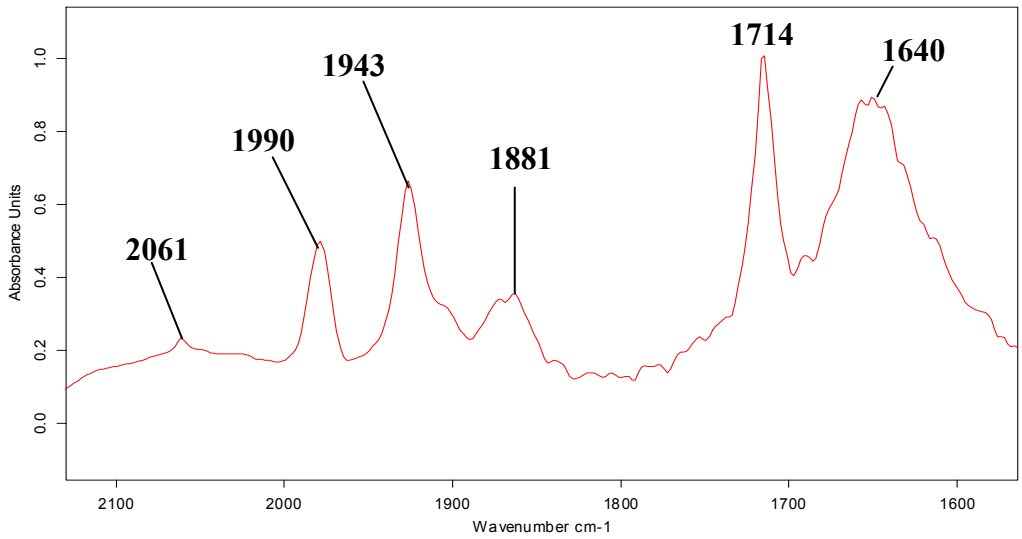

Figure 2.12: **HP-IR spectra for the reaction of $Mo(CO)_6$ with CH_3ONa (1:5) under N_2 pressure in THF after addition of 1.25 ml MeOH, temperature is 16 ^oC.**

2.3 Summary

Addition of $Mo(CO)_6$ to the system of methoxide carbonylation of methanol under CO atmosphere increased the amount of methyl formate produced. The effect of solvent is very important in this reaction. Excess methanol increases the formation of methoxide ion, while reactions in THF and triglyme produce lower amounts of methyl formate. This is probably due to the inability of THF and triglyme to protonate the metalloester [$(CO)_5Mo(COOCH_3)^-$]. The same solvent effect was observed under H_2, syngas and N_2.

Addition of $Mo(CO)_6$ to the methoxide carbonylation of methanol under syngas produced more methyl formate in methanol solution. This is probably due to the presence of hydrogen in syngas which assists in the hydrogenation of the metalloester and the protonation of the metalloester by methanol. A stoichiometric increase in the $Mo(CO)_6$ ratio under syngas (1:1) increased the amount of methyl formate produced, with a 1:2 ratio of $Mo(CO)_6/KOCH_3$ producing more methyl fomate compared to the other ratios. This shows that $Mo(CO)_6$ does not react with water in the water gas shift argument as there is no linear response of methyl formate to the increase in $Mo(CO)_6$ concentration. It was expected that an increase in $Mo(CO)_6$ will result in a linear increase in methyl formate produced. Longer chain (C2-C5) alcohols were also produced in triglyme. Addition of hydrogen to the reaction of $Mo(CO)_6$ & $KOCH_3$ produced comparable amounts of methyl formate as the reaction performed under CO.

HP-IR studies of $Mo(CO)_6$ & $KOCH_3$ (1:5) performed under CO produced the metalloester, which diminished to eliminate methyl formate and regenerate $Mo(CO)_6$ (**Scheme 2.4**). If the same reaction is performed under H_2, a metalloester is formed which then diminishes to form the bridged hydride μ-$HMo_2(CO)_{10}^-$. Addition of excess CH_3O^- under H_2 results in the formation of a *bis*(methoxycarbonyl) complex characterized by ester peaks at 1680 $cm^{-1}$and 1600 cm^{-1}. A peak characteristic of a mono hydride ($HMo(CO)_5^-$) was only observed at higher temperatures (100 ^oC).

HP-IR studies of $Mo(CO)_6/KOCH_3$ (1:5) under syngas showed the formation of a metalloester and a bridged hydride (μ-$HMo_2(CO)_{10}^-$) which disappeared after few minutes of reaction to form a methoxide complex ($Mo(CO)_5OCH_3^-$) as the final organometallic product in the reaction. It is interesting to note that a *bis*(methoxycarbonyl) complex was not observed under CO, which implies that some excess CH_3O^- catalyzes the carbonylation reaction to form methyl formate.

There were no other organic products observed for the reactions performed under syngas atmosphere in THF & MeOH mixture.

2.4 References

[1] (a) I. Y. Guzman-Jiminez, J. W. van Hal, K. H Whitmire, Organometallics, 22 (2003) 1914; (b) D. J. Forster, J. Am. Chem. Soc., 98 (1976) 846

[2] G. Jenner, Appl. Catal. A: General, 121 (1995) 25

[3] W. Bertleff, M. Roeper, X. Sava, Carbonylation, Wiley-VCH Verlag GmbH & Co, (2007) pp. 1-26

[4] G. Bud, H. U. Hog, J. Mol. Catal. A: Chemical, 95 (1995) 45

[5] M. Fontaine, Y. Castanet, A. Mortreux, F. Petit, J. Catal., 167 (1997) 324

[6] G. Jenner, Tetrahedron lett., 37 (1990) 3887

[7] D. J. Darensbourg, R. L. Gray, C. Ovalles, Mol. J. Catal., 41 (1987) 329

[8] E. Gerard, H. Gotz, S. Pellegrini, Y. Castnet, A. Morteux, Appl. Catal. A: General, 170 (1998) 297

[9] M. Mlekuz, F. Joo, H. Alper, Organometallics, 6 (1987) 1591

[10] G. Lavigne, N. Lugan, P. Kalck, J. M. Soulie, O. Leroge, J. Y. Saillard, J. F. Halet, J. Am. Chem. Soc., 114 (1992) 10669

[11] In *Chem Abstr.*; BASF: Britain, 21 (1925) 2477

[12] S. P. Tonner, D. L. Trim, M. S. Wainwright, N. W. Cant, J. Mol. Catal., 18 (1983) 215

[13] D. Mahajan, US Patent 0158270 A1 (2003)

[14] D. Mahajan, US Patent 6921733 (2005)

[15] P. G. Jessop, Y. Hsiao, T. Ikariya, R. Noyori, J. Am. Chem. Soc., 118 (1996) 344

[16] P. G. Jessop, F. Joo, C. Tai, Coord. Chem. Rev., 245 (2004) 2425

[17] D. J. Darensbourg, C. Ovalles, M. Pala, J. Am. Chem. Soc., 105 (1983) 5937

[18] D. J. Darensbourg,; C. Ovalles, J. Am, Chem. Soc., 106 (1984) 3750

[19] D. J. Darensbourg, A. Rokicki, M. Y. Darensbourg, J. Am. Chem. Soc., 103 (1981) 3223

[20] D. J. Darensbourg, A. Rokicki, Organometallics, 1 (1982) 1685

[21] R. J. Trautman, D. C. Gross, P. C. Ford, J. Am. Chem. Soc., 107 (1985) 2355

[22] P. C. Ford, Acc. Chem. Res., 14 (1981) 31

[23] D. J. Darensbourg, R. L. Gray, C. Ovalles, M. Pala, J. Mol. Catal., 29 (1985) 285

[24] M. Marchiona, L. Basini, A. Argno, M. Lami, F. Ancillotti, J. Mol. Catal., 75 (1992) 147

[25] A. Bates, M. T. Muraoka, R.Trautman, J. Inorg. Chem., 32 (1993) 2651

[26] H. E. Bryndza, Organometallics, 4 (1985) 1686

[27] R. Bertani, G. Cavinato, L. Toniolo, G. Vasapollo, J. Mol. Catal., 84 (1993**)** 165

[28] D. J. Darensbourg, M. Y.Darensbourg, Inorg. Chem., 9 (1970**)** 1691

[29] M. Y. Darensbourg, H. L. Condor, D. J. Darensbourg, C. Hasday, J. Am. Chem. Soc., 95 (1973) 5919

[30] D. A. Nguyen, T. Sridhar, Ind. Eng. Chem. Res., 35 (1996**)** 3044

[31] D. Mahajan, Top. Catal., 32 (2005) 209

[32] R. S. Sapienza, W. A. Sleiger, T. E. O'Hare, D. Mahajan, US Patent 4614749 (**1**986), US Patent 4619946 (1986), US Patent 4623634 (1986), US Patent 4935395 (1990), US Patent 4992480 (1991)

[33] M. Marchionna, M. Lami, F. Ancillotti, R. Ricci, Ital. Patent 20028/A (1988)

[34] S. Ohyama, E. S. Lee, K. Aika, J. Mol. Catal. A: Chemical, 138 (1999**)** 305

[35] D. C. Gross, P. C. Ford, J. Am. Chem. Soc., 107 (1985) 585

[36] M. Xiang, D. Li, H. Xiao, J. Zhang, W. Li, B. Zhong, Y. Sun, Catal. Today, 131 (2008) 489

[37] X. Li, L. Feng, Z. Liu, B. Zhong, D. B. Dadyburjor, E. L. Kugler, Ind. Eng. Chem. Res., 37 (1998) 3853

[38] L. Gang, Z. Chengfang, C. Yanqing, Z. Zhibin, N. Yianhui, C. Linjun, Y. Fong, Appl. Catal. A., 150 (1997) 243

[39] M. Xiang, D. Li, W. Li, B. Zhong, Y. Sun, Catal. Commun., 8 (2007) 88

[40] L. Damoense, M. Datt, M. Green, C. Steenkamp, Coord. Chem. Rev., 248 (2004) 2393

[41] I. T. Horvath, J. M. Millar, Chem. Rev., 91 (1991) 1339

[42] D. J. Darensbourg, K. K. Klausmeyer, J. D. Draper, J. A. Chojnacki, J. H. Reibenspies Inorg. Chim. Acta., 270 (1998) 405

[43] R. A. Andrian, M. Y. Yaklin, K. K. Klausemeyer, Organometallics, 23 (2004) 1352

[44] D. C. Gross, P. C. Ford, J. Am. Chem. Soc., 107 (1985) 585

[45] M. Y. Darensbourg, S. Slater, J. Am. Chem. Soc., 103 (1981) 5914

[46] R. G. Hayter, J. Am. Chem. Soc., 88 (1966) 4376

[47] M. Y. Darensbourg, J. C. Deaton, Inorg. Chem., 20 (1981) 1644

[48] L. Marko, Z. Nagy-Magos, J. Organomet. Chem., 285(1985) 193

[49] F. A. Cotton, D. J. Darensbourg, B. W. S. Kolthammer, J. Am. Chem. Soc., 103 (1981), 398

[50] F. A. Cotton, D. J. Darensbourg, B. W. S. Kolthammer, R. Kudaroski, Inorg. Chem., 21 (1982), 1656

[51] A. P. Abbott, A. V. Malkov, N. Zimmermann, J. B. Raynor, G. Ahmed, J. Steele, P. Kocǒvský, Organometallics, 16 (1997) 3690

3. CHAPTER 3

Nucleophilic activation of coordinated carbon monoxide. Reactions of $Mo(CO)_6$, $Ph_3PMo(CO)_5$ and $[CpMo(CO)_3(PR_3)]^+$ with alkoxides.

3.1 Introduction

Reactions of nucleophiles with metal carbonyls have been a subject of interest for the past two or three decades.[1] Emphasis has been with nucleophiles such as hydrides and hydroxides, since they produce intermediates which were thought to be generated under catalytic processes related to carbon monoxide conversion.[2-4] The intermediacy of transition metal formyl complexes, as the initial step in the catalytic reduction of CO by H_2, has been considered by many researchers as an alternative in understanding the homogeneous catalytic carbon chain length propagation from carbon monoxide to organic products.[2] In search of a new homogeneous catalyst for CO reduction, attention has been focused on the synthesis of metal formyl complexes *via* reduction of metal coordinated CO by hydride ions at room temperature (eqn.1).[5,6]

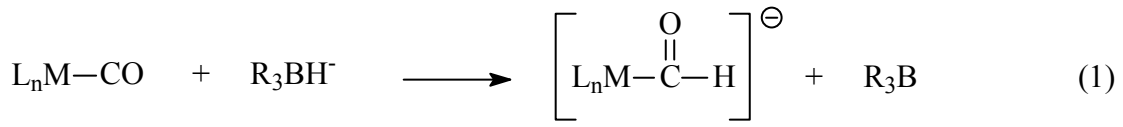

$L_nM{-}CO + R_3BH^- \longrightarrow [L_nM{-}C(=O){-}H]^{\ominus} + R_3B$ (1)

L= CO, PR_3

The hydroxide (OH^-) ion had been utilized as a cocatalyst in the process called the water gas shift reaction (WGSR, eqn. 2).

$CO + H_2O \rightleftharpoons CO_2 + H_2$ (2)

The importance of the WGSR had been sparked by the necessity of producing gaseous and liquid hydrocarbon fuels from non-petroleum sources such as coal.[7] This process involves the reaction of carbon monoxide with water catalyzed by metal carbonyls, such as ruthenium, iron, molybdenum and tungsten, to produce carbon dioxide and hydrogen in alkaline solution (eqn. 2).

An intensive study by the Ford group has revealed that a key step in the mechanism of the WGSR is a nucleophilic attack of the hydroxide ion on the metal coordinated carbon monoxide to form hydroxycarbonyl adducts, eqn. 3.[1,7]

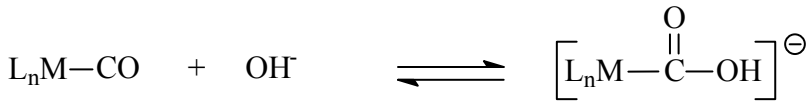

(3)

L= CO, PR_3

There are, however, many reactions involving nucleophilic activation of coordinated carbon monoxide. The common reactions are the syntheses of metal carbene complexes using metal carbonyls and organolithium reagents (eqn. 4) and/or Grignard reagents.[8-10]

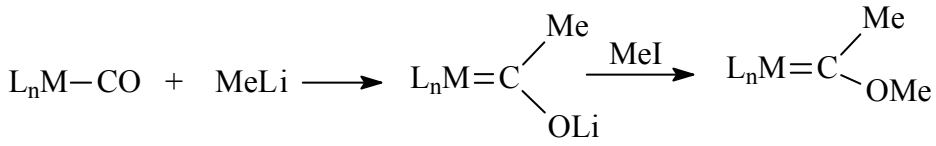

(4)

M= W, L = CO

Hydroxide and methoxide nucleophiles have also been employed as cocatalysts in many metal carbonyl catalyzed reactions, such as the reductive carbonylation of nitroaromatics,[11] the reduction of CO, base catalyzed carbonylation of organic halides to esters and the hydroformylation of olefins by CO/H_2O mixtures.[12,13] The methoxide is also known as the catalyst in the carbonylation of methanol to methyl formate.[14] The instability of the hydroxycarbonyl adducts formed in equation 3, lead to the development of the fairly stable methoxycarbonyl adducts (eqn. 5), so as to understand their chemistry.[1,15-17]

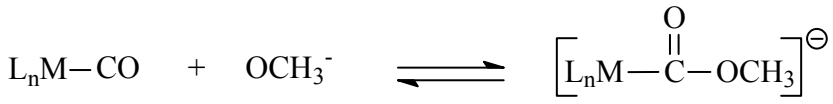

(5)

L= CO, $P(OCH_3)_3$

Ford *et al.*[15] performed kinetic studies on the reaction of group 8 metal carbonyls with the methoxide ion and the reactions of their methoxycarbonyl adducts with hydrogen and phosphite

($P(OR)_3$) ligands. Results showed that the rate of the $NaOCH_3$ reaction with metal carbonyl complexes is solvent dependent with a second order rate constant in pure methanol as well as with (90/10) THF/CH_3OH mixtures.[16]

The mononuclear metal carbonyls reacted faster than the trinuclear complexes, but under comparable conditions, the order of mononuclear metal carbonyl reactivity with $NaOCH_3$ is $Os(CO)_5 > Ru(CO)_5 > Fe(CO)_5$.[16,18] The reactivity of trinuclear metal carbonyls with $NaOCH_3$ in methanol follows the order, $Fe_3(CO)_{12} > Ru_3(CO)_{12} > Os_3(CO)_{12}$.[12,18] However, replacement of one CO by $P(OCH_3)_3$ in the mononuclear metal carbonyls led to the deactivation of the remaining carbonyls towards nucleophilic attack by $NaOCH_3$.

The reactivity of the methoxycarbonyl complexes of group 8 metals was demonstrated with the $Ru_3(CO)_{11}(COOCH_3)^-$ adduct. The lability of $Ru_3(CO)_{11}(COOCH_3)^-$ allowed the substitution of one CO with $P(OCH_3)_3$. This ligand substitution is associated with a negative charge on the complex which tends to labilize the carbonyl groups, in contrast to $Ru(CO)_4P(OCH_3)_3$, where activation of the terminal carbonyls was reduced due to electronic effects. The lability of $Ru_3(CO)_{11}(COOCH_3)^-$ allowed the study of the hydrogenation of the $Ru_3(CO)_{11}(COOCH_3)^-$ complex to form methyl formate and $HRu_3(CO)_{11}^-$ (eqn. 6).[19]

$$Ru_3(CO)_{11}(COOCH_3)^- + H_2 \longrightarrow HRu_3(CO)_{11}^- + HCOOCH_3 \qquad (6)$$

Bates *et al*.[17] performed kinetic studies on group 6 metal carbonyls using $W(CO)_6$ as the model with methoxide, and found that the reactivity is two orders of magnitude lower than that of group 8 metal carbonyls. This was associated with the CO force constant values of $W(CO)_6$ compared to the group 8 metal carbonyls. Group 8 metal carbonyls appeared to have larger force constants than $W(CO)_6$ (**Chapter 1**, **Table 1.2**) , which increased their reactivity towards nucleophiles.[20,21] Similar to the mononuclear substituted group 8 metal carbonyl, $Ru(CO)_4(P(OCH_3)_3$, substitution of one CO in $W(CO)_6$ with PPh_3 gave no evidence for the formation of a $[W(CO)_4(PPh_3)(COOCH_3)]^-$ species for the same reason. Unlike the trinuclear group 8 methoxycarbonyl intermediate, $[Ru_3(CO)_{11}(COOCH_3)]^-$; labilization of the tungsten methoxycarbonyl intermediate, $[W(CO)_5(COOCH_3)]^-$, was reported to be unsuccessful. The compound, $W(CO)_5(COOCH_3)^-$, is more unstable than group 8 methoxycarbonyls and it loses CO even under CO atmosphere to form the $W(CO)_5OCH_3^-$ complex.[17] The methoxycarbonyl

compound ($W(CO)_5(COOCH_3)^-$) is reported to react with water to give $W(CO)_6$ and the μ-$HW_2(CO)_{10}^-$ species. Based on the results from the HPIR studies (Chapter 2), the aim of the work discussed in this chapter was to synthesize different types of metalloesters (alkoxycarbonyl complexes) by nucleophilic reactions of alkoxides with $Mo(CO)_6$ under CO and N_2, in order to understand the the nature of the intermediates formed, as observed under HPIR in Chapter 2.

3.2 Results and Discussions

Schlenk tube reaction of $Mo(CO)_6$ with Methoxide Ion. Addition of $[K^+][OCH_3^-]$ in methanol to $Mo(CO)_6$ in pure THF results in the formation of a yellow solution and a cream white precipitate. The precipitate was tentatively assigned as a methoxycarbonyl derivative, $[K^+][Mo(CO)_5(COOCH_3)^-]$. The compound was analysed by IR and NMR spectroscopy (**Table 3.1**). These instruments (IR and especially ^{13}C NMR) have been reported to be the most used and successful diagnostic tools in characterizing the formation of various alkoxycarbonyl (metallesters) complexes.[1] The methoxycarbonyl derivative was found to be thermally stable, but moisture sensitive, and insoluble in all tested organic solvents but dissolving completely in water. The chemical properties of this precipitate suggest the formation of an ionic compound with a tight interaction with the K^+ ion. There are two possible ways in which K^+ ion can interact with the methoxycarbonyl anionic group ($-COOCH_3$). The first possibility involves the location of the negative charge on the metal center, allowing the direct sigma bonding of an ester group to the metal center (**A, Scheme 3.1**). The second possibility involves the delocalization of the electrons to the oxygen of the ester carbonyl to form a carbene type complex (**B, Scheme 3.1**). However, the NMR results support the formation of a methoxycarbonyl complex **A,** as no carbene peak was observed in the ^{13}C NMR spectra (**Table 3.1**).

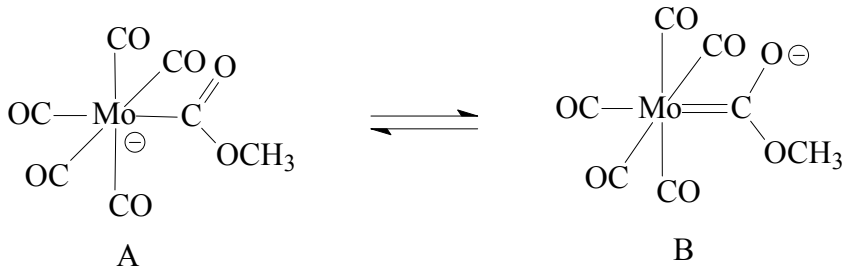

Scheme 3.1: Possible resonance structures of the molybdenum methoxycarbonyl adduct.

The insolubility of potassium methoxycarbonylatopentacarbonylmolybdate(0), $[K^+][Mo(CO)_5(COOCH_3)^-]$, in organic solvents prompted the use of other longer chain alkyl groups and bigger counter ions in the reaction with the intention of increasing the solubility of this species in organic solvents. Room temperature metathesis of $[K^+][Mo(CO)_5(COOCH_3)^-]$ with bulky counter ions, such as Et_4NCl, *n*-Bu_4NI and PPNCl was unsuccessful, probably due to a tight interaction of the K^+ ion to the metalloester (**A, Scheme 3.1**) and the insolubility of $[K^+][Mo(CO)_5(COOCH_3)^-]$ in organic solvents.

Alkyl groups were chosen with the aim of not decreasing the nucleophilicity of the alkoxide.[22] For example, a tertiary alkoxide such a *t*-butoxide is known to be more nucleophilic (basic) than methoxide. The alkoxides studied, besides potassium methoxide, were potassium *t*-butoxide, potassium *t*-amyl alkoxide and sodium triphenylmethoxide, based on increasing hydrophobicity of the alkyl groups (**Table 3.1**). The compounds were also characterized by IR and NMR spectroscopy. The formation of the metal coordinated ester (Mo-$COOCH_3$) group was confirmed by peaks at 178-184 ppm in the ^{13}C NMR spectra. Terminal carbonyls were not observed in the ^{13}C NMR spectra. Peaks for terminal carbonyls were, however, observed in the IR spectra. The formation of the metal coordinated ester (Mo-$COOCH_3$) was confirmed by peaks at 1735-1480 cm^{-1} depending on the nature of the nucleophile, L_nM, and the formal charge on the complex.[1]

However, changing the alkyl groups did not change the solubility/behavior of the complexes formed, with the exception of the triphenylmethoxycarbonylpentacarbonyl molybdate(0) complex, which did not dissolve even in water. Attempts to grow crystals of these potassium metalloesters in THF and H_2O resulted in the formation of molybdenum oxalato clusters, **Figure 3.1**.

The oxalato cluster crystallizes in a monoclinic form with a space group of P2(1)/c. The crystal shows networked oxo clusters with an octahedral molybdenum atom surrounded by six oxygen atoms. Some of the oxygen atoms surrounding molybdenum are linked to an oxalate type carbon structure (C1-C2 in Fig. 13). The structure is symmetric with four molybdenum atoms. The structure further shows ionic bonding of the potassium counter ion (K) from $[K^+][Mo(CO)_5(COO$*t*Amyl$)]$ with eight oxygen atoms. The C1-C2 bond distance is 1.557(3) Å and is within the range of known molybdenum oxalate clusters (**Table 3.2**).[23] The O-C distances are 1.226 (3)-1.271(2) Å and are within the range of the known Mo

oxalate complexes.[23] The Mo-O bond distances are within the range of 1.717(2)-2.208(2) Å, and the K-O bond distances are within the range of 2.739(2)-3.221(2) Å.

Table 1.1: IR and ^{1}H & ^{13}C NMR (D_2O) data for the Mo metalloester complexes

Compound	IR (KBr)/cm^{-1} $\nu CO_{terminal}$	ν(COOR[a]) group	^{1}H NMR/ppm[b]	^{13}C NMR/ppm[b]
$K[Mo(CO)_5(COOCH_3)]$	2043,1956,1880	1655	3.16 (s,3H)	55 (CH_3) 178 (COOR)
$K[Mo(CO)_5(COOC(CH_3)_3]$	1987,1955,1885	1725	3.16 (s,9H)	56 (CH_3) 82 ($C(CH_3)_3$) 174 (COOR)
$K[Mo(CO)_5(COOC(CH_3)_2CH_2CH_3)]$	1986, 1941, 1885	1662	0.7 (t,3H), 1.0 (s,6H), 1.3 (q,2H)	4.9 (CH_3) 24 ($C(CH_3)_2$) 32 (CH_2) 64 ($C(CH_3)_2$ 184 (COOR)
$K[Mo(CO)_5(COOCPh_3)]$	1978,1953,1894	1600	-	-

a = R is $-CH_3$, $-C(CH_3)_3$, $-C(CH_3)_2CH_2CH_3$, b = NMR was performed in D_2O

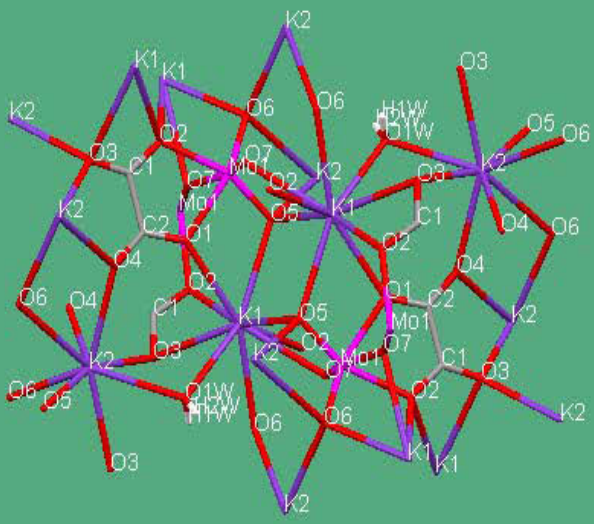

Figure 3.1: Crystal structure of the $C_8H_{12}K_8Mo_4O_{32}$ cluster.

$[PPN][OCH_3]$ was prepared by reacting *bis*(triphenylphosphine) iminium chloride (PPNCl) and potassium methoxide ($KOCH_3$) in methanol at room temperature. The reaction between $[PPN][OCH_3]$ and $Mo(CO)_6$ was monitored by IR spectroscopy (**Table 3.3**) in a mixture of THF and methanol. Addition of a THF solution of $Mo(CO)_6$ to a $[PPN][OCH_3]$ methanolic solution at room temperature resulted in the formation of a yellow solution, $[PPN][Mo(CO)_5(COOCH_3)]$, after 17 hours of stirring (eqn. 7). The solution was evaporated to dryness to give a dark yellow solid.

$$[PPN][OCH_3] + Mo(CO)_6 \xrightarrow[RT,\ 17\ hrs]{THF/MeOH} [PPN][Mo(CO)_5(COOCH_3)] \qquad (7)$$

The solubility was improved and the moisture sensitivity of the product reduced by using the bis(triphenylphosphine) ammonium counter ion (PPN). This product dissolved completely in methanol. IR (MeOH) bands for the terminal carbonyls of the product were observed at 2043(w) cm^{-1}, 1942(vs) $cm^{-1}$and 1879(m) cm^{-1}, respectively. The ester carbonyl group ($-CO_2CH_3$) was

observed as a broad band at 1607 cm^{-1}, which is shifted from the ester position of the free organic ester compounds, which appears at 1750-1730 cm^{-1}.

Table 3.2: Selected bond lengths for $C_8H_{12}K_8Mo_4O_{32}$ cluster

Bond		Length (Å)	Bond		Length (Å)
Mo1	O1	2.208(2)	O3	K2	2.743(2)
Mo1	O2	2.196(2	O3	K2	2.760(2)
Mo1	O6	1.717(2)	O3	K1	2.926(2)
Mo1	O5	1.730(2)	C1	C2	1.557(3)
Mo1	O7	2.119(2)	K2	O1W	2.930(3)
O1	C2	1.267(3)	K2	O6	3.221(2)
O1	K1	2.745(2)	K2	O5	2.759(2)
O2	C1	1.271(2)	K2	O4	3.015(2)
O2	K1	2.949(2)	K2	O3	2.743(2)
O6	K2	3.221(2)	O1W	H2W	0.85(5) 1
O6	K2	2.739(2)	O1W	H1W	0.80(5) 1
O6	K1	2.826(2)	O1W	K1	2.869(3)
O5	K1	2.928(2)	K1	O5	2.928(2)
O5	K2	2.759(2)	K1	O2	2.949(2)
O7	Mo1	1.781(2)	K1	O6	2.826(2)
O7	K1	2.805(2)	K1	O7	2.805(2)
O4	C2	1.229(3)	K1	O3	2.926(2))
O4	K2	3.015(2)	O4	K2	2.787(2)
O3	C1	1.226(3)			

The ν(C=O) value of the ester carbonyl at 1607 cm^{-1} is in the range obtained by Petz[24] and Garlaschelli *et al.*[25] for the metal coordinated $–CO_2CH_3$ group. This position (1607 cm^{-1}) is also not far from the range (1700-1610 cm^{-1}) obtained by Angelici for similar compounds, however that depends on the type of a nucleophile and the metal center.[1,26] The shift is linked to the metal back donation effect of the metal attached to an ester group. NMR analysis of the product supported the formation of the desired product. ^1H NMR spectrum recorded in deuterated methanol showed a singlet at 3.34 ppm for the methyl group of $–CO_2CH_3$. The aromatic rings for the PPN were observed as multiplets at 7.49-7.69 ppm (J_{H-H} = 8.26 Hz) respectively. The ^{13}C NMR spectrum showed the methyl carbon for $–CO_2CH_3$ at 49.9 ppm and the phenyl groups for PPN at 128-135 ppm, respectively. In the ^{13}C NMR analysis, the ester ($-COOCH_3$) carbonyl was observed at 170 ppm, while the terminal carbonyls were observed at 202 ppm and 210 ppm, respectively.

Addition of [*n*-Bu_4N][OCH_3] methanolic solution to a THF solution of $Mo(CO)_6$ at room temperature also resulted in the formation of a yellow solution, of [*n*-Bu_4N][$Mo(CO)_5(COOCH_3)$]. Evaporation under vacuum resulted in a dark yellow solid. The IR analysis (**Table 3.3**) of this compound was done in methanol as the compound is more soluble in polar solvents. The terminal carbonyls appeared at 2043(m) cm^{-1}, 1936(s) cm^{-1} and 1872 (m) cm^{-1}. The peak for an ester carbonyl group ($-CO_2CH_3$) appeared at 1604(m, br) cm^{-1}.[1] The three-band pattern of νCO bands is consistent with a C_{4v} symmetry and indicates that the methoxycarbonyl has occupied an axial site of an octahedral $Mo(CO)_5L$. The slight shift in the peak positions noticed between the PPN^+ and *n*-Bu_4N^+ salts shows the slight difference in the bonding of these counter ions with the anion; *n*-Bu_4N^+ showed a tighter interaction with the anion, $Mo(CO)_5(COOCH_3)^-$. This is probably because of the difference in the sizes of these counter ions. The shift in the position of the ester carbonyl group for *n*-Bu_4N^+ supports that *n*-Bu_4N^+ has a tighter interaction with the anion, as was proposed by Trautman *et al.*[16] A ^1H NMR experiment with [*n*-Bu_4N][$Mo(CO)_5(COOCH_3)$] was carried out in deuterated methanol. The peaks for the counter ion [*n*-Bu_4N]$^+$ appeared at 1.01 ppm (triplet, J_{H-H} = 7.35 Hz) for the methyl ($-CH_3$) group, 1.40 ppm (sextet, J_{H-H} = 7.40 Hz) for a methylene group ($-CH_2-$) group, 1.65 ppm (quintet, J_{H-H} = 5.34 Hz) for another methylene group and 3.24 ppm (triplet, J_{H-H} = 8.58 Hz) for the methylene group attached to nitrogen ($–CH_2N^+$), respectively. The peak at 3.24 ppm is shifted downfield due to the electron withdrawing effect of nitrogen. The methyl of the ester group ($-CO_2CH_3$) appeared as a singlet at 3.34 ppm. The ^{13}C NMR experiment supported the formation

of the proposed compound, [*n*-Bu_4N][$Mo(CO)_5(COOCH_3)$], with peaks for the counter ion [*n*-Bu_4N]$^+$ appearing at 14 ppm (CH_3-), 21 ppm (-CH_2-), 25 ppm (-CH_2-) and 59 ppm (-CH_2N), respectively. The methyl group of –CO_2CH_3 in [$Mo(CO)_5(COOCH_3)$]$^-$ appeared at 50 ppm. The ester carbonyl peak was observed at 170 ppm, which supports the formation of structure A in **Scheme 3.1** with the negative charge on the metal center. The terminal carbonyls were observed at 202 ppm and 206 ppm. The effect of the counter ion is also clearly shown in the peak position of the terminal carbonyls in the ^{13}C NMR experiment, corresponding to the peak shift observed in the IR spectra of these compounds. The peak at 206 ppm for the [*n*-Bu_4N]$^+$ complex supports the stronger interaction of this counter ion with the metalloester. This peak was observed at 210 ppm for the [PPN]$^+$ complex.

Addition of 18-crown-6 ether to the potassium methoxycarbonyl complex, [K^+][$Mo(CO)_5(COOCH_3)$], in a mixture of THF and MeOH gave a dark yellowish oily product (eqn. 8).

$$KOCH_3 + Mo(CO)_6 \xrightarrow[RT,\ 2\ h]{20ml\ THF/MeOH} [K^+][Mo(CO)_5(COOCH_3)^-] \xrightarrow[RT,\ 2\ h]{0.4\ ml\ 18\text{-}crown\text{-}6} [K(18\text{-}crown\text{-}6)^+][Mo(CO)_5(COOCH_3)^-] \quad (8)$$

IR analysis (**Table 3.3**) of the oily product in a THF/MeOH mixture showed peaks for the terminal carbonyls at 2040(w) cm^{-1}, 1943(vs) cm^{-1} and 1879(m) cm^{-1}. The peak for an ester carbonyl group (-CO_2CH_3) was observed as a broad peak at 1652(m, br) cm^{-1} which supports the successful formation of [K(18-crown-6)][$Mo(CO)_5(COOCH_3)$]. The appearance of a peak due to the methoxycarbonyl group at higher frequency corresponds to a weaker interaction of the capsulated potassium counter ion ([K(18-crown-6)]$^+$) with the methoxycarbonyl group (**Scheme 3.1**), in contrast to the interaction of the PPN^+ and *n*-Bu_4N^+ ions. The successful capsulation of potassium in [K^+][$Mo(CO)_5(COOCH_3)$] was supported by an improved solubility of the formed product in methanol. ^{13}C NMR analysis of [K(18-crown-6)][$Mo(CO)_5(COOCH_3)$] showed a peak for the methyl group of –CO_2CH_3 at 49.6 ppm and a peak at 71 ppm was assigned to the equivalent –CH_2- group of 18-crown-6 ether. Ester peaks were observed at 170 and 178 ppm, which shows that there were probably two isomers formed. The terminal carbonyls were observed at 202 and 210 ppm respectively. A methanolic solution of [K(15-crown-5)$_2$][OCH_3]

was prepared separately by refluxing 15-crown-5 ether with $KOCH_3$ solution for 30 minutes under CO,[27] followed by the addition of a THF solution of $Mo(CO)_6$ to form an orange solution (eqn. 9).

$$[K(15C5)_2^+][OCH_3^-] + Mo(CO)_6 \xrightarrow[\Delta\ ,\ 30\ min]{THF/MeOH} [K(15C5)_2^+][Mo(CO)_5(COOCH_3)^-] \qquad (9)$$

15C5 = 15- crown-5

The reaction was monitored by IR spectroscopy (**Table 4**). After evaporation in *vacuo*, the dark yellow oily product was dissolved in methanol and analyzed by IR in the region of 2100-1400 cm^{-1}. The peaks characteristic of $[K(15\text{-crown-}5)_2][Mo(CO)_5(COOCH_3)]$ were observed at 2042(w) cm^{-1}, 1944(vs) cm^{-1} and 1880(m) cm^{-1} for the terminal carbonyls, similar to the peaks observed for the PPN^+ salt. However, an ester carbonyl band for $[K(15\text{-crown-}5)_2][Mo(CO)_5(COOCH_3)]$ was observed at higher wavenumbers than those of the $[PPN]^+$ and $[n\text{-}Bu_4N]^+$ complexes. The peak that appeared at 1654 cm^{-1} wavenumbers, implies that there is a weak interaction of the formed potassium capsulated counter ion $[K(15\text{-crown-}5)_2]^+$ with the anion, $[Mo(CO)_5(COOCH_3)]^-$. The ^1H NMR analysis of this compound was also performed in deuterated methanol, with peaks for an ester methyl group ($-COOCH_3$) observed as a singlet at 3.34 ppm. A singlet for 15-crown-5 ether was observed at 3.65 ppm. The ^{13}C NMR analysis showed a methyl peak at 49.9 ppm ($-COOCH_3$), methylene groups of 15-crown-5 ether at 71 ppm and an ester carbonyl peak was observed at 161 ppm. The terminal carbonyls were observed at 202 and 210 ppm, respectively, which supports the synthesis of a novel capsulated potassium 15-crown-5 complex. Attempts to grow crystals of the product in a mixture of methanol and hexane were unsuccessful.

The third attempt in solubilizing the metalloester was ligand substitution in molybdenum carbonyl by triphenylphosphine (PPh_3) and the cyclopentadienyl (Cp) group. Unlike $Ph_3PW(CO)_5$,[17] which did not react, the reaction of $Ph_3PMo(CO)_5$ with three equivalents of $KOCH_3$ solution at room temperature, monitored by infrared spectroscopy (**Table 3.3**), resulted in the formation of $[K^+][\ Ph_3PMo(CO)_4(COOCH_3)^-]$ after 16 hours of stirring (eqn. 10). A cream white solid was obtained.

$$Ph_3PMo(CO)_5 \quad + \quad 3\ KOCH_3 \xrightarrow[RT,\ 16\ hrs]{THF/MeOH} [K^+][Ph_3PMo(CO)_4(COOCH_3)^-] \quad (10)$$

It is important to note that a reaction between a one to one equivalent of $Ph_3PMo(CO)_5$ and $KOCH_3$ did not succeed even under refluxing conditions, probably due to the same electronic effect observed by Bates *et al.* and Ford *et al.*[17,19]

IR (THF) analysis of $[K^+][Ph_3PMo(CO)_4(COOCH_3)]$ showed peaks at 2073(m) cm^{-1}, 1990(m) cm^{-1}, 1947(vs) $cm^{-1}$and 1604(m, br) cm^{-1}. The peaks at 2073, 1990 and 1947 cm^{-1} were associated with the terminal carbonyls, while the broad peak at 1604 cm^{-1} was related to the -CO_2CH_3 group. The solubility of the metalloester in organic solvents improved slightly, since the solid product dissolved only in DMSO-d_6. The compound was also analyzed by NMR spectroscopy. Three carbonyl peaks at 205(d) ppm, 210(d) ppm and 234 ppm were observed in the ^{13}C NMR spectrum.

The solubility of the metalloester in organic solvents improved slightly, since the solid product dissolved only in DMSO-d_6. The compound was also analyzed by NMR spectroscopy. Three carbonyl peaks at 205(d) ppm, 210(d) ppm and 234 ppm (s) were observed in the ^{13}C NMR spectrum. The two doublets at 205 and 210 ppm support the coupling of phosphorus from PPh_3 with terminal carbonyls. The coupling constant (J_{P-C}) for the doublet at 205 ppm was 8.9 Hz, which confirms the coupling of PPh_3 with a *cis* terminal carbonyl of $[K^+][Ph_3PMo(CO)_4(COOCH_3)^-]$. The coupling constant (J_{P-C}) for the doublet at 210 ppm was 22 Hz supporting the coupling of PPh_3 with a *trans* terminal carbonyl. The peak assigned to a carbonyl of $–CO_2CH_3$ was observed at 166 ppm. The methyl peak of $–CO_2CH_3$ was observed at 48.6 ppm and the phenyl groups of PPh_3 were observed between 128-140 ppm respectively. The stability of these compounds also increased after the ligand substitution by PPh_3.

Metathesis of $KOCH_3$ by PPNCl followed by reaction with $Ph_3PMo(CO)_5$ resulted in the formation of a $[PPN][Ph_3PMo(CO)_4(COOCH_3)]$, which was characterized by Attenuated Total Reflance (ATR) bands at 2073(m) cm^{-1}, 1994(m) cm^{-1}, 1913(s) cm^{-1}, 1890(sh) cm^{-1}, 1600(sh) cm^{-1} and 1592 (s) cm^{-1}. ^1H NMR in deuterated methanol showed a singlet peak at 3.34 ppm characteristic of a $–CO_2CH_3$ methyl group. The aromatic peaks for PPN^+ were observed as multiplets at 7.2-7.6 ppm (J_{H-H} = 8.26 Hz). Successful synthesis of the product was also confirmed by ^{13}C NMR analysis in deuterated methanol, with the methyl group peak of $–CO_2CH_3$

observed at 49.9 ppm. The peaks for the aromatic groups were observed at 128-134 ppm. An ester carbonyl peak was observed at 170 ppm, while only two peaks were observed at 207(d) and 211(d) ppm for the terminal carbonyls. The doublets in the terminal carbonyls are due to the coupling of phosphorus from PPh_3 with the carbonyl groups. A coupling constant (J_{P-C}) of 8.90 Hz for the peaks at 207 ppm supports the coupling of PPh_3 with a *cis* carbonyl. A coupling constant of 22 Hz for the peak at 211 ppm supports a coupling of PPh_3 with a *trans* carbonyl.

Table 3.3: IR data of the Mo metalloester compounds

Compound	**Color**	**IR(cm^{-1}) *ν*(CO)**	***ν*(-COOR)**
$[PPN][Mo(CO)_5(COOCH_3)]$[a]	dark yellow	2043(w), 1942(vs), 1879(m)	1607(m)
$[n\text{-}Bu_4N][Mo(CO)_5(COOCH_3)]$[a]	dark yellow	2042(m), 1936(vs), 1872(m)	1604(m, br)
$[K(15\text{-crwon-}5)_2][Mo(CO)_5(COOCH_3)]$[a]	dark brown oil	2042(w), 1944(vs), 1880(m)	1654 (m, br)
$[K(18\text{-crwon-}6)][Mo(CO)_5(COOCH_3)]$[a]	dark brown oil	2040(w), 1943(vs), 1879(m)	1652(m, br)
$[K][Ph_3PMo(CO)_4(COOCH_3)]$[b]	cream white	2073(m), 1990(m), 1947(vs)	1604(m, br)
$[PPN][Ph_3PMo(CO)_4(COOCH_3)]$[c]	cream white	2073(m), 1994(m), 1913(s), 1890(sh)	1600(sh) 1592(s)
$CpMo(CO)_3I$[d]	dark brown	2042 (s), 1966 (s)	
$[CpMo(CO)_3][OTf]$[d]	dark brown	2070(s), 1990(vs), 1711(vs)	
$[CpMo(CO)_3(PPh_3)][OTf]$[d]	yellow	2060 (s), 1995(sh), 1975 (m, br)	
$CpMo(CO)_2(PPh_3)(COOCH_3)$[d]	yellow	1958(m), 1875(vs)	1610(m, br)
$CpMo(CO)_2(PMe_3)(COOCH_3)$[d]	yellow	1954(s), 1874(s)	1622(m)
$CpMo(CO)_2(PPh_3)(COOCH_2CH_3)$[d]	yellow	1955(m), 1874(s)	1607(m)

a = IR was performed in methanol, b = IR was performed in THF, c = ATR solid state, d = IR was performed in CH_2Cl_2

A molybdenum dimer, $[CpMo(CO)_3]_2$, was synthesized by a known method of refluxing a THF solution of NaCp with $Mo(CO)_6$ to form a red solution, which was then mixed with an acid solution of ferric sulphate to form fine purple crystals of $[CpMo(CO)_3]_2$. The dimer was then cracked by adding iodine in dichloromethane solution and stirred at room temperature to yield $CpMo(CO)_3I$ as a brown solid. $CpMo(CO)_3I$ was characterized by an IR spectroscopy which showed characteristic peaks at 2042(s) cm^{-1} and 1966(s) cm^{-1}. The compound, $CpMo(CO)_3I$, was then reacted with silver triflouromethanesulfonate (AgOTf) to form a dark purple solution of $[CpMo(CO)_3][OTf]$ with *ν*(CO) bands shifted to 2070(s) cm^{-1}, 1990(vs) cm^{-1} and 1711(vs) cm^{-1}. The peak at 1711 cm^{-1} was associated to the vibration of S=O bonds for the triflouromethanesulfonate. The dark purple solution of $[CpMo(CO)_3][OTf]$ was then reacted with PR_3 (R= Ph and Me) overnight to form a light yellow solid product, $[CpMo(CO)_3(PR_3)][OTf]$, with characteristic IR peaks at 2060(s) cm^{-1}, 1995(sh) cm^{-1} and 1975(m, br) cm^{-1} (**Scheme 3.2**).[28] ^1H NMR analysis of the yellow product showed multiplet peaks characteristic of PPh_3 at 7.2-7.6 ppm (J_{H-H} = 8.26 Hz)and a Cp singlet peak at 5.8 ppm.

When a two mole equivalence of trimethyl phosophine was added to a dichloromethane solution of $[CpMo(CO)_3][OTf]$, the dicarbonyl-(η^5-cyclopentadienyl)-*bis*(trimethylphosphine)-molybdenum(II) trifluoromethanesulfonate, $[CpMo(CO)_2(P(CH_3)_3)_2][OTf]$, **Figure 3.2**, compound was formed.[29] Yellow crystals suitable for X-ray crystallography were obtained in a mixture of CH_2Cl_2 and hexane at room temperature. The compound, $[CpMo(CO)_2(PR_3)_2][OTf]$, crystallized in the monoclinic form with a space group of $P2_1/n$. The Cp ligand is bonded to molybdenum through all carbon atoms. The bond distances between Mo-Cp carbon atoms range from 2.3123 (19)-2.362 (2) Å. The Mo-P bond distances ranges between 2.4729 (5)-2.4751 (5) Å, Mo-P12 being 2.4729 (5) Å, shorter than Mo-P13, probably due to the triflate anion being adjacent to it. The Mo-CO bond distances are between 1.9581 (19)-1.9683 (19) Å, with Mo-$C_{17}O$ being shorter than Mo-$C_{16}O$. The bond angle between P13-Mo1-P12 is 130.342 (16)^o while the bond angle between C17-Mo1-C16 is 108.55 (8)^o, respectively. Bond lengths and bond angles are given in **Appendix 1**.

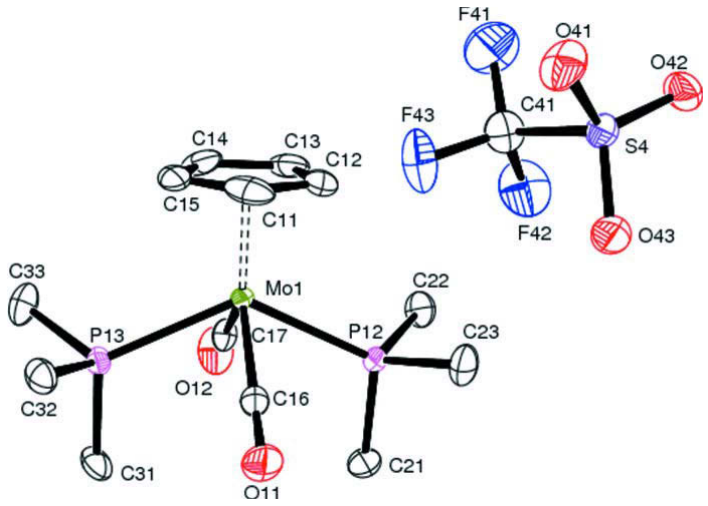

Figure 3.2: Crystal structure of $[CpMo(CO)_2(PMe_3)_2][OTf]$.

A methanolic solution of CH_3ONa was added to the dichloromethane solution of $[CpMo(CO)_3(PR_3)][OTf]$ at room temperature to form a yellow solution of $[CpMo(CO)_2(PPh_3)(COOCH_3)]$, which was charactized by IR spectroscopy (**Table 3.3**). The *v*CO peaks for $[CpMo(CO)_2(PPh_3)(COOCH_3)]$ were observed at 1958(m) cm^{-1} and 1875(vs) cm^{-1} for the two terminal carbonyls. These peaks are similar to those of a carboxylic acid derivative, $[CpMo(CO)_2(PPh_3)(COOH)]$, published by Gibson *et al.*[30] A metal coordinated ester (Mo-$COOCH_3$) peak was observed as a broad peak at 1610(m, br) cm^{-1}. The solubility of the compound was improved in organic solvents, but it was unstable due to air/oxygen in the solvent and decomposed with time to form a red-brown oily product with *v*CO peaks at 1960(sh) cm^{-1}, 1936(s) cm^{-1}, 1872(sh) cm^{-1} and 1855(s) cm^{-1}. The fast decomposition of $[CpMo(CO)_2(PPh_3)(COOCH_3)]$ prohibited further characterization of this compound with other instruments. Grubbs *et al*. also published the synthesis of a neutral intramolecular metalloester *trans* $(\eta^5\text{-}C_5H_4)CH_2CH_2O_2CM(CO_2)PPh_3$ (M = Mo and W) which also showed *v*(CO) peaks at 1970(s) cm^{-1}, 1881(vs) cm^{-1} and 1613(m) cm^{-1}.[31] Their $[CpMo(CO)_2(PPh_3)(COOCH_3)]$ type complex showed similar thermal instability.[31]

The ^1H NMR analysis of $[CpMo(CO)_2(PPh_3)(COOCH_3)]$ was performed in acetone-d_6 and dichloromethane-d_2. The fast decomposition of the product in dichloromethane-d_2 prevented the ^{13}C NMR analysis of $CpMo(CO)_2(PPh_3)(COOCH_3)$ in this solvent (CD_2Cl_2). The ^{13}C NMR analysis of $CpMo(CO)_2(PPh_3)(COOCH_3)$ was therefore performed in acetone-d_6. A slow decomposition of the product was monited by NMR spectroscopy. In acetone-d_6, a singlet peak

for the methyl group of Mo-$COOCH_3$ was observed at 3.49 ppm; a Cp peak was observed as a singlet at 5.15 ppm and a multiplet for the aromatic rings of PPh_3 were observed at 7.2-7.6 ppm. The peaks shifted slightly in dichloromethane-d_2 solvent, with a methyl peak observed as a singlet at 3.54 ppm, Cp peak was observed at 5.08 ppm and the aromatic peaks were observed at 7.37-7.45 ppm (J_{H-H} = 8.26 Hz). ^{13}C NMR analysis in acetone-d_6 showed a methyl group peak at 69 ppm, a Cp peak was observed at 95.7 ppm, aromatic ring carbon atoms of PPh_3 were observed at 128-136 ppm and terminal carbonyls at 209 ppm and 240 ppm.

Synthesis of an ethyl derivative of $CpMo(CO)_2(PPh_3)(COOCH_3)$ was also attempted by following the same procedure (**Scheme 3.2**), except that $NaOCH_2CH_3$ was used instead of $NaOCH_3$. Due to decomposition, only the IR and ^1H NMR analysis was performed. IR analysis of $CpMo(CO)_2(PPh_3)(COOCH_2CH_3)$ in dichloromethane showed *v*CO peaks at 1955(m) cm^{-1}, 1874(s) cm^{-1} and 1607(m) cm^{-1}, similar to the methyl derivative. The ^1H NMR analysis was done in dichloromethane-d_2 and showed a triplet for a methyl group at 1.2 ppm (J_{H-H} = 2.25 Hz), a quartet for a methylene group at 4.0 ppm (J_{H-H} = 7.28 Hz) and a doublet for a Cp group at 5.08 ppm (J_{H-H} = 1.62 Hz). The multiplets for the aromatic groups of PPh_3 were observed at 7.2-7.6 ppm. The compound decomposed with time before the ^{13}C NMR analysis could be performed.

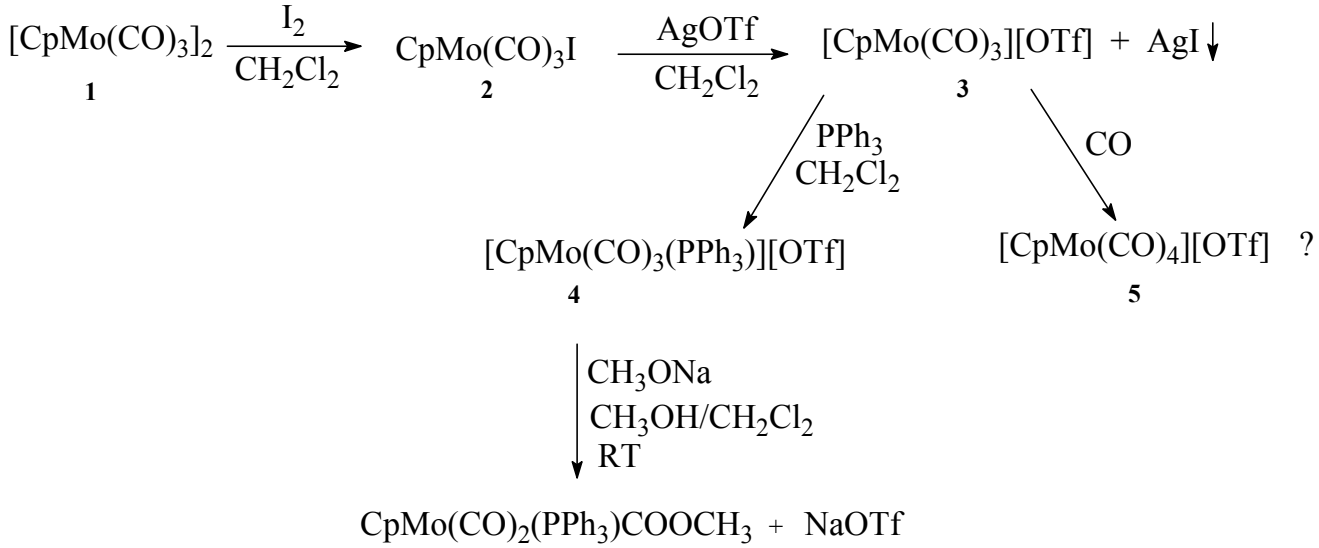

Scheme 3.2: Synthesis of $CpMo(CO)_2(PPh_3)(COOCH_3)$ from $[CpMo(CO)_3(PPh_3)][OTf]$ and CH_3ONa.

A $P(CH_3)_3$ derivative $\{CpMo(CO)_2(P(CH_3)_3)(COOCH_3)\}$ was synthesized following the same method (**Scheme 3.2**). The successful synthesis of $P(CH_3)_3$ derivatives, $[CpMo(CO)_3(PMe_3)][OTf]$ and $\{CpMo(CO)_2(P(CH_3)_3)(COOCH_3)\}$ was confirmed by IR spectroscopy. The *v*CO peaks for $[CpMo(CO)_3(PMe_3)][OTf]$ in dichloromethane solution were observed at 2055(s) cm^{-1}, 1990(sh) cm^{-1}, 1963(s) cm^{-1}, 1884(s) cm^{-1} and 1711(s) cm^{-1}. After addition of an equivalent amount of a methanolic solution of $NaOCH_3$ to a dichloromethane solution of $[CpMo(CO)_3(PMe_3)][OTf]$, the *v*CO peaks were shifted to 1954(s) cm^{-1}, 1874(s) cm^{-1} and 1622(m) cm^{-1}. The metal coordinated ester carbonyl was clearly seen at 1622 cm^{-1}, which was shifted slightly from the ester position of $CpMo(CO)_2(PPh_3)(COOCH_3)$. ^1H NMR analysis in chloroform-*d* showed a singlet for the methyl group ($-COOCH_3$) at 3.40 ppm, a doublet for the methyl group of $P(CH_3)_3$ at 1.6(d) ppm and a singlet for a Cp peak at 5.4 ppm, respectively. Attempts to grow a crystal of $\{CpMo(CO)_2(P(CH_3)_3)(COOCH_3)\}$ were unsuccessful.

3.3 Summary

Reactions of some Mo carbonyl compounds ($Mo(CO)_6$, $Ph_3PMo(CO)_5$ and $[CpMo(CO)_3][OTf]$) in Schlenk tubes with nucleophiles (alkoxides) gave alkoxycarbonyl complexes, also known as metalloesters compounds ($Mo\text{-}COOCH_3$). The reaction of $Mo(CO)_6$ with methoxides ($NaOCH_3$ or $KOCH_3$) resulted in the formation of water soluble complexes which were characterized as $K[Mo(CO)_5(COOCH_3)]$ or $Na[Mo(CO)_5(COOCH_3)]$. The same types of complexes were obtained when bulkier nucleophiles ($(CH_3)_3COK$, $CH_3CH_2(CH_3)_2COK$) were also used. Attempts to grow crystals suitable for X-ray crystallography from the reaction product of *t*-amyloxide with $Mo(CO)_6$ resulted in the formation of a novel oxaloto molybdenum cluster with an octahedral Mo surrounded by oxygen atoms.

Addition of crown ethers (18-crown-6 or 15-crown-5) to $K[Mo(CO)_5(COOCH_3)]$ in THF improved its solubility in organic solvents, and the IR data (**Table 3.1**) supported the formation of the proposed compound. This supports the belief that the potassium cation was tightly bound to the anion $[Mo(CO)_5(COOCH_3)]^-$ to form the water soluble salt.

Metathesis of $K[Mo(CO)_5(COOCH_3)]$ with bulkier counter ions (Et_4NCl, PPNCl and *n*-Bu_4NI) was not successful, due to the poor solubility of the potassium complex in the organic solvents. Apart from the poor solubility there is also the fact that the interaction of potassium as opposed to the ammonium cation would have been favoured, hence thermodynamically the metathesis reaction was not favoured. However, an alternative synthesis of the PPN and *n*-Bu_4N

alkoxycarbonyl complexes by reaction of [PPN][OCH_3] and/or [*n*-Bu_4N][OCH_3] with $Mo(CO)_6$ at room temperature was successful. There was a small shift in the IR peak positions of [PPN][$Mo(CO)_5(COOCH_3)$] compared to [*n*-Bu_4N][$Mo(CO)_5(COOCH_3)$], due to the counterion effect; the solubility and stability of the compounds was also improved by the introduction of bulkier counter ions. The ligand substitution of CO in $Mo(CO)_6$ by PPh_3 had improved the stability and solubility of the metalloester compounds formed. Successful synthesis of K[$Ph_3PMo(CO)_4(COOCH_3)$] was only achievable at a stoichiometric ratio of 1:3. The metathesis of K[$Ph_3PMo(CO)_4(COOCH_3)$] with PPNCl was unsuccessful. Its PPN analogy was also achieved by reacting [PPN][OCH_3] with $PPh_3Mo(CO)_5$ for 17 hours at room temperature.

Cp type metalloesters, ($CpMo(CO)_2(PPh_3)COOCH_3$ and $CpMo(CO)_2(PPh_3)COOCH_2CH_3$) derivatives were successfully synthesized but found to be thermally unstable. Their solubility in organic solvents was improved, but no crystals could be grown.

3.4 References

[1] P. C. Ford, A. Rokicki, Adv. Organomet. Chem., 81 (1988) 141

[2] C. P. Casey, S. M. Neuman, J. Am. Chem. Soc., 98 (1976) 5395

[3] W. Tam, G. Lin, J. A. Gladysz, Organometallics, 1 (1982) 525

[4] D. H. Gibson, K. Owens, T. Ong, J. Am. Chem. Soc., 106 (1984) 1125

[5] J. R. Sweet, W. A. G. Graham, J. Am. Chem. Soc., 104 (1982) 2811

[6] W. Tam, G. Lin, J. A. Gladysz, Organometallics, 1 (1982) 525

[7] P. C. Ford, Acc. Chem. Res., 14 (1981) 31

[8] E. O. Fischer, A. Maasbol, Angew. Chem. Int. Ed., 3 (1964) 580

[9] D. J. Darensbourg, M. Y. Darensbourg, Inorg. Chem., 9 (1970) 1691

[10] M. Y. Darensbourg, H. L. Conder, D. J. Darensbourg, C. Hasday, J. Am. Chem. Soc., 95 (1973) 5919

[11] H. Alper, K. E. Hashem, J. Am. Chem. Soc., 103 (1981) 6514

[12] E. J. Corey, L. S. Hegedus, J. Am. Chem. Soc., 91 (1969) 1233

[13] D. C. Gross, P. C. Ford, J. Am. Chem. Soc., 107 (1985) 585

[14] M. J. Chen, H. M. Feder, J. W. Rathke, J. Am. Chem. Soc., 104 (1982) 7346

[15] D. J. Taube, R. van Eldik, P. C. Ford, Organometallics, 6 (1987) 125

[16] R. J. Trautman, D. C. Gross, P. C. Ford, J. Am. Chem. Soc., 107 (1985) 2355

[17] A. Bates, M. T. Muaroka, R. J. Trautman, Inorg. Chem., 32 (1993) 2651

[18] D. C. Gross, P. C. Ford, Inorg. Chem., 21 (1982) 1704

[19] D. J. Taube, A. Rokicki, M. Anstock, P. C. Ford, Inorg. Chem., 26 (1987) 526

[20] D. J. Darensbourg, M. Y. Darensbourg, Inorg. Chem., 9 (1970) 1691

[21] M. Y. Darensbourg, H. L. Conder, D. J. Darensbourg, C. Hasday, J. Am. Chem. Soc., 95 (1973) 5919

[22] C. A. Brown, J. Chem. Soc., Chem. Comm., 1974, 680

[23] M. Cindric´, N. Strukana, V. Vrdoljak a, T. Fuss a, G. G. B. Kamenar, Inorg. Chim. Acta, 309 (2000) 77

[24] W. Petz, J. Organomet. Chem., 105 (1976) C19

[25] L. Garlaschelli, S. Martinengo, P. Chini, F. Canziani, R. Bau, J. Organomet. Chem., 213 (1981) 379

[26] R. J. Angelici, Acc. Chem. Res., 5 (1972) 335

[27] M. L. Cole, C. Jones, P. C. Junk, J.Chem. Soc. Dalton Trans., (2002) 896

[28] J. Markham, K. Menard, A. Cutler, Inorg. Chem., 24 (1985) 1581

[29] S. Jali, H. B. Friedrich, M. D. Bala, Acta Cryst., E64 (2008) m1401

[30] D. H. Gibson, K, Owens, T, Ong., J. Am. Chem. Soc., 106 (1984) 1125

[31] T. S. Coolbaugh, B. D. Santarsiero, R. H. Grubbs. J. Am. Chem. Soc., 106 (1984) 6310

4. CHAPTER 4

The synthesis, characterization and reactions of short chain molybdenum alkoxycarbonyl complexes $[Mo(CO)_5(COOR)]^-$ (R= Me, Et, ^iPr) and $[Mo(CO)_4(COOR)_2]^{2-}$ (R = ^iPr)

4.1 Introduction

Alkoxycarbonyl (metalloester) complexes are believed to be intermediates in some important catalytic reactions, including the carbonylation of alcohols and organic halides,[1-3] hydroformylation, hydrocarbonylation of olefins,[4] the Fischer-Tropsh synthesis and synthesis of alkyl carbonates and oxalates.[5,6] The complexes are obtained by the nucleophilic attack of an alkoxide anion and/or hydroxide on the electrophilic carbon atom of carbon monoxide coordinated to a transition metal, as shown in eqn. 1 and as discussed in the previous chapters.[7-13]

$$M_x(CO)_y + Nu \underset{K_{-1}}{\overset{K_1}{\rightleftharpoons}} M_x(CO)_{y-1}(C(=O)Nu)^- \quad (1)$$

adduct

Nu = OR^-, H^-, R^-, NH_2 etc
M = Transition metals
R = Alkyl groups

As mentioned in **Chapter 1**, there are many possible ways of synthesizing transition metal alkoxycarbonyl complexes, which do not involve nucleophilic attack of an alkoxide. For example, some group 10 (Ni, Pd and Pt) alkoxycarbonyl complexes have been synthesized by the migration of an alkoxide to the metal coordinated carbon monoxide (eqn. 2).[14]

$$M{-}OCH_3 + CO \longrightarrow \left[\begin{array}{c} CO \\ | \\ M{-}OCH_3 \end{array} \right]^{\ddagger} \longrightarrow M{-}COOCH_3 \quad (2)$$

M= group 10 transtion metal

Other group 10 alkoxycarbonyl complexes had been synthsized by reacting square planar metal complexes, suspended in an alcohol, under 10-50 atm of CO in the presence of trialkylamine at 50-70 ^{o}C.[15] "*Apart from the methods discussed above, another interesting approach for the synthesis of alkoxycarbonyls is the insertion of carbon dioxide into a metal heteroatom bond (eqn. 3). These reactions are interesting given the fact that they represent a means to CO_2 activation.*

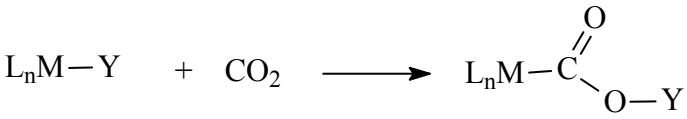

(3)

However, this route is limited by an unfavorable insertion of CO_2 to give the carbon-coordinated alkoxycarbonyl isomer (M-COOR) as opposed to the more favorable insertion yielding oxygen-coordinated carboxylates (M-OCOR)."[16]

Group 6 metal carbonyls have been used for the carbonylation of methanol to methyl formate and reported in the literarature. Ohyama *et al*. have reported a system for the synthesis gas (syngas (1:2)) carbonylation of methanol to methyl formate using a $Mo(CO)_6/KOCH_3$ catalyst,[18] while Darensbourg *et al*. have reported the $W(CO)_6/KOCH_3$ version using pure carbon monoxide.[19] In analyzing the steps involved in the transformations, a methoxycarbonyl anion, $[W(CO)_5(COOCH_3)]^-$, has been proposed to be involved, but a detailed analysis was not presented to support the conclusions and only the electrospray ionization spectroscopy (ESI) data was given.[20] Also, none of the previous reports have succeeded in isolating the intermediates involved in the reactions. Hence an efficient method for the synthesis of molybdenum alkoxycarbonyl complexes (Mo-COOR, R = $-CH_3$, $-CH_2CH_3$, $-CH(CH_3)_2$) and an investigation of the role played by the methoxycarbonyl complex, [PPN][$Mo(CO)_5$(COOMe)], in the catalytic carbonylation of methanol to methyl formate under synthesis gas atmosphere was undertaken.

Since the nucleophilic reactions of alkoxides with $Mo(CO)_6$ and the nature of the formed intermediates is understood (Chapter 3), the aim of the work presented in this chapter was (i) to improve the synthesis by changing the solvent and the conditions of the reaction. (ii) To test the catalytic effect of the intermediate $[Mo(CO)_5(COOCH_3)]^-$ in the production of methyl formate under hydrogen and syngas (1:1) atmospheres.

4.2 Results and Discussion

Anhydrous *bis*(triphenylphosphine)iminium chloride (PPNCl) was reacted with an equivalent amount of $NaOCH(CH_3)_2$) in dry isopropanol to give $[PPN][OCH(CH_3)_2]$. Addition of $Mo(CO)_6$ to this refluxing mixture under a CO atmosphere produced a yellow solution and a yellowish-brown precipitate after refluxing for *ca.* 35 min, eqn. 4.[21]

$$Mo(CO)_6 + [M^{+'}][OR^-] \longrightarrow [M'^+][Mo(CO)_5(COOR')^-] \quad (4)$$

M'= PPN, Ph_4As
R'= $-CH_3$, $-CH_2CH_3$, $-CH(CH_3)_2$

The yellow-brown precipitate was identified as the $[PPN][Mo(CO)_5(OCH(CH_3)_2)]$ complex. After separation by cannula, the yellow filtrate was dried under *vacuum* to yield $[PPN][Mo(CO)_5(COOCH(CH_3)_2)]$ as a yellow solid. IR (MeOH) analysis of the yellow product showed peaks at 2042(w) cm^{-1}, 1942(s) cm^{-1} and 1880(m) cm^{-1} for the terminal carbonyls. The ν(C=O) band for the metal coordinated ester (Mo-$COOCH_3$) was observed at 1665(m, br) cm^{-1}. ^1H NMR analysis (**Table 4.1**) was performed in CD_3OD, and showed a doublet at 1.13 ppm (J_{H-H} = 6.06 Hz) for the equivalent methyl groups ($-CH_3$) of the isopropyl moiety. A septet for the methylidine group (-CH-) was observed at 3.91 ppm (J_{H-H} = 6.20 Hz). The aromatic peaks for the counter ion (PPN) were observed as multiplets between 7.25-7.69 ppm (J_{H-H} = 8.26 Hz). Since ^{13}C NMR is also a diagnostic tool for the successful analysis of the alkoxycarbonyl complexes,[16] a ^{13}C NMR analysis of $[PPN][Mo(CO)_5(COOCH(CH_3)_2)]$ in CD_3OD showed characteristic peaks at 25 ppm for the methyl groups ($-CH_3$) and the methylidyne peak (-CH-) was observed at 65 ppm. The alkoxycarbonyl peak (metalloester, Mo-$COOCH(CH_3)_2$) was observed at 170 ppm, similar to the complexes discussed in Chapter 3. The terminal carbonyls for the complex were observed at 202 and 210 ppm, respectively. The compound was found to melt (Mp) at 204-205 ^oC. The successful synthesis of the compound was also confirmed by an elementary analysis (**Chapter 5**), which showed the expected percentage of the elements analyzed (CHN). After a few days, the compound decomposed even under a CO atmosphere, to form a molybdenum alkoxide. This decomposition was followed by observing changes in the IR bands under the same solvent. This is not unusual, as Bates *et al.* reported a similar behavior for the tungsten metalloester complex, $[PPN][W(CO)_5(COOCH_3)]$.[8]

In the absence of CO atmosphere, the alkoxycarbonyl product, $[PPN][Mo(CO)_5(COOCH(CH_3)_2)]$, also decomposes to form an alkoxide complex which was confirmed by both IR and NMR data to be the novel $[Mo(CO)_5(OCH(CH_3)_2)]^-$ complex (**Table 4.1**). Infrared analysis of this compound did not show the characteristic peak of an alkoxycarbonyl at 1700-1600 cm^{-1} and showed the terminal carbonyls at 2045(w) cm^{-1}, 1939(vs) $cm^{-1}$and 1873(m) cm^{-1}, which correspond to the C_{4v} type complexes of $LMo(CO)_5$. ^1H NMR analysis in CD_3OD showed a doublet at 1.13 ppm (J_{H-H} = 6.06 Hz) for the methyl groups ($-CH_3$), a septet for the methylidyne group (-CH-) was observed at 3.91 ppm (J_{H-H} = 6.20 Hz) and the aromatic peaks were observed as multiplets at 7.25-7.69 ppm (J_{H-H} = 8.26 Hz), respectively. In the ^{13}C NMR analysis, there was no alkoxycarbonyl peak between 160-180 ppm, only the terminal carbonyls were observed at 202 ppm and 207 ppm, supporting the formation of the molybdenum alkoxide complex, $[Mo(CO)_5(OCH(CH_3)_2)]^-$.

Table 4.1: Infrared[a] and NMR[b] spectral data for $[PPN][Mo(CO)_5(COOR)]$, R= Me, Et & ^{i}Pr, $[Ph_4As][Mo(CO)_5(OCH(CH_3)_2]$ and $[Ph_4As]_2[Mo(CO)_5(COOCH(CH_3)_2)_2]$

Compound	IR /ν(CO) cm^{-1}	^1H NMR /ppm	^{13}C NMR /ppm	Mp (°C)
$[PPN][Mo(CO)_5(COOCH(CH_3)_2)]$	2042(w),1942(s), 1880(m), 1665(m,br), 1589(m)[c]	1.13(*d*),3.91(*s*), 7.25-7.69(m)	25,65,128-135(*m*), 170[d], 202[e], 210	204-205
$[PPN][Mo(CO)_5(COOCH_2CH_3)]$	2043(w),1938(vs), 1871(m), 1656(s,br), 1590(m)[c]	1.12(*t*),3.57(*q*), 7.2-7.6 (*m*)	18, 58, 126-137(m), 170[d], 202, 210	230-231
$[PPN][Mo(CO)_5(COOCH_3)]$	2065(w),1930(vs), 1864(m), 1644(m,br), 1590(m)[c]	3.34(*s*), 7.2-7.6(*m*)	49,127-134(m), 170[d], 202, 206	214-215
$[Ph_4As][Mo(CO)_5(OCH(CH_3)_2]$	2045(w),1939(vs), 1873(m)	1.13(*d*),3.91(s), 7.25-7.69(m)	25, 65, 125-136(m), 202, 207	223-224
$[Ph_4As]_2[Mo(CO)_4(COOCH(CH_3)_2)_2]$	2074(vw),1939(s),1871(m),1708(m), 1659(m, br)	1.15(*d*),3.92(s), 7.2-7.6(m)	25, 65, 130-140(m),161, 170, 202, 207	310 (dec)

a = methanolic solution, b = CD_3OD, c =C(O)-OR is a weak vibration of the C=O band. d = ester carbonyl. For R= isopropyl the ester peak appeared at 167 ppm in acetone-d_6. e = terminal carbonyl which appeared at 210(*d*) and 214 ppm in acetone-d_6. dec= decomposed

The effect of the counterion in the molybdenum alkoxide complex, $[Mo(CO)_5(OCH(CH_3)_2)]^-$, was very prominent. The tetraphenylarsonium salt (Ph_4As^+) and *bis*(triphenylphosphine)iminium salt (PPN^+) compounds were obtained as precipitates in the reactions of $Mo(CO)_6$ with $[Ph_4As][OCH(CH_3)_2]$ and $[PPN][OCH(CH_3)_2]$. A significant chemical shift was observed in the ^{13}C NMR spectra for the terminal carbonyls of the formed molybdenum alkoxide complexes, one of the peaks was shifted from 207 ppm for $[Ph_4As]^+$ to 210 ppm when the counterion was $[PPN]^+$.

Room temperature crystallization of $[PPN][Mo(CO)_5(COOCH(CH_3)_2]$ in dry acetonitrile gave yellow crystals of the molybdenum-oxo cluster, $[PPN]_2[Mo_6O_{19}]$ (**Figure 4.1**). The structure of $[PPN]_2[Mo_6O_{19}]$ had previously been reported and characterized, showing an oxygen centered octahedral environment involving six molybdenum atoms.[22,23]

When solutions of $[PPN][Mo(CO)_5(COOCH(CH_3)_2)]$ and $[PPN][Mo(CO)_5(OCH(CH_3)_2)]$ were exposed to ambient light, the compounds decomposed in air to form the known cluster compound, $[PPN]_2[Mo_6O_{19}]$, which is a version of the reported oxygen centered polyoxomolybdate compound with a Lindqvist-type structure (**Figure 4.1**). Lindqvist clusters, are normally oxides of group 5 or group 6 transition metals in their higher oxidation states.[24] The crystal crystallizes in the triclinic form with a space group of P-1. The structure shows an anion that is bonded to the counterion through hydrogens. For the counter ion PPN, the bond distances between P (1)-N (1) and N (1)-P (2) are slightly different with the former being 1.571 (2) Å and the latter being 1.566 (2) Å. The bond angle (P (1)-N(1)-P (2)) is 149°. The anion is symmetric with O (4) occupying the center position of the cluster. All molybdenum atoms are octahedral surrounded by six oxygen atoms. The bond distances between the center oxygen, O (4), to the surrounding molybdenum atoms (Mo(1) to Mo(3)) are slightly different (**Table 4.2**). The O(4)-Mo(1) distance is 2.3281(2) Å, while its reflection O(4)-Mo(1)a {O(4)-Mo(1)1} has a distance of 2.3281(2) Å as expected. The distance between O(4) and Mo(2) or Mo(2)a is 2.2994(2) Å. The distance between O(4) and Mo(3) is 2.3255(2) Å and it is slightly longer than the O(4)-Mo(1) distance by 0.0026 Å. This suggests a slightly distorted octahedron structure of the anion, $Mo_6O_{19}^{2-}$. The distances between terminal oxygen atoms (O(2), O(5) and O(10)) to the molybdenum atoms (Mo(1), Mo(2) and Mo(3)) are approximately equivalent to each other; the O(2)-Mo(1) distance is 1.684(2) Å, while the distance between O(5)-Mo(2) is 1.679(2) Å and the distance between O(10)-Mo(3) is 1.690(2) Å. The bond angles from the surrounding molybdenum atoms passing to the centered O(4) to other surrounding molybdenum atoms formed

a right angle, e.g. Mo(2)1-Ô(4)-Mo(1)1= 90.271(9) degrees. The other bond angles, for example, Mo(1)-O(6)-Mo(3) are between 110-116.99(9) degrees (see **Appendix 2**).

Table 4.2: Selected bond lengths [Å] for $[PPN]_2[Mo_6O_{19}]$

Bond	Length	Bond	Length
O(1)-Mo(2)	1.883(2)	O(6)-Mo(1)	1.878(2)
O(1)-Mo(1)	1.966(2)	O(6)-Mo(3)	1.990(2)
O(2)-Mo(1)	1.684(2)	O(7)-Mo(3)	1.861(2)
O(3)-Mo(1)	1.875(2)	O(7)-Mo(2)	2.006(2)
O(3)-Mo(2)1	1.956(2)	O(8)-Mo(3)	1.8694(19)
O(4)-Mo(2)1	2.2994(2)	O(8)-Mo(1)1	1.986(2)
O(4)-Mo(2)	2.2994(2)	O(9)-Mo(2)1	1.858(2)
O(4)-Mo(3)1	2.3255(2)	O(9)-Mo(3)	1.994(2)
O(4)-Mo(3)	2.3255(2)	O(10)-Mo(3)	1.690(2)
O(4)-Mo(1)1	2.3281(2)	Mo(1)-O(8)1	1.986(2)
O(4)-Mo(1)	2.3281(2)	Mo(2)-O(9)1	1.858(2)
O(5)-Mo(2)	1.679(2)	Mo(2)-O(3)1	1.956(2)

The chemistry of these and related polyoxometallate compounds have been extensively studied by Pope and Müller.[25] A comprehensive coverage of a broad range of topics within polyoxometallate chemistry has also been published,[26] while several reports have appeared detailing crystal structures of $[Mo_6O_{19}]^{2-}$ with various counter ions.[27-31] The bond distances of the terminal Mo-O bonds range from 1.679(2)-1.690(2) Å in the crystal data, which is slightly longer than Mo-O bond distances of $[HN_3P_3(NMe_2)_6][Mo_6O_{19}]$ discussed by Allcock *et al.,*[28] whose crystal data show a range of 1.676(4)-1.678(4) Å. Hoppe *et al.*[30] found bond distances which range from 1.671(5)-1.673(5) Å for terminal Mo-O bonds of $[PPN]_2[Mo_6O_{19}]$, also slightly shorter than the terminal Mo-O bond distance in the $[PPN]_2[Mo_6O_{19}]$ crystal. The distance for bridging Mo-O bonds ranges from 1.875(2)-2.006 (2) Å in the crystal data for $[PPN]_2[Mo_6O_{19}]$ and is comparable with the known distance which range from 1.855 (4)-2.005(4) Å. Both ranges

are slightly different to the range (1.882(5)-1.981(5) Å) reported by Hoppe *et al.*[28,30] Bond angles for bridging Mo(1)-O(6)-Mo(3) and other bridges are similar to the reported data.

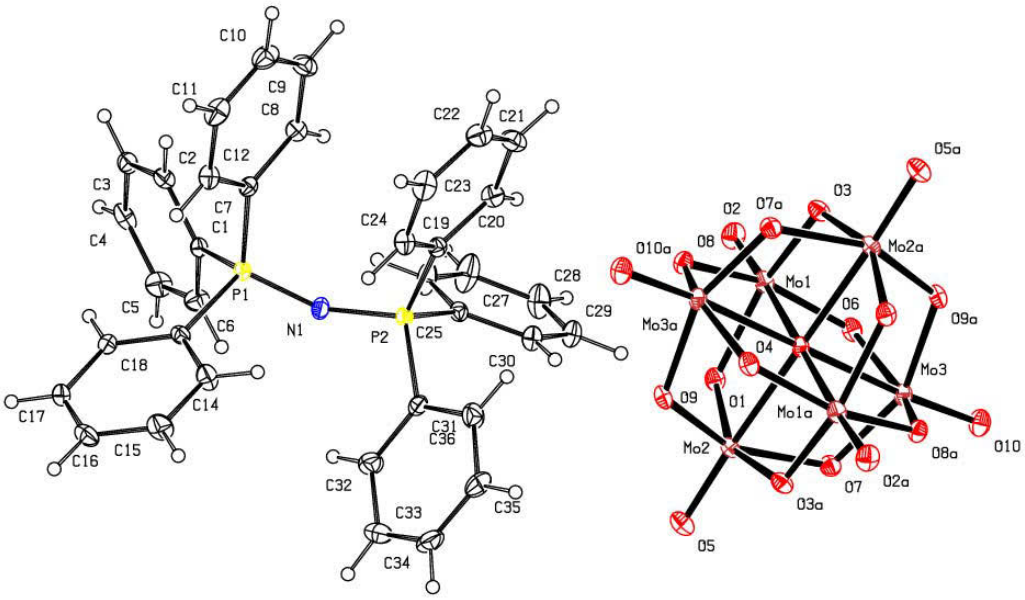

Figure 4.1: Crystal structure of $[PPN]_2[Mo_6O_{19}]$.

A detailed study of the mechanism for the formation of $[PPN]_2[Mo_6O_{19}]$ showed that it is formed *via* a decarbonylation pathway and the process is catalyzed by ambient light even under an inert (N_2) atmosphere. The pathway to the molybdenum oxo cluster (**Scheme 4.1**) is regarded as the UV initiated sequential decarbonylation of the metalloester $[PPN][Mo(CO)_5(COOCH(CH_3)_2)]$ via the metal alkoxide $[PPN][Mo(CO)_5(OCH(CH_3)_2)]$.

$$[PPN][Mo(CO)_5(COOCHC(CH_3)_2)] \xrightarrow[-CO]{\text{room light}} [PPN][Mo(CO)_5OCHC(CH_3)_2] \xrightarrow[-CO]{\text{room light}} [PPN]_2[Mo_6O_{19}]$$

Scheme 4.1: Decarbonylation of $[PPN][Mo(CO)_5(COOCH(CH_3)_2)]$ to $[PPN]_2[Mo_6O_{19}]$.

When the solution of $[PPN][Mo(CO)_5(COOCH(CH_3)_2)]$ was left in the absence of light under N_2 atmosphere, the cluster compound, $[PPN]_2[Mo_6O_{19}]$, was not obtained, but the crystals of $[PPN]_2[Mo_6O_{19}]$ were readily obtained under these conditions (N_2 atm) after the solution was

exposed to ambient light. The crystals were also grown in air under ambient light, which supports the photolysis theory.

It is interesting to note that formation of an oxo-complex such as $[PPN]_2[Mo_6O_{19}]$ *via* the metalloester utilized in this report is a novel route, that until now has not been reported. Thakur *et al.*[32] recently published a new synthetic method to Lindqvist polyoxometallate clusters of Mo and W from the metal alkoxycarbene complexes of group 6 transition metals. The authors believe that the polyoxometallate cluster formation is catalysed by tetrabutylammonium bromide (TBAB) in the presence of sodium hydroxide (eqn. 5).

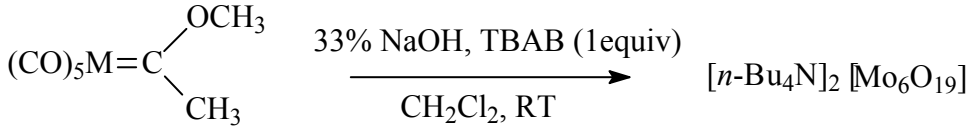

(5)

M=Mo, W

In our study the ethoxy and the methoxy derivatives were also prepared and isolated in dry solvents by using NaOEt in ethanol and NaOMe in methanol.[21] The spectral data for $[PPN][Mo(CO)_5(COOR)]$, R= Me, Et & ^{i}Pr and $[Ph_4As]_2[Mo(CO)_5(OCH(CH_3)_2)]$ in methanol are reported in **Table 4.1**.

The IR spectral data of these compounds ($[PPN][Mo(CO)_5(COOR)]$, R = Et and Me) in methanol showed terminal carbonyl peaks at 2042(w) cm^{-1}, 1943(s) cm^{-1} and 1880(m) cm^{-1} and have a similar pattern to the normal C_{4v} type compounds of $LMo(CO)_5$. The alkoxycarbonyl (metalloester) peaks appeared at 1644-1665 cm^{-1}, which is within the range of values (1700-1610 cm^{-1}) reported for similar compounds, although the range depends on the type of a nuclephile (Nu) and the metal center (L_nM) used.[10] However, Ford *et al.* claimed a range of 1735-1480 cm^{-1} for alkoxycarbonyl peaks in IR spectroscopy.[16]

The IR spectral data of the complex $[PPN][Mo(CO)_5(COOEt)]$ (**Table 4.1**) is analogous to that of the isopropyl derivative, but the alkoxycarbonyl peak was observed at 1656 cm^{-1}. The ^{1}H NMR analysis in CD_3OD showed a triplet at 1.12 ppm (J_{H-H} = 2.25 Hz) for a methyl group ($-CH_3$), a quartet for a methylene peak ($-CH_2-$) was observed at 4 ppm (J_{H-H}=7.28 Hz) and multiplets for the aromatic peaks of the counterion (PPN) were observed between 7.2-7.6 ppm (J_{H-H} = 8.26 Hz).

^{13}C NMR analysis for [PPN][$Mo(CO)_5(COOEt)$] showed peaks at 18 ppm for the methyl group ($-CH_3$) and the methylene group ($-CH_2-$) was observed at 58 ppm. The aromatic peaks were observed as multiplets between 126-137 ppm. A characteristic peak for an alkoxycarbonyl complex was observed at 170 ppm, in a similar position to the isopropyl derivative. The terminal carbonyls were observed at 202 ppm and 210 ppm respectively, supporting a successful synthesis of [PPN][$Mo(CO)_5(COOEt)$]. The compound melted at 230-231 ^oC and was also analyzed by elementary analysis (**Chapter 5**), which showed the expected values (CHN). Based on the IR and NMR data, the results suggest that the complex is structuraly similar to the isopropyl derivative.

A noticeable change in the comparative data of [PPN][$Mo(CO)_5(COOCH_3)$] was found in the IR data, which showed bands at 2065(w) cm^{-1}, 1930(vs) cm^{-1}, 1864(m) cm^{-1} for the terminal carbonyls. The peak at 2065 cm^{-1} was not observed in the ethyl and isopropyl derivatives. The alkoxycarbonyl peak was also shifted by 12-20 cm^{-1} relative to those of the ethyl and isopropyl derivatives. The peak was observed at 1644 cm^{-1} which is, however, within the reported region for metalloesters.**[10,16]** ^1H NMR analysis in CD_3OD showed a singlet at 3.34 ppm for the methyl group ($-CH_3$), and the multiplets for the aromatic peaks of the counterion (PPN) were observed between 7.2-7.6 ppm (J_{H-H} = 8.26 Hz), respectively. ^{13}C NMR showed a peak for the methyl group ($-CH_3$) at 49 ppm and aromatic peaks were observed at 125-136 ppm. A significant peak for an alkoxycarbonyl group ($Mo-COOCH_3$) was observed at 170 ppm, in a similar position to the ethyl and isopropyl derivatives. The terminal carbonyls were observed at 202 ppm and 206 ppm.

The tetraethylammonium derivative, [Et_4N][$Mo(CO)_5(COOCH_3)$], was also synthesized by refluxing [Et_4N][OCH_3] with an equivalent amount of $Mo(CO)_6$ in methanolic solution. The yellow solution was evaporated under vacuum to form a dark yellow solid. The solid was dissolved in methanol and IR analysis showed ν(CO) peaks at 2043(w) cm^{-1}, 1942(vs) cm^{-1}, 1880(m) cm^{-1} for the terminal carbonyls. An alkoxycarbonyl peak was observed at 1644(m, br) cm^{-1}. ^1H NMR analysis was performed in CD_3OD and showed a triplet at 1.3 ppm (J_{H-H} = 2.25 Hz) for the methyl group ($-CH_3$) of the counterion, [Et_4N^+] and a quartet for the methylene group ($-CH_2-$) was observed at 3.3 ppm (J_{H-H} = 7.28 Hz). The methyl group of the alkoxycarbonyl group ($-COOCH_3$) was observed as a singlet at 3.34 ppm. ^{13}C NMR data in CD_3OD showed a methyl group ($-CH_3$) for the counterion at 7.66 ppm and a methyl group of the alkoxycarbonyl group ($-COOCH_3$) was observed at 49.9 ppm. A methylene peak ($-CH_2-$) was observed at 53.3 ppm, while the metalloester peak was observed at 170 ppm. Only one terminal carbonyl was

observed at 202 ppm, and this might be due to the relexation time of the carbonyl groups. Attempts to grow crystals in acetonitrile resulted in the formation of the novel molybdenum oxo-cluster $[Et_4N]_2[Mo_4O_{13}]$, as brown crystals with no centered oxygen atom like $[PPN]_2[Mo_6O_{19}]$, **Figure 4.2**.

The crystal crystallizes in the monoclinic form with a space group of P 2_1/n. The anion $[Mo_4O_{13}]^{2-}$ is symmetric with octahedral and tetrahedral molybdenum atoms surrounded by oxygen atoms. The molecular structure does not show any Mo-Mo bonding in the structure but some molybdenum atoms are joined by oxygen bridges, for example Mo (1) and Mo (3) are bridged by O (1). The bond distances between O (1)-Mo (1) and O (1)-Mo (3) are similar with the former being 1.917 (4) Å and the latter being 1.915 (4) Å. Mo (2) and Mo (3) are bridged by O (2) which also bridges Mo (2) to Mo (1). The bond distance between O (2)-Mo (3) is 2.421 (4) Å, O (2)-Mo (1) is 2.461 (4) Å and O (2)-Mo (2) 1 is 1.791(4) shorter than the two.

Clearly, this structure has different apertures of molybdenum oxides with some being four membered rings and others being six membered rings like zeolite structures. Mo (1) is bridged to Mo (4) by both O (4) and O (7) to form a four membered ring aperture. The bond distances between the terminal oxygen and molybdenum atoms, O (11)-Mo (1) and O (14)-Mo (1) are 1.703(4) Å. The bond distance between O (13)-Mo (2) is 1.722 (3) Å. The bond distances between O (12)-Mo (3) and O (15)-Mo (3) are 1.707 (4) Å and 1.708 (4) Å. The bond distances between the terminal oxygen atoms {O (16) and O (18)} and Mo (4) are 1.701 (4) Å and 1.707 (4) Å respectively. Bond angles are shown in **Appendix 3**.

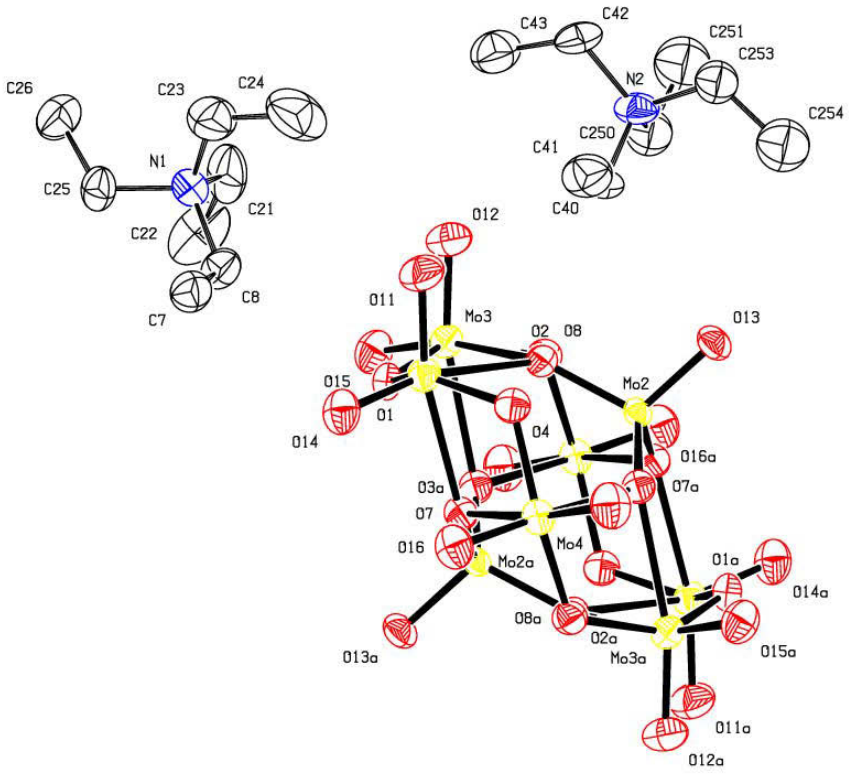

Figure 4.2: Crystal structure of $[Et_4N]_2[Mo_4O_{13}]$.

Addition of an excess of $[Ph_4As][OCH(CH_3)_2]$ to $[Mo(CO)_6]$ (4:1 molar ratio) in isopropanol resulted in the formation of a dark brown precipitate. On the basis of the IR and NMR data, this compound was tentatively formulated as $[Ph_4As]_2[Mo(CO)_4(COOCH(CH_3)_2)_2]$. The compound was dissolved in methanol and the IR anlysis was performed, which showed 5 bands at 2074(vw) cm^{-1}, 1939(s) cm^{-1}, 1871(m) cm^{-1}, 1708(m) cm^{-1} and1659(m, br) cm^{-1}. The peaks at 1708 cm^{-1} and 1659 cm^{-1} were associated to the possible formation of a *bis*(alkoxycarbonyl) type complex. The ^1H NMR analysis in CD_3OD showed a doublet at 1.13 ppm (J_{H-H}= 6.06 Hz) for the equivalent methyl groups ($-CH_3$) of the isopropyl moiety, a septet for the methylidyne (-CH-) peak was observed at 3.9 ppm (J_{H-H}= 6.20 Hz) and the peaks for the counterion (Ph_4As^+) were observed as multiplets between 7.2-7.6 ppm (J_{H-H} = 8.26 Hz). ^{13}C NMR spectrum showed a peak for the methyl groups ($-CH_3$) at 25 ppm, the methylidyne peak (-CH-) was observed at 65 ppm, and the aromatic peaks for the counterion (Ph_4As^+) were observed between 130-140 ppm as multiplets. Two alkoxycarbonyl peaks were observed at 161 ppm and 170 ppm, respectively, in support of the two IR bands for the alkoxycarbonyl peaks observed at 1708 cm^{-1} and 1659 cm^{-1}. The appearance of two alkoxycarbonyl peaks at 161 and 170 ppm suggests a non-symmetric product.

The two terminal carbonyl peaks were observed at 202 and 207 ppm, respectively. The compound did not melt, but it decomposed at 310 ^{o}C. However, it is important to note that this compound was only obtainable when the counterion was Ph_4As^+, attempts to repeat this reaction using a PPN^+ salt did not produce a *bis*(alkoxycarbonyl) complex. Formation of this type of complex is not unusual for the group 6 metal carbonyls, a *bis*(carbomyl) tungstate complex, $[W\{C(OLi)N^iPr_2\}_2(CO)_4]$, **Scheme 4.2**, has been published by Fischer *et al*. in 1984.[33,34] Carbomyls are also formed through a nucleophilic attack of an amine (nucleophile) to the metal coordinated carbonyl group, similar to the formation of alkoxycarbonyl complexes.[10]

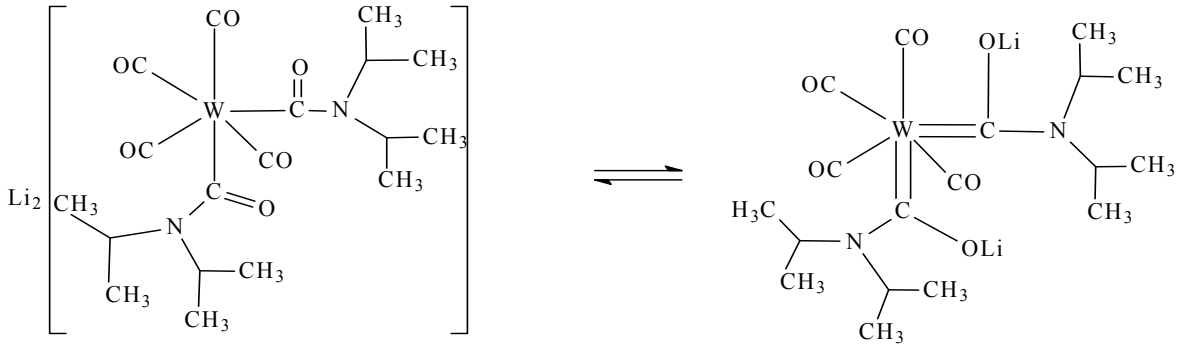

Scheme 4.2: Resonance structure of *bis*(carbomyl) tungstate, $[W\{C(OLi)N^iPr\}_2(CO)_4]$.[33,34]

The formation of *bis*(alkoxycarbonyl) complexes is also known for platinum and palladium complexes, and it was also claimed to be the possible intermediate in the synthesis of α-ketoamides and oxalate esters.[14,35,36] *Bis*(alkoxycarbonyl) complexes of iron are also known and they also eliminate oxalate esters by a reductive C-C coupling between two alkoxycarbonyl (ester) ligands.[37-39] They are synthesized by the reaction of oxalyl chloride with tetracarbonyl(alkoxycarbonyl) iron anions, ($[(CO)_4Fe(CO_2R)]^-$, R= Me, *t*-Bu, allyl, 1,1'-dimethylallyl) which is obtained by a nucleophilic addition of an alkoxide on $Fe(CO)_5$.[40] It is interesting that studies had also claimed the synthesis of iron tris(alkoxycarbonyl) complexes by the nucleophilic addition of *t*-BuOK on the terminal carbonyl of $[(CO)_4Fe(CO_2R)_2]^-$ (eqn. 6),[40] which confirms that a reaction of metal carbonyls with excess alkoxide can result in the formation of *bis* or *tris*(alkoxycarbonyl) complexes.

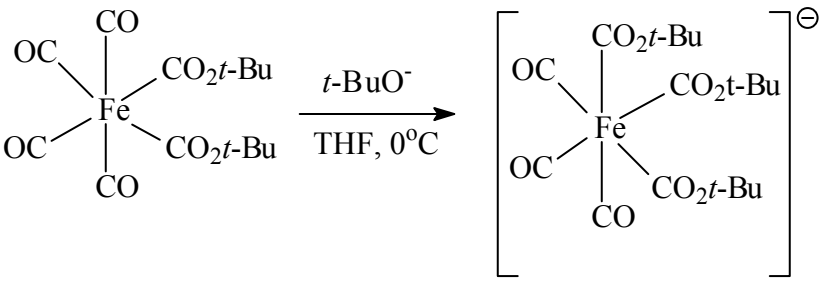

(6)

The observation of two alkoxycarbonyl peaks in both the IR and ^{13}C NMR data suggest a non-symmetric product. Attempts to grow crystals of this compound were unsuccessful.

4.3 Catalytic effect of [PPN][Mo(CO)$_5$(COOCH$_3$)] in CO hydrogenation to methyl formate

$Mo(CO)_6$ was selected for this study because it was claimed by several patents[41] to enhance the production of methyl formate and methanol from synthesis gas, in a reaction catalyzed by a homogeneous $Ni(CO)_4/KOCH_3$ system.[42] Based on this work, Marchionna *et al.*[43] proposed a mechanism for the $Ni(CO)_4/KOCH_3$ catalytic system which involved a nickel metalloester, $[Ni(CO)_3(COOCH_3)]^-$, as an intermediate to the formation of methyl formate and methanol. In 1999, Ohyama *et al.*[18] examined the role played by group 6 metal carbonyls (Cr, Mo, W) and $Ni(CO)_4$ in this reaction but did not isolate any metalloester intermediates.

Our studies support, at least in part, the proposed mechanism by Morchionna *et al.*[43] as the fundamental reaction of $Mo(CO)_6$ with $KOCH_3$ results in the formation of $[Mo(CO)_5(COOCH_3)]^-$. From the preliminary results for methyl formate synthesis under syngas atmosphere (eqn.7), it is clear that heating the synthesized $[PPN][Mo(CO)_5(COOCH_3)]$ in methanol for 24 hours does not produce methyl formate. This was confirmed by gas chromatography and GC-MS analysis of the organic solvent after the reaction. The same results were obtained when a methanolic solution of $[PPN][Mo(CO)_5(COOCH_3)]$ was reacted with hydrogen in a reactor.

$$[PPN][Mo(CO)_5(COOCH_3)] \xrightarrow[\Delta]{\text{methanol}} HCOOCH_3 + HCOOH \qquad (7)$$

However, methyl formate was formed using $[PPN][Mo(CO)_5(COOCH_3)]$ under 1700 kPa of syngas (1:1) at 125 ^oC (eqn. 8) together with $Mo(CO)_6$ (**Table 4.3**).

$$[PPN][Mo(CO)_5(COOCH_3)] + CO + H_2 \xrightarrow[\Delta]{\text{methanol}} HCOOCH_3 + Mo(CO)_6 + \text{other products} \quad (8)$$

Table 4.3: Amount of methyl formate produced from $[PPN][Mo(CO)_5(COOCH_3)]$

Catalyst[a] + gas	Time (hours)	Solvent	% Conversion	Moles of MF (mmoles)	% Yield
H_2	24	MeOH	-	-	-
Syngas	24	MeOH	6	6.42	7.50
Syngas[b]	24	THF	6	2.65	3.09
Syngas +$KOCH_3$	24	THF	32	7.43	8.66

a = catalyst is $[PPN][Mo(CO)_5(COOCH_3)]$, b = 0.9 % of methanol was produced and an unquantified amount of formic acid.

A high-pressure infrared study ($[PPN][Mo(CO)_5(COOCH_3)]$, 5 Bar syngas (1:1)) supported the formation of $Mo(CO)_6$, as the metalloester peaks at 1942 cm^{-1} and 1880 cm^{-1} diminished with the concomitant growth of the $Mo(CO)_6$ peak at 1986 cm^{-1}. There was no evidence of the formation of a mono or bridged hydride ($HMo(CO)_5^-$/μ-$HMo_2(CO)_{10}^-$) species in the reaction. A small amount of methanol was generated when THF was used as a solvent (eqn. 9). Formic acid is probably formed by the degradation of methyl formate due to hydrolysis.

$$[PPN][Mo(CO)_5(COOCH_3)] + CO + H_2 \xrightarrow[\Delta]{\text{THF}} HCOOCH_3 + HCOOH + CH_3OH + \text{other products} \quad (9)$$

Addition of 5ml of $KOCH_3$ in a THF solution of $[PPN][Mo(CO)_5(COOCH_3)]$ increased the amount of methyl formate produced, and this is probably due to the normal carbonylation of methanol to methyl formate. The conversion of syngas also increased from 6 % to 32 %.

4.4 Summary and conclusion

Reaction of molybdenum hexacarbonyl with nucleophiles RO^- [R= CH_3, CH_2CH_3, $CH(CH_3)_2$)] in respective alcoholic solvent under reflux gave alkoxycarbonyl complexes. Relative to the free CO, metal coordinated carbon monoxide was strongly activated by the alkoxides. The polarity of the solvents did not influence the equilibrium rate of reaction under reflux. During the synthesis of alkoxycarbonyl complexes, a molybdenum alkoxide complex, $[Mo(CO)_5(OCH(CH_3)_2)]^-$, was formed through a direct substitution of CO by alkoxide which competed with the nucleophilic attack to form the alkoxycarbonyl complex. Addition of excess isopropoxide ($[Ph_4As][OCH(CH_3)_2]$ to $Mo(CO)_6$ solution resulted in the formation of a *bis*(isoproxycarbonyl) complex. All mono substituted alkoxycarbonyl complexes ($Mo(CO)_5(COOR)^-$, R= Me, Et and ^{i}Pr), on standing under CO atmosphere slowly decarbonylate to form molybdenum alkoxide complexes ($Mo(CO)_5OR^-$).

The mono substituted isopropoxycarbonyl complex ($Mo(CO)_5(COO^iPr)^-$) slowly decarbonylates on standing and in solution to form the molybdenum isopropoxide complex ($Mo(CO)_5O^iPr)^-$ even under CO atmosphere. The molybdenum isopropoxide complex in solution further decarbonylates to form the stable molybdenum oxo cluster, $[PPN]_2[Mo_6O_{19}]$, when exposed to ambient light. A tetraethylammonium pentacarbonyl molybdenum methoxycarbonylato derivative, $[Et_4N][Mo(CO)_5(COOCH_3)]$, also decomposed in solution to form an oxo cluster compound, $[Et_4N]_2[Mo_4O_{13}]$, however, this cluster does not have a centered oxygen atom like $[PPN]_2[Mo_6O_{19}]$.

There is a significant role played by the methoxycarbonyl intermediate ($[PPN][Mo(CO)_5(COOCH_3)]$) in the production of methyl formate from $Mo(CO)_6$ and $KOCH_3$. Formation of methyl formate from ($[PPN][Mo(CO)_5(COOCH_3)]$) and syngas regenerates $Mo(CO)_6$. Addition of potassium methoxide to a methanolic solution of ($[PPN][Mo(CO)_5(COOCH_3)]$) under sygas increased the amount of methyl formate formed. An HPIR study of $[PPN][Mo(CO)_5(COOCH_3)]$ under syngas suggests the decomposition of the metalloester with the formation of $Mo(CO)_6$. A possible mechanism for the formation of methyl formate from $[PPN][Mo(CO)_5(COOCH_3)]$ involves the breakdown of the metalloester through protonation by methanol to eliminate the $Mo(CO)_5$ intermediate (**Scheme 4.3**). The $Mo(CO)_5$ intermediate is then carbonylated to form $Mo(CO)_6$.

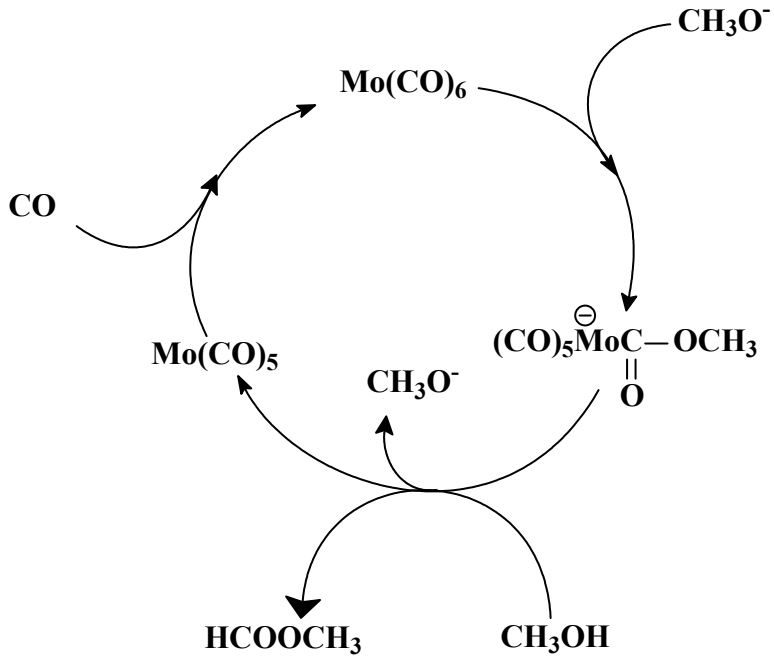

Scheme 4.3: **Mechanism for the formation of methyl formate from $Mo(CO)_6/KOCH_3$ under syngas *via* $[PPN][Mo(CO)_5(COOCH_3)]$ intermediate.**

4.5 References

[1] G. Cardaci, G. Bellachioma, P. F. Zanazzi, J. Chem. Soc. Dalton Trans., (1987) 473

[2] R. Bertani, G. Cavinto, L. Tonoilo, G. Vasapollo, J. Organomet. Chem., 84 (1993) 165

[3] E. J. Corey, L. S. Hegedus, J. Am. Chem. Soc., 91 (1969) 1233

[4] (a) R. Bertani, G. Cavinato, G. Facchin, L. Toniolo, A. Vavasori, J. Organomet. Chem., 466 (1994) 273; (b) C. D. Wood, P. E. Garrou, Organometallics, 3 (1984) 170; (c) D. Milstien, J. L. Huckaby, J. Am. Chem. Soc., 104 (1982) 6150

[5] G. Vasapollo, L. Toinolo, G. Cavinato, F. Bigoli, M. Lanfrachi, M. A. Pellinghelli, J. Organomet. Chem., 481 (1994) 173

[6] X. Yin, J. Andersen, A. Cotton, J. Moss, J. Organomet. Chem., 564 (1998) 267

[7] P. C. Ford, A. Rokicki, Adv. Organomet. Chem., 28 (1988) 139

[8] A, Bates, M. T. Muraoka, R. J. Trautman, Inorg. Chem., 32 (1993) 2651

[9] D. J. Darensbourg, M. Y. Darensbourg, Inorg. Chem., 9 (1970) 1691

[10] R. J. Angelici, Acc. Chem. Res., 5 (1972) 335

[11] (a) R. J. Trautman, D. C. Gross, P. C. Ford, J. Am. Chem. Soc., 107 (1985) 2355 (b) D. C. Gross, P. C. Ford, J. Am. Chem. Soc., 107 (1985) 585

[12] M. Y. Darensbourg, H. L. Condor, D. J. Darensbourg, C. Hasday, J. Am. Chem. Soc., 95 (1973) 5919

[13] L. Schwartburd, E. Poverenov, L. J. W. Shimon, D. Milstein, Organometallics, 26 (2007) 2931

[14] (a) H. E. Bryndza, Organometallics, 4 (1985) 1686; (b) G. D. Smith, B. E. Hanson, J. S. Merola, F. J. Waller, Organometallics, 12 (1993) 568; (c) S. A. Macgregor, G. W. Neave, Organometallics, 22 (2003) 4547; (d) S. A. Macgregor, G. W. Neave, Organometallics, 23 (2004) 891

[15] R. Bertani, G. Cavinato, L. Toniolo, G. Vasapollo, J. Mol. Catal., 84 (1993) 165

[16] P.C. Ford, A. Rokicki, Adv. Organomet. Chem., 81 (1988) 141

[17] A. R. Cutler, P. K. Hanna, J. C. Vites, Chem. Rev., 88 (1988) 1363

[18] S. Ohyama, E. S. Lee, K. Aika, J. Mol. Catal. A: Chemical, 138 (1999) 305

[19] D. J. Darensbourg, R. L. Gray, C. Ovalles, M. Pala, J. Mol. Catal., 29 (1985) 285

[20] V. N. Nemykin, P. Basu, Inorg. Chim. Acta, 358 (2005) 2876

[21] (a) L. Garlaschelli, M. C. Malatesta, S. Martinengo, F. Demartin, M. Manassero, M. Sansoni, J. Chem. Soc. Dalton Trans., (1986) 777; (b) L. Garlaschelli, S. Martinengo, C. Chini, F. Canziani, R. Bau, J. Orgnometal. Chem., 213 (1981) 379

[22] C. Rocchiccioli-Deltcheff, R. Thouvenot, M. Fouassier, Inorg. Chem., 21 (1982) 30

[23] Y. Xia, P. Wu, Y. Wang, H. Guo, Crystal growth & design, 6 (2006) 253

[24] (a) S. Hoppe, J. L. Stark, K. H. Whitmire, Act. Cryst., C53 (1997) 68; (b) N. Strukan, M. Cindric, M. Devcic, G. Giester, B. Kamenar, Acta. Cryst., C56 (2000) e278; (c) J. Li, J. Cluster Science, 13 (2002) 137; (d) N.H. Hur, W.G. Klemperer, R. C. Wang, Inorg. Synth., 27 (1990) 77; (e) M. Che, M. Fournier, J.P. Launay, J. Chem. Phys., 71 (1979) 1954

[25] (a) M. T., Pope, Heteropoly and Isopoly Oxometalates; Springer-Verlag: New York, 1983; (b) M. T., Pope; A. Müller, Angew. Chem., Int. Ed. Engl., 30 (1991) 34; (c) M. T., Pope, A. Müller, Eds.; Polyoxometalates: from platonic solids to anti-retroViral activity; Kluwer Academic Publishers: Dordrecht, The Netherlands, 1994

[26] C. L., Hill, Chem. Rev., 98 (1998) 8

[27] Garner, C. D.; Howlander, N. C.; Mabbs, F. E.; McPhail, A. T.; Miller, R. W.; Onan, K. D. J. Chem. Soc., Dalton Trans., (1978) 1582

[28] H. R. Allcock, E. C. Bisell, E. T. Shwall, Inorg. Chem., 12 (1973) 2963

[29] R. A. Roesner, S. C. McGrath, J. T. Brockman, J. D. Moll, D. X. West, J. K. Swearingen, A. Castineiras, Inorg. Chim. Acta, 342 (2003) 37

[30] S. Hoppe, J. L. Stark, K. H. Whitmire Acta Cryst., (1997). C53, 68-70

[31] N. Strukan, M. Cindric, M. Devcic, G. Giester, B. Kamenar, Acta Cryst., (2000). C56, e278

[32] A. Thakur, A, Chakraborty, V, Ramkumar, S, Ghosh, J. Chem. Soc. Dalton Trans., (2009) 7552

[33] E. O. Fischer, R. Reitmeier, K. Z. Ackermann, Naturforsch.,B., 39 (1984) 668

[34] S. Anderson, D. J. Cook, A. F. Hill, Organometallics, 16 (1997) 5595

[35] F. Ozawa, H. Yanagihara, A. Yamamoto, J. Org. Chem., 51 (1986) 415; (b) F. Ozawa, H. Soyama, H.Yanagihara, I. Aoyama, H. Takino, K. Izawa, A. Yamamoto, J. Am. Chem. Soc., 107 (1985) 3235

[36] V. Giuseppe, T. Luigi, C. Giovanni, B. Francesco; L. Maurizio; P. M. Angela. J. Organomet. Chem., 481 (1994) 173

[37] J. Y. Salaun, G. Le Gall, P. Laurent, H. des Abbayes, J. Organomet. Chem., 441 (1992) 99

[38] P. Laurent, J. Y. Salaun, G. Legall, M. Sellin, H. Desabbayes, J. Organomet. Chem., 466 (1994) 175

[39] J. Salaun, P. Laurent, H. des Abbayes, Coord. Chem. Rev., 178–180 (1998) 353

[40] N. L. Gall, D. Luart, J. Y. Salau¨n, J. Talarmin, H. des Abbayes, L. Toupet, N. Menendez, F. Varret, Organometallics, 21 (2002), 1775

[41] D. Mahajan, US Patent 6921733 (2005)

[42] R. S. Sapienza, W. A. Sleiger, T. E. O'Hare, D. Mahajan, US Patent 4614749 (1986), US Patent 4619946 (1986), US Patent 4623634 (1986), US Patent 4935395 (1990), US Patent 4992480 (1991)

[43] M. Marchiona, L. Basini, A. Argno, M. Lami, F. Ancillotti, J. Mol. Catal., 75 (1992) 147

5. CHAPTER 5

Experimental

5.1 General

All synthesis experiments were performed under carbon monoxide or nitrogen atmospheres using Schlenk line techniques. Chemically pure tetrahydrofuran (Merck), hexane and diethyl ether (Merck) were distilled over sodium/benzophenone and stored over sodium wire. Dichloromethane (Merck) was distilled over phosphorus pentoxide (P_2O_5) and stored over molecular sieves, type 4A. Methanol (Promark chemicals and/or Sigma Aldrich ≥ 99.99 %), ethanol (Sigma Aldrich ≥ 99.99%) and isopropanol (Sigma Aldrich ≥ 99.98%) were distilled over magnesium turnings and iodine and stored over molecular sieves, type 3A. Acetonitrile (Merck 99.99%) was distilled over P_2O_5 and stored over molecular sieves, type 3A. Triglyme (Sigma Aldrich, triethylene glycol dimethyl ether, 99%) was dried over sodium wire and used without distillation. Molecular sieves (type 3A and 4A from Sigma Aldrich) were dried in a furnace at 250-300 ^oC for 10 hours and cooled in a desiccator before use.

Potassium methoxide ($KOCH_3$, Fluka), potassium *t*-butoxide ($KOC(CH_3)_3$, Fluka), molybdenum hexacarbonyl ($Mo(CO)_6$, Sigma Aldrich and Acros), dicyclopentadiene (Fluka, 95%), triphenylphopsphine (Fluka), *bis*(triphenylphosphine) iminium chloride (PPNCl, Sigma Aldrich), 18-crown-6 ether (Sigma Aldrich), 15-crown-5 ether (Sigma Aldrich), tetrabutylammonium iodide (*n*-Bu_4NI, Sigma Aldrich) were purchased. Sodium isopropoxide ($NaOCH(CH_3)_2$), sodium methoxide ($NaOCH_3$), sodium ethoxide ($NaOCH_2CH_3$) and potassium *t*-amyloxide ($KOCH_2C(CH_3)_2CH_3$) were synthesized from chemically pure alcohols. All gases (CO, 99.99%; syngas (1:1) and H_2, 99.99%) were purchased from Afrox and used without any further purification. Melting points were recorded on an Ernst Leitz Wetzlar hot-stage microscope and are uncorrected. Elemental analyses were performed on a LECO CHNS elemental analyzer. Infrared spectra were recorded on a Nicolet Impact 400D 5DXFT- spectrophotometer in the range 4000-400 cm^{-1} and/or Perkin Elmer (FT-IR spectrophotometer, spectrum RX 1), either in solution using a liquid cell with NaCl windows (Aldrich 99.99%), as KBr (Sigma Aldrich 99.99%) discs or Attenuated Total Reflectance (ATR spectrum 100) equipped with ZnSe crystal. High pressure Infrared (HPIR) spectra were recorded at Sasol research and development, using a Bruker EQUINOX 55 Infrared equipped with a CaF_2 high pressure transmission cell. NMR spectra were

recorded on Varian 300 MHz, Varian Inova 400 MHz, Bruker 400 MHz and Bruker 600 MHz spectrometers. NMR solvents, chloroform-*d* (Sigma Aldrich, 99.8%), acetone-d_6 (Sigma Aldrich, 99.5%), methanol-d_4 (Sigma Aldrich, 99.8%), and water-d_2 (Sigma Aldrich) were used as purchased. The precursors $[CpMo(CO)_3]_2$, $CpMo(CO)_3I$, $[CpMo(CO)_3][OTf]$, $[CpMo(CO)_3(PR_3)][OTf]$ (R=Me, Ph) and $Ph_3PMo(CO)_5$ were all prepared by literature methods or sometimes modified methods.

5.2 Experimental methods for the data discussed in Chapter 2

The experiments were conducted to verify the effect of $Mo(CO)_6$ and solvent in the carbonylation of methanol using different gases (CO, H_2 and syngas (1:1) and syngas (1:2)) using a pipe reactor, **Figure 5.1**. The solvents studied were methanol, THF and triglyme and were selected based on their polarity.

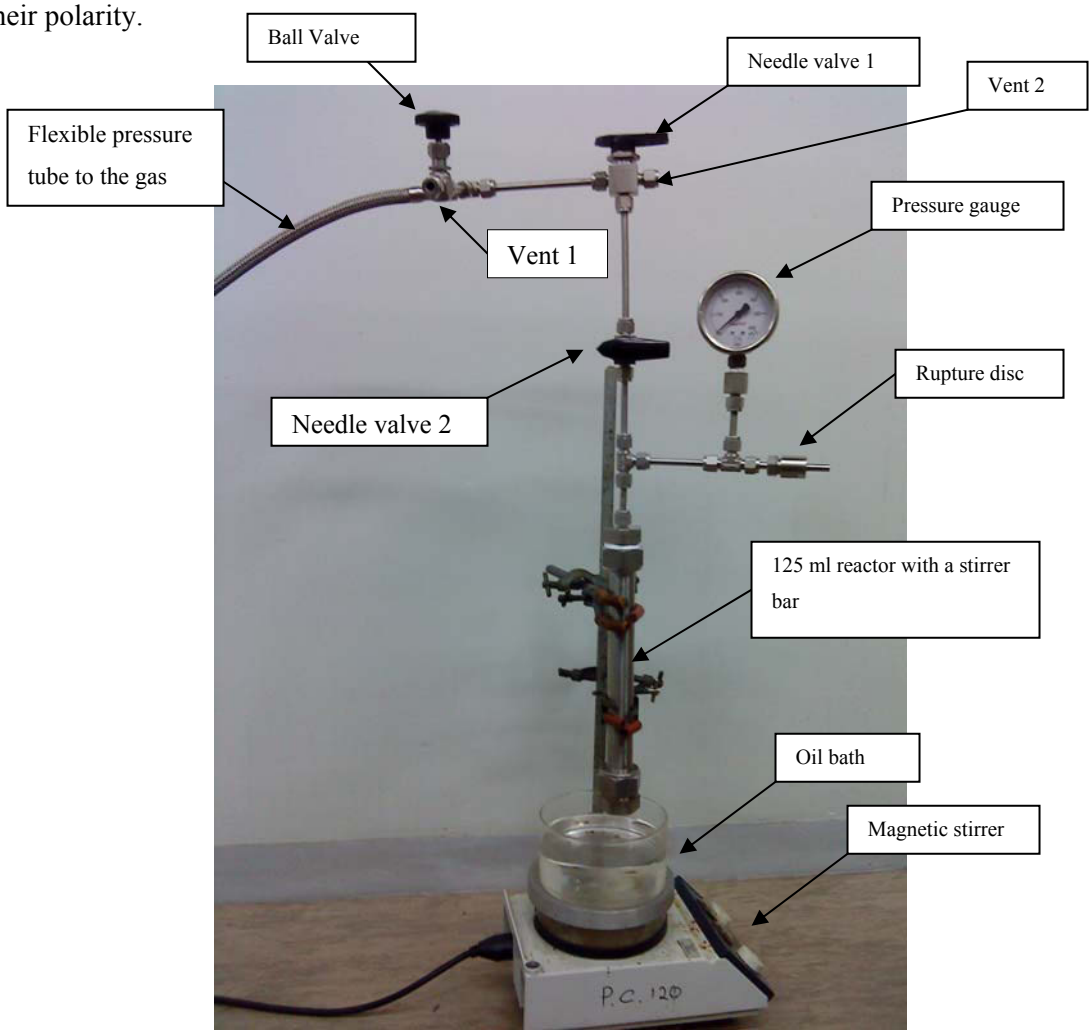

Figure 5.1: Pipe reactor.

5.2.1 Gas Chromatography (GC)

Organic products were analyzed by a Perkin Elmer Clarus 500 gas chromatography. The GC was equipped with a flame ionization detector. Column specifications and GC parameters are given below.

Carrier gas; Hydrogen

Column: Elite-Petro, 50 m x 0.2 mm x 0.5 μm Film thickness

Injector Temperaure: 250 ^{o}C

Detector Temperature: 270 ^{o}C

Maximum oven temperature: 320 ^{o}C

Split: on

Attenuation: 0

Oven programme:

Initial temp: 40 ^{o}C for 5 min

Ramp 1: 10.0 ^{o}C. min^{-1} to 80 ^{o}C, held for 5 min

Ramp 2: 20.0 ^{o}C. min^{-1} to 120 ^{o}C, held for 5 min

Ramp 3: 30.0 ^{o}C. min^{-1} to 270 ^{o}C, held for 15 min

5.2.2 CO carbonylation of methanol catalyzed by potassium methoxide ($KOCH_3$) in methanol

Potassium methoxide solution (10 ml, 2.5 g, 35 mmol) was added to 20 ml of dry methanol and transferred to a pipe reactor. The reactor was then purged three times with carbon monoxide and

charged to a pressure of 1600 kPa. Thereafter the reactor was heated for 24 hrs at 160 ^{o}C in an oil bath. After the reaction, the reactor was cooled to room temperature by dipping it in an ice bath. The organic products were analyzed by gas chromatography and GC-mass spectrometry.

5.2.3 CO carbonylation of methanol catalyzed by potassium methoxide ($KOCH_3$) in tetrahydrofuran

The experimental procedure is the same as in experiment 5.2.2 expect that the solvent is THF.

5.2.4 CO carbonylation of methanol catalyzed by potassium methoxide ($KOCH_3$) in triglyme

The experimental procedure is the same as in experiment 5.2.2 expect that the solvent is triglyme.

5.2.5 Syngas carbonylation of methanol catalyzed by potassium methoxide ($KOCH_3$) in methanol

Potassium methoxide solution (10 ml, 2.5 g, 35 mmol) was added to 20 ml of dry methanol and transferred to a pipe reactor. The reactor was purged three times with synthesis gas and charged to a pressure of 1600 kPa. The reactor was then heated for 24 hrs at 160 ^{o}C in an oil bath. After the reaction, the reactor was cooled to room temperature by dipping it in an ice bath. The organic products were analyzed by gas chromatography and GC-mass spectroscopy.

5.2.6 Syngas carbonylation of methanol catalyzed by potassium methoxide ($KOCH_3$) in tetrahydrofuran

The experimental procedure is the same as in experiment 5.2.5 expect that the solvent is THF.

5.2.7 Syngas carbonylation of methanol catalyzed by potassium methoxide ($KOCH_3$) in triglyme

The experimental procedure is the same as in experiment 5.2.5 expect that the solvent is triglyme.

5.2.8 CO carbonylation of methanol catalyzed by $Mo(CO)_6/KOCH_3$ (1:4) in methanol

To dry methanol (20 ml) was added $Mo(CO)_6$ (2.64 g, 10 mmol). Potassium methoxide solution (10 ml, 2.5 g, 35 mmol) was added to the $Mo(CO)_6$ solution and transferred to a pipe reactor. The reactor was purged three times with carbon monoxide and charged to a pressure of 1600 kPa. The reactor was subsequently heated for 24 hrs at 160 ^oC in an oil bath. After the reaction, the reactor was cooled to room temperature by dipping it in an ice bath. The organic products were analyzed by gas chromatography and GC-mass spectroscopy.

5.2.9 CO carbonylation of methanol catalyzed by $Mo(CO)_6/KOCH_3$ (1:4) in tetrahydrofuran

The experimental procedure is the same as in experiment 5.2.8 expect that the solvent is THF.

5.2.10 CO carbonylation of methanol catalyzed by $Mo(CO)_6/KOCH_3$ (1:4) in triglyme

The experimental procedure is the same as in experiment 5.2.8 expect that the solvent is triglyme.

5.2.11 Syngas carbonylation of methanol catalyzed by $Mo(CO)_6/KOCH_3$ (1:4) in methanol

To dry methanol (20 ml) was added $Mo(CO)_6$ (2.64 g, 10 mmol). Potassium methoxide solution (10 ml, 2.5 g, 35 mmol) was added to the $Mo(CO)_6$ solution and transferred to a pipe reactor. The reactor was then purged three times with synthesis gas (syngas) and charged to a pressure of 1600 kPa. The reactor was subsequently heated for 24 hrs at 160 ^oC in an oil bath. After the reaction,

the reactor was cooled to room temperature by dipping it in an ice bath. The organic products were analyzed by gas chromatography and GC-mass spectroscopy.

5.2.12 Syngas carbonylation of methanol catalyzed by $Mo(CO)_6/KOCH_3$ (1:4) in tetrahydrofuran

The experimental procedure is the same as in experiment 5.2.11 expect that the solvent is THF.

5.2.13 HPIR reaction of $Mo(CO)_6$ and $KOCH_3$ (1:5) under CO pressure

$Mo(CO)_6$ (50 mg, 0.1893 mmol) was dissolved in 20 ml of dry THF and transferred to a Parr reactor equipped with an IR window. A methanolic solution of $KOCH_3$ (0.3 ml, 66.39 mg, 0.9468 mmol) was added. A 5 bar of CO was charged and the reaction was monitored from room temperature to 100 ^oC. The first spectrum was collected after 1 min reaction time. The reaction was then monitored for 30 min and spectra collected every 5 min.

5.2.14 HPIR reaction of $Mo(CO)_6$ and $KOCH_3$ (1:5) under H_2 pressure

The experimental procedure is the same as in experiment 5.2.13 expect that the experiment was performed under H_2 atmosphere.

5.2.15 HPIR reaction of $Mo(CO)_6$ and $KOCH_3$ (1:5) under syngas (1:1) pressure

The experimental procedure is the same as in experiment 5.2.13 expect that the experiment was performed under syngas (1:1) atmosphere.

5.2.16 HPIR reaction of $Mo(CO)_6$ and $KOCH_3$ (1:5) under N_2 pressure, the effect of methanol in the formation of methyl formate

The experimental procedure is the same as in experiment 5.2.13 expect that the experiment was performed under N_2 atmosphere.

5.2.17 HPIR reaction of $Mo(CO)_6$ and $NaOCH_3$ (1:5) under N_2 pressure, the effect of methanol in the formation of methyl formate.

$Mo(CO)_6$ (50 mg, 0.1893 mmol) was dissolved in 20 ml of dry THF and transferred to a Parr reactor equipped with an IR window. $NaOCH_3$ (50 mg, 0.9256 mmol) was added to the THF solution. 5 bar of N_2 was charged and the reaction was monitored from room temperature to 100 ^oC. The first spectrum was collected after 1 min reaction time. The reaction was then monitored for 30 min and spectra collected after every 5 min. IR (THF, cm^{-1}) ν(CO) 1990, 1881, a broad peak at 1790-1507 cm^{-1}. Methanol (1.25 ml) was then added under H_2 atm, IR (THF/MeOH, cm^{-1}) ν(CO) 2061(w), 1990 ($Mo(CO)_6$), 1943(s), 1881(m), 1714(vs), 1600(s,br).

5.2.18 Syngas carbonylation of methanol catalyzed by $Mo(CO)_6/KOCH_3$ (1:2) in tetrahydrofuran

To dry THF (20 ml) was added $Mo(CO)_6$ (5.28 g, 20 mmol) was added. Potassium methoxide solution (10 ml, 2.5 g, 35 mmol) was added to the $Mo(CO)_6$ solution and this mixture was transferred to a pipe reactor. The reactor was then purged three times with synthesis gas (syngas) and charged to a pressure of 1600 kPa. The reactor was heated for 24 hours at 160 ^oC in an oil bath. After the reaction, the reactor was cooled to room temperature by dipping it in an ice bath. The organic products were analyzed by gas chromatography and GC-mass spectroscopy.

5.2.19 Syngas carbonylation of methanol catalyzed by $Mo(CO)_6/KOCH_3$ (2:1) in tetrahydrofuran

The experimental procedure is the same as in experiment 5.2.18 expect that the experiment was performed at a ratio of (2:1) $Mo(CO)_6/KOCH_3$.

5.2.20 Syngas carbonylation of methanol catalyzed by $Mo(CO)_6/KOCH_3$ (1:4) in triglyme

The experimental procedure is the same as in experiment 5.2.11 expect that the solvent is triglyme.

5.2.21 The effect of hydrogen in the formation of methyl formate from $Mo(CO)_6/KOCH_3$ (1:4) in methanol

To dry methanol (20 ml) was added $Mo(CO)_6$ (2.64 g, 10 mmol). Potassium methoxide solution (10 ml, 2.5 g, 35 mmol) was added to the $Mo(CO)_6$ solution and transferred to a pipe reactor. The reactor was then purged three times with hydrogen and charged to a pressure of 1100 kPa. The reactor was subsequently heated for 24 hrs at 160 ^oC in an oil bath. After the reaction, the reactor was cooled to room temperature by dipping it in an ice water. The organic products were analyzed by gas chromatography and GC-mass spectroscopy.

5.2.22 The effect of hydrogen in the formation of methyl formate from $Mo(CO)_6/KOCH_3$ (1:4) in tetrahydrofuran

The experimental procedure is the same as in experiment 5.2.21 expect that the solvent is THF.

5.2.23 The effect of hydrogen in the formation of methyl formate from $Mo(CO)_6/KOCH_3$ (1:4) in triglyme

The experimental procedure is the same as in experiment 5.2.21 expect that the solvent is triglyme.

5.3 Experimental methods for the Data discussed in Chapter 3

5.3.1 Synthesis of $K[Mo(CO)_5(COOCH_3)]$

To dry THF (20 ml) was added $Mo(CO)_6$ (0.5 g, 1.894 mmol). Potassium methoxide solution (0.5 ml, 0.13 g, 1.894 mmol) was added. The mixture was stirred at room temperature for 1 hour and a yellow solution and white precipitate was formed. The precipitate and filtrate were seperated by cannula and dried under vacuum to form a yellow solid (filtrate) and a cream white solid (precipitate). IR of the yellow solid (KBr, cm^{-1}) ν(CO) 2043(w), 1956(s), 1880(m), 1655(m). ^1H NMR (D_2O, ppm): [δ] 3.16 (s, 3H). ^{13}C NMR (D_2O, ppm): [δ] 55 (CH_3), 178 ($COOCH_3$).

5.3.2 Synthesis of $K[Mo(CO)_5(COOC(CH_3)_3)]$

To dry THF (20 ml) was added $Mo(CO)_6$ (0.5 g, 1.894 mmol). Potassium *t*-butoxide solution (1.90 ml, 0.21 g, 1.894 mmol) was added. The mixture was stirred at room temperature for 1 hour and a yellow solution was formed. The solution was dried under vacuum to yield a light yellow solid (50%). IR (KBr, cm^{-1}) ν(CO) 1987(m), 1955(s), 1885(m), 1725(m). ^1H NMR (D_2O, ppm): [δ] 3.16 (s, 9H). ^{13}C NMR (D_2O, ppm): [δ] 56 (CH_3), 82 ($C(CH_3)_3$), 174 ($COOC(CH_3)_3$).

5.3.3 Synthesis of $K[Mo(CO)_5(COOC(CH_3)_2CH_2CH_3)]$

To dry THF (20 ml) was added $Mo(CO)_6$ (0.5 g, 1.894 mmol). Potassium *t*-amyloxide (0.24g, 1.894 mmol) was added. The mixture was stirred at room temperature for 1 hour and a yellow solution was formed. The solution was dried under vacuum to form a yellow solid. IR (KBr, cm^{-1}) ν(CO) 1986(m), 1941(s), 1885(m), 1662(m). ^1H NMR (D_2O, ppm): [δ]0.7 (t,3H),1.0 (s,6H),1.3 (q,2H). ^{13}C NMR (D_2O, ppm): [δ] 4.9 (CH_3), 24 ($C(CH_3)_2$), 32 (CH_2), 64 ($C(CH_3)_2$), 184 ($COOC(CH_3)_2CH_2CH_3$).

5.3.4 Effect of 18-crown-6 to the solubility of $[K^+][Mo(CO)_5(COOCH_3)^-]$, synthesis of $[K(18\text{-crown-6})][Mo(CO)_5(COOCH_3)]$

To dry THF (20 ml) was added $Mo(CO)_6$ (0.5 g, 1.894 mmol). Potassium methoxide solution (0.5 ml, 0.13 g, 1.894 mmol) was added. The mixture was stirred at room temperature for 2 hours and a yellow solution and white precipitate was formed. The reaction was monitored by IR before addition of 18-crown-6. IR (νCO) (THF/MeOH) before addition of 18-crown-6 showed peaks at 1918(s), 1862(m) and 1682(w, br) cm^{-1}. To this solution was added 18-crown-6 (0.4 ml, 1.879 mmol) and the solution was stirred at room temperature for 2 hours. IR (THF/MeOH, cm^{-1}) (νCO) 2040(vw), 1943(vs), 1879(m), 1855(sh), 1652(m, br). ^1H NMR (CD_3OD, ppm): [δ] 3.34 (s, 3H), 3.61 (s, 24H). ^{13}C NMR (CD_3OD, ppm): [δ] 49.6 (CH_3), 71 (18-crown-6, -CH_2-), 161, 170, 178, ($COOCH_3$), 202, 210 (terminal CO).

5.3.5 Synthesis of $[K(15\text{-crown-}5)_2][OCH_3]$

15-crown-5 (1.6 ml, 8.08 mmol) was added dropwise to a 20 ml THF solution of $KOCH_3$ (0.3 ml, 4.04 mmol) at room temperature. The light yellowish brown solution was then stirred for 1hour under nitrogen atmosphere. The $[K(15\text{-crown-}5)_2][OCH_3]$ THF solution was kept for experiment 5.3.6.

5.3.6 Synthesis of $[K(15\text{-crown-}5)_2][Mo(CO)_5(COOCH_3)]$

$Mo(CO)_6$ (1.07 g, 4.04 mmol) was added to a 20 ml light yellowish brown solution of $[K(15\text{-crown-}5)_2][OCH_3]$. The solution was then stirred at room temperature for 2 hours to form a yellow precipitate and a yellow solution. The solution was filtered by cannula and dried under vacuum. The filtrate gave 1.36 g of brown oil. IR (νCO) (CH_3OH, cm^{-1}) 2042(w), 1944(s), 1880(m) and 1654(m, br). ^1H NMR (CD_3OD, ppm): [δ] 3.33 (s, 3H), 3.65 (s, 20H). ^{13}C NMR (CD_3OD, ppm) [δ] 49.86 (CH_3), 71 (15-crown-5, -CH_2-), 161 ($COOCH_3$), 202, 210 (terminal CO).

5.3.7 Synthesis of $[K(18\text{-crown-}6)][OCH_3]$

18-crown-6 (0.86 ml, 4.04 mmol) was added dropwise to a 20 ml of dry MeOH solution of $KOCH_3$ (0.3 ml, 4.04 mmol) and refluxed while stirring for 1 hour. A clear solution was observed. The $[K(18\text{-crown-}6)][OCH_3]$ solution was kept for experiment 5.3.8.

5.3.8 Synthesis of $[K(18\text{-crown-}6)][Mo(CO)_5(COOCH_3)]$

$Mo(CO)_6$ (1.07 g, 4.04 mmol) was added to a 20 ml refluxing solution of $[K(18\text{-crown-}6)][OCH_3]$. The mixture was then further refluxed while stirring for 2 hours to form a yellow solution. A yellow solution was then separated by cannula and dried under vacuum. A dark-brown oil was obtained (1.20 g). IR (νCO) (CH_3OH, cm^{-1}) 1938(s), 1870(m), 1654(s, br) and 1611(sh). ^1H NMR (CD_3OD, ppm): [δ] 3.34 (s, 3H), 3.61 (s, 24H). ^{13}C NMR (CD_3OD, ppm): [δ] 49.68 (CH_3), 71 (18-crown-6, -CH_2-), 161, 170, 178 ($COOCH_3$), 202, 205 (terminal CO).

5.3.9 Synthesis of [PPN][OCH_3]

PPNCl (2.00 g, 3.5 mmol) was dissolved in 6 ml of dry methanol. $KOCH_3$ solution (1 ml, 0.25 g, 3.5 mmol) was added. The solution was then stirred at room temperature for 30 min to form a white (KCl) precipitate. The solution was kept for experiment 5.3.10.

5.3.10 Synthesis of [PPN][$Mo(CO)_5(COOCH_3)$]

$Mo(CO)_6$ (0.924 g, 3.5 mmol) was dissolved in 20 ml of dry THF. [PPN][OCH_3] methanol solution (7 ml, 3.5 mmol) was added, the solution was stirred at room temperature for 17 hrs to form a yellow solution. The yellow solution was dried under vacuum to form a yellow-brown solid (1.63 g). The solid was sublimed to give a pure product. IR (CH_3OH, cm^{-1}) ν(CO) 2042(w), 1942(vs), 1879(m), 1607(m, br). ^1H NMR (CD_3OD, ppm): [δ] 3.34 (s, 3H), 7.2-7.6(m, 15H, J_{H-H} = 8.26 Hz). ^{13}C NMR (CD_3OD, ppm): [δ] 49.87 (CH_3), 128-135 (CH, Ph), 170 ($COOCH_3$), at 202, 210 (terminal CO). Mp. 214-215 ^oC.

5.3.11 Synthesis of [*n*-Bu_4N][OCH_3]

n-Bu_4NI (1.29 g, 3.5 mmol) was dissolved in 6 ml of dry methanol. 1ml (0.25 g, 3.5 mmol) of $KOCH_3$ solution was added. The solution was then stirred at room temperature for 30 min to form a white precipitate. The solution was kept for experiment 5.3.12.

5.3.12 Synthesis of [*n*-Bu_4N][$Mo(CO)_5(COOCH_3)$]

$Mo(CO)_6$ (0.924 g, 3.5 mmol) was dissolved in 20 ml of dry THF. [*n*-Bu_4N][OCH_3] methanolic solution (11 ml, 3.5 mmol) was added and the solution was stirred at room temperature for 17 hrs to form a yellow solution. The yellow solution was dried under vacuum to form a dark-yellow solid (1.98 g). The solid was sublimed to give a pure product. IR (MeOH, cm^{-1}) (νCO) 2043(w), 1936(s), 1872(m), 1604(m, br). M.p.> 250 ^oC (dec). ^1H NMR (CD_3OD, ppm): [δ] 1.01 (t, 12H, J_{H-H}= 7.35 Hz), 1.40 (s, 8H, J_{H-H}= 7.40 Hz), 1.65 (q, 8H, J_{H-H}= 5.34 Hz), 3.24 (t, 8H, J_{H-H}= 8.58 Hz), 3.34 (s, 3H). ^{13}C NMR (CD_3OD, ppm):[δ] 49.87 (CH_3), 128-135 (Ph), 170 ($COOCH_3$), 202, 210 (terminal CO).

5.3.13 Synthesis of $[K^+][Ph_3PMo(CO)_4(COOCH_3)^-]$

$Ph_3PMo(CO)_5$ (1 g, 2.007 mmol) was dissolved in 20 ml dry THF. $KOCH_3$ methanolic solution (3ml, 0.751g, 6.021 mmol) was added. The mixture was stirred at room temperature for 16 hours. A creamy solution was formed and dried under vacuum to form a cream white solid. M.p. = 160-163 ^oC; IR (THF, cm^{-1}) (νCO) 2072(m), 1990(m), 1947(vs), 1900(sh), 1604(m,br), 1592(m,br). ^1H NMR (DMSO-d_6, ppm): [δ] 3.16s, 3H), 7.2-7.6 (m, 15H, J_{H-H} = 8.26 Hz). ^{13}C NMR (DMSO-d_6, ppm): [δ] 48.5 (CH_3), 128-156 (Ph), 166 ($COOCH_3$), 205 (d, J= 8.90 Hz), 210 (d, J= 22 Hz), 234 (terminal CO).

5.3.14 Synthesis of $[PPN][Ph_3PMo(CO)_4(COOCH_3)]$

$Ph_3PMo(CO)_5$ (1 g, 2.007 mmol) was dissolved in 20 ml dry THF. [PPN][OCH_3] methanolic solution (3ml, 6.021 mmol) was added. The mixture was stirred at room temperature for 16 hours. A creamy solution was formed and dried under vacuum to form a cream white solid. M.p. = 124-126 ^oC; IR (νCO) (ATR, cm^{-1}) 2073(m), 1994(m), 1913(vs), 1890(sh), 1600(sh), 1592(s). ^1H NMR (DMSO-d_6, ppm): [δ] 3.16 (s, 3H), 7.2-7.6 (m, 15H, J_{H-H} = 8.26 Hz). ^{13}C NMR (DMSO-d_6, ppm): [δ] 48.5 (CH_3), 128-156 (Ph), 170 ($COOCH_3$), 207 (d, J= 8.90 Hz), 211 (d, J= 22 Hz) (terminal CO).

5.3.15 Synthesis of $[CpMo(CO)_3]_2$

$Mo(CO)_6$ (21.0 g, 600 mmol) was added to a 50 ml THF solution of NaCp. The mixture was refluxed for 14 hours to form a reddish-brown solution. 250 ml water solution of ferric sulphate (20 g) was acidified by 15 ml of acetic acid, then mixed with the reddish-brown solution over 30 minutes. Fine purple crystals of $[CpMo(CO)_3]_2$ precipitated and were filtered off, washed with water, methanol and pentane then dried. The product was purified by recrystallization in acetone.

5.3.16 Synthesis of $CpMo(CO)_3I$

$[CpMo(CO)_3]_2$ (0.82 g, 1.674 mmol) was dissolved in 100 ml of deoxygenated CH_2Cl_2. I_2 (2 g, 11.4 mmol) was dissolved in 2 ml of CH_2Cl_2 and added to the solution of $[CpMo(CO)_3]_2$, the mixture was then stirred for 30 min at room temperature. $Na_2S_2O_3$ (2 g, 12.65 mmol) was dissolved in 10 ml of deionised water and added to the CH_2Cl_2 solution. The mixture formed two

layers which were separated by a separating funnel and the organic layer was dried by adding anhydrous $MgSO_4$. The organic solution was then evaporated to dryness under vacuum to produce a dark-red solid (0.42 g). IR (CH_2Cl_2, cm^{-1}) (νCO) 2042(s), 1966(s). ^{13}C NMR ($CDCl_3$, ppm): [δ] 90 (Cp), 206 (CO).

5.3.17 Synthesis of [CpMo(CO)$_3$][OTf]

$CpMo(CO)_3I$ (0.1 g, 26.88 mmol) was dissolved in 50 ml CH_2Cl_2. AgOTf (0.14 g, 53.80 mmol) was added, the mixture was stirred for 5 hours under argon atm to form a dark purple solution and brown (AgI) precipitate. The solution was filtered by cannula and dried under vacuum. A dark-purple product (60 mg) was obtained. IR (CH_2Cl_2, cm^{-1}) (νCO) 2070(s), 1992(s, br).

5.3.18 Synthesis of [CpMo(CO)$_3$(PPh$_3$)][OTf]

$[CpMo(CO)_3][OTf]$ (0.32 g, 80.65 mmol) was dissolved in 20 ml CH_2Cl_2. PPh_3 (0.4 g, 80.65 mmol) was added. The reaction was stirred overnight at room temperature to form a light yellowish-brown solution. A yellow solid was precipitated by adding a mixture of Et_2O and hexane in a ratio of 10:1. The solid was filtered and dried under vacuum. IR (CH_2Cl_2, cm^{-1}) (νCO) 2060(s), 1999(m), 1979(s).

5.3.19 Synthesis of CpMo(CO)$_2$(PPh$_3$)(COOCH$_3$)

$[CpMo(CO)_3(PPh_3)][OTf]$ (0.38 g, 57.84 mmol) was dissolved in 40 ml CH_2Cl_2. CH_3ONa (0.30 g, 55.53 mmol) was added to the CH_2Cl_2 solution of $[CpMo(CO)_3(PPh_3)][OTf]$. 20 drops of dry methanol were added and the solution was stirred for 1h 30 min at room temperature. The solvent was dried under vacuum to yield a yellow solid (0.18 g). IR (νCO) (CH_2Cl_2, cm^{-1}) 1958(m), 1875(s), 1610(m). ^1H NMR (acetone-d_6, ppm): [δ] 3.49 (s, 3H), 5.15 (s, 5H), 7.2-7.6 (m, 15H, J_{H-H} = 8.26 Hz). ^{13}C NMR (acetone-d_6, ppm): [δ] 69.7 (CH_3), 95.7 (Cp), 120-140 (Ph), 209, 240 (CO).

5.3.20 Synthesis of CpMo(CO)$_2$(PPh$_3$)(COOCH$_2$CH$_3$)

$[CpMo(CO)_3(PPh_3)][OTf]$ (0.1 g, 0.1523 mmol) was dissolved in 40 ml CH_2Cl_2. CH_3CH_2ONa (0.1 g, 1.470 mmol) was added to the CH_2Cl_2 solution of $[CpMo(CO)_3(PPh_3)][OTf]$. 6 drops of

dry ethanol were added and the solution was stirred for 1h 30 min at room temperature. The solvent was dried under vacuum to yield a yellow solid (0.18g). IR (CH_2Cl_2, cm^{-1}) *v*(CO) 1954(m), 1875(s), 1612(m). ^1H NMR (CD_2Cl_2, ppm): [δ] 1.2 (t, 3H, J_{H-H} = 2.25 Hz), 4.0 (q, 2H, J_{H-H} = 7.28 Hz), 5.08 (d, 5H, J_{H-H} = 1.62 Hz), 7.2-7.6 (m, 15H, J_{H-H} = 8.26 Hz).

5.4 Experimental methods for the Data discussed in Chapter 4

5.4.1 Synthesis of [PPN][Mo(CO)$_5$(COOCH(CH$_3$)$_2$)]

Anhydrous PPNCl (1 g, 1.742 mmol) was dissolved in dry isopropanol (20 ml) in a Schlenk-tube and a solution of [$NaOCH(CH_3)_2$] (0.14 g, 1.742 mmol) in isopropanol (2 ml) was added. The mixture was stirred and warmed until a white NaCl precipitate was formed. $Mo(CO)_6$ (0.46 g, 1.742 mmol) was added and the mixture was refluxed for 35 min until a yellow solution formed. The resulting solution was cooled, and then filtered by cannula to another Schlenk tube leaving a yellowish brown precipitate. The yellow solution was evaporated under vacuum until a yellow oily product was formed. The oil was triturated with hexane until a yellow solid formed, which was then dried under *vacuum* to yield 0.78 g (52%) of yellow product. Mp. 204-205 ^oC. Elemental analyses, Calculated: %C = 62.73; %H = 4.33; % N = 1.63. Found: %C = 62.66; %H = 4.81; % N = 1.91. The $[Ph_4As]^+$ complex was obtained by a similar procedure using Ph_4AsCl instead of PPNCl. 0.49 g (33 %) of a yellow-brown precipitate was obtained. IR (CH_3OH, cm^{-1}) *v*(CO) 2042(w), 1942(s), 1880(m), 1665(m, br), 1589(m). ^1H NMR (CD_3OD, ppm): [δ] 1.13 (*d,* 6H, J_{H-H} = 6.06 Hz), 3.91 (*q,* 1H, J_{H-H} = 6.20 Hz), 7.2-7.6 (m, 15H, J_{H-H} = 8.26 Hz). ^{13}C NMR (CD_3OD, ppm): [δ] 25 ($CH(CH_3)_2$), 65 ($CH(CH_3)_2$, 128-135 (*m,* Ph), 170 ($COOCH_3$), 202**,** 210 (CO).

5.4.2 Synthesis of [PPN][Mo(CO)$_5$(COOCH$_2$CH$_3$)]

This compound was prepared as described for the isopropyl derivative, but using dry ethanol (20 ml) and NaOEt. PPNCl (1 g, 1.742 mmol) and NaOEt (0.12 g,1.742 mmol) in ethanol (20 ml) were first warmed then stirred until a white NaCl precipitate was formed, followed by addition of an equimolar amount of $Mo(CO)_6$, then the mixture was refluxed for 35 min. A dark yellow solid was obtained (0.74 g, 50 %). Mp. 230-231 ^oC. Elemental analysis data, Calculated: %C= 62.35; %H= 4.16; %N= 1.65. Found: %C= 61.83; %H= 4.86; %N= 1.83. IR (CH_3OH, cm^{-1}) *v*(CO) 2043(w), 1938(vs), 1871(m), 1656(s,br), 1590(m). ^1H NMR (CD_3OD, ppm): [δ] 1.12 (*t,* 3H, J_{H-H}

= 2.25 Hz), 3.57 (*q,* 2H, J_{H-H} = 7.28 Hz), 7.2-7.6 (*m,* 15H, J_{H-H} = 8.26 Hz). ^{13}C NMR (CD_3OD, ppm): [δ] 18 (CH_3), 58 (CH_2), 126-137 (m, Ph), 170 ($COOCH_2CH_3$), 202, 210 (CO).

5.4.3 Synthesis of [PPN][Mo(CO)$_5$(COOCH$_3$)]

This compound was prepared as described for the isopropyl and ethyl derivatives but using dry methanol (20 ml) and NaOMe. PPNCl (1 g ,1.742 mmol) and 0.16 g (1.742 mmol) of NaOMe in methanol (20 ml) were first warmed then stirred until a white NaCl precipitate is formed, followed by addition of an equimolar amount of $Mo(CO)_6$ then refluxed for 35 min. Adark yellow solid was obtained (1.02 g, 70 %). Mp. 214-215 ^{o}C. IR (CH_3OH, cm^{-1}) *ν*(CO) 2065(w), 1930(vs), 1864(m), 1644(m,br), 1590(m). ^{1}H NMR (CD_3OD, ppm): [δ] 3.34(*s,* 3H), 7.2-7.6(*m,* 15 H, J_{H-H} = 8.26 Hz). ^{13}C NMR (CD_3OD, ppm): [δ] 49 (CH_3), 127-134 (m, Ph), 170 ($COOCH_3$), 202, 206 (CO).

5.4.4 Synthesis of [Ph$_4$As]$_2$[Mo(CO)$_4$(COOCH(CH$_3$)$_2$)$_2$]

$NaOCH(CH_3)_2$ (0.58 g, 6.968 mmol) was dissolved in 20 ml of dry isopropanol. Ph_4AsCl (1.5 g, 6.968 mmol) was added, the mixture was then warmed while stirring for 30 min to form a white NaCl precipitate. This was followed by addition of $Mo(CO)_6$ (0.46 g, 1.742 mmol) then refluxed for 30 min. The ratio of $Mo(CO)_6$ to $NaOCH(CH_3)_2$ used was 1:4. A dark brown precipitate was formed and separated by cannula, then triturated with hexane to remove isopropanol. 0.94 g (47 %) of the product was obtained. Mp. 310 ^{o}C (dec). IR (CH_3OH, cm^{-1}) *ν*(CO) 2074(vw), 1939(s), 1871(m), 1708(m), 1659(m,br). ^{1}H NMR (CD_3OD, ppm): [δ] 1.15 (*d,* 6H, J_{H-H} = 6.06 Hz), 3.92 (*q,* 1H, J_{H-H} = 6.20 Hz), 7.2-7.6 (m, 15H). ^{13}C NMR (CD_3OD, ppm): [δ] 25 ($CH(CH_3)_2$), 65 ($CH(CH_3)_2$), 130-140 (m, Ph, J_{H-H} = 8.26 Hz), 161 ($COOCH(CH_3)_2$), 170 ($COOCH(CH_3)_2$), 202, 207 ($Mo(CO)_4$).

5.4.5 Blank catalytic testing of [PPN][Mo(CO)$_5$(COOCH$_3$)], methanol effect in the production of methyl formate

[PPN][$Mo(CO)_5(COOCH_3)$] (0.23 g, 0.2669 mmol) was dissolved in 20 ml of dry methanol. The reactor was heated for 24 hours at 160 ^{o}C in an oil bath. After the reaction, the reactor was cooled to room temperature by dipping it in ice bath. The organic products were analyzed by gas chromatography and GC-mass spectroscopy.

5.4.6 Catalytic testing of [PPN][$Mo(CO)_5(COOCH_3)$] under hydrogen in methanol

[PPN][$Mo(CO)_5(COOCH_3)$] (0.23 g, 0.2669 mmol) was dissolved in 20 ml of dry methanol. The reactor was then purged three times with hydrogen and charged to a pressure of 1200 kPa. The reactor was heated for 24 hours at 160 ^oC in an oil bath. After the reaction, the reactor was cooled to room temperature by dipping it in ice bath. The organic products were analyzed by gas chromatography and GC-mass spectroscopy.

5.4.7 Catalytic testing of [PPN][$Mo(CO)_5(COOCH_3)$] under syngas (1:1) in methanol

[PPN][$Mo(CO)_5(COOCH_3)$] (0.23 g, 0.2669 mmol) was dissolved in 20 ml of dry methanol. The reactor was then purged three times with synthesis gas (syngas) and charged to a pressure of 1600 kPa. The reactor was heated for 24 hours at 160 ^oC in an oil bath. After the reaction, the reactor was cooled to room temperature by dipping it in ice bath. The organic products were analyzed by gas chromatography and GC-mass spectroscopy.

5.4.8 Catalytic testing of [PPN][$Mo(CO)_5(COOCH_3)$] under syngas (1:1) in THF

[PPN][$Mo(CO)_5(COOCH_3)$] (0.23 g, 0.2669 mmol) was dissolved in 20 ml of dry THF. The reactor was then purged three times with synthesis gas (syngas) and charged to a pressure of 1600 kPa. The reactor was heated for 24 hours at 160 ^oC in an oil bath. After the reaction, the reactor was cooled to room temperature by dipping it in ice bath. The organic products were analyzed by gas chromatography and GC-mass spectroscopy.

5.4.9 Catalytic testing of [PPN][$Mo(CO)_5(COOCH_3)$] + $KOCH_3$ under syngas (1:1) in THF

[PPN][$Mo(CO)_5(COOCH_3)$] (0.23 g, 0.2669 mmol) was dissolved in 20 ml of dry THF. Potassium methoxide solution (5 ml, 1.25 g, 17.5 mmol) was added to the [PPN][$Mo(CO)_5(COOCH_3)$] solution and transferred to a pipe reactor. The reactor was then purged three times with synthesis gas (syngas) and charged to a pressure of 1600 kPa. The reactor was heated for 24 hours at 160 ^oC in an oil bath. After the reaction, the reactor was

cooled to room temperature by dipping it in ice bath. The organic products were analyzed by gas chromatography and GC-mass spectroscopy.

5.4.9.1 Synthesis of [*n*-$Bu_4N]_2[Mo_6O_{19}$]

MoO_3 (1 g, 6.947 mmol) was added to 50 ml round bottom flask. *n*-Bu_4NI (0.79 g, 2.319 mmol) was added to the round bottom flask. Dionized water (40 ml) was added and the mixture was refluxed for 4 hours to form a yellow-green precipitate. The precipitate was filtered by a crucible, washed with hot hexane and recrystallized in acetone and filtered again to remove excess MoO_3. 1.88 g of the product was obtained. IR (ATR, cm^{-1}) 1030(w), 987(w), 949(vs) ν(Mo-O) $_{\text{stretching}}$, 880(w), 789(vs, br) ν(Mo-O-Mo) $_{\text{bending}}$, 424(s) ν(Mo=O). Uv/Vis (CH_3CN, nm) 222.5, 258.9, 325.8.

6. CHAPTER 6

Conclusion and overview

Catalytic carbonylation of methanol by $KOCH_3$ or $NaOCH_3$ is a well known process commerciallised by BASF. From the claims made by BNL, this process is clearly dominating in the production of methyl formate, and this is also shown in the study of Ohyama *et al*. for the effects of group 6 metal carbonyl compounds in the production of methanol and methyl formate under syngas.

The role played by $Mo(CO)_6$ in the $KOCH_3$ catalysed carbonylation of methanol to methyl formate was studied extensively in the work reported in this thesis by using HPIR, IR and NMR spectroscopy. The results presented here shows a slight increase in the amount of methyl formate due to $Mo(CO)_6$, while dimethyl ether was observed even without the addition of $Mo(CO)_6$.

Addition of $Mo(CO)_6$ to the methoxide carbonylation ($Mo(CO)_6/KOCH_3$) (1:4) of methanol reaction under CO atmosphere slightly increased the amount of methyl formate produced compared to the $KOCH_3$ catalyst. The effect of solvent was very significant in the methoxide carbonylation of methanol. A catalytic reaction performed in methanol yielded more methyl formate than a reaction performed in THF and triglyme. There are probably two reasons for a high yield of methyl formate in methanol: (i) the first possibility is the regeneration of the methoxide ion (CH_3O^-), and (ii) the second possibility is the ability of methanol to protonate the metalloester $[(CO)_5Mo(COOCH_3)^-]$ to eliminate methyl formate which cannot occur in THF and triglyme.

The same solvent effect was observed under H_2, syngas and N_2. The catalytic reaction of $Mo(CO)_6$ with $KOCH_3$ ($Mo(CO)_6/KOCH_3$) under a H_2 atmosphere produced methyl formate and the amount produced was also dependant on the solvent. The reaction performed in methanol also produced slightly more methyl formate than in THF and triglyme. Addition of hydrogen in the reaction ($Mo(CO)_6/KOCH_3$) produced comparable amounts of methyl formate as for the reaction performed under CO. Addition of $Mo(CO)_6$ to the methoxide carbonylation ($Mo(CO)_6/KOCH_3$) of methanol reaction under syngas (1:1) produces more methyl formate than carbonylation with the $KOCH_3$ catalyst. Comparing the amount of methyl formate produced under CO and syngas in methanol showed more methyl formate produced under synags than under a CO atmosphere. This is probably due to the hydrogen in syngas which assists in the

hydrogenation of the metalloester. A stoichiometric increase in the $Mo(CO)_6$ ratio under syngas (1:1) increased the amount of methyl formate produced, with a 1:2 ratio of $Mo(CO)_6/KOCH_3$ producing more methyl fomate compared to other ratios. Longer chain (C2-C5) alcohols were also produced in triglyme under syngas.

HP-IR studies of $Mo(CO)_6/KOCH_3$ (1:5) performed under CO atmosphere showed the metalloester, which diminishes and eliminates methyl formate and regenerates $Mo(CO)_6$. If the same reaction is performed under H_2 atmosphere, a metalloester is formed then diminishes to form the bridged hydride μ-$HMo_2(CO)_{10}^-$. Addition of excess CH_3O^- under H_2 atmosphere results in the formation of a *bis*(methoxycarbonyl) complex characterized by ester peaks at 1680 cm^{-1} and 1600 cm^{-1}. A peak characteristic of a mono hydride species was only observed at higher temperatures (100 ^oC).

HP-IR studies of $Mo(CO)_6/KOCH_3$ (1:5) under syngas also showed the formation of a metalloester and after some time a bridged hydride (μ-$HMo_2(CO)_{10}^-$) which also disappeared after few minutes of the reaction to form a methoxide complex ($Mo(CO)_5OCH_3^-$) as the final organometallic product of the reaction. It is interesting to note that a *bis*(methoxycarbonyl) complex was not observed under CO atmosphere, which implies that some excess CH_3O^- catalyzes the carbonylation reaction to form methyl formate. There were no other organic products observed under syngas atmosphere after the reaction in THF/MeOH mixture.

Metal carbonyl compounds ($Mo(CO)_6$, $Ph_3PMo(CO)_5$ and $[CpMo(CO)_3][OTf]$) reacted with nucleophiles (alkoxides) to form alkoxycarbonyl complexes, also known as metalloesters compounds ($Mo\text{-}COOCH_3$). The reaction of $Mo(CO)_6$ with methoxide ($NaOCH_3$ or $KOCH_3$) resulted in the formation of water soluble complexes which were characterized as $K[Mo(CO)_5(COOCH_3)]$ or $Na[Mo(CO)_5(COOCH_3)]$. The same types of complexes were obtained when bulkier nucleophiles ($(CH_3)_3COK$, $CH_3CH_2(CH_3)_2COK$) were used. Attempts to grow crystals suitable for X-ray crystallography from the reaction product of *t*-amyloxide with $Mo(CO)_6$ resulted in the formation of a novel oxaloto molybdenum cluster with an octahedral Mo surrounded by oxygen atoms.

Addition of crown ethers (18-crown-6 and 15-crown-5) to $K[Mo(CO)_5(COOCH_3)]$ in THF improved its solubility in organic solvents, and the IR data (**Table 2**) supported the formation of the proposed compound. This supports the belief that the potassium cation was tightly bound to the anion $[Mo(CO)_5(COOCH_3)]^-$ to form the water soluble salt.

Metathesis of $K[Mo(CO)_5(COOCH_3)]$ with bulkier counter ions (Et_4NCl, PPNCl and *n*-Bu_4NI) was not successful, due to the poor solubility of the potassium complex in the organic solvents, such as $CHCl_3$, MeOH, DMSO, DMF, THF and others. Apart from the poor solubility there is also the fact that the interaction of potassium as opposed to the ammonium cation would have been favoured, hence thermodynamically the metathesis reaction was not significantly viable. However, an alternative synthesis of the PPN and *n*-Bu_4N alkoxycarbonyl complexes by reaction of $[PPN][OCH_3]$ and/or $[n\text{-}Bu_4N][OCH_3]$ with $Mo(CO)_6$ was successful, but required longer reaction times at room temperature. There was a small shift in the IR peak positions of $[PPN][Mo(CO)_5(COOCH_3)]$ compared to $[n\text{-}Bu_4N][Mo(CO)_5(COOCH_3)]$ due to the counterion effect; solubility and stability of the compounds was also improved by the introduction of bulkier counter ions. The ligand substitution of CO in $Mo(CO)_6$ by PPh_3 improved the stability and solubility of the metalloester compounds formed. Successful synthesis of $K[Ph_3PMo(CO)_4(COOCH_3)]$ was only achievable at a stoichiometric ratio of 1:3. The metathesis of $K[Ph_3PMo(CO)_4(COOCH_3)]$ with PPNCl was unsuccessful. Its PPN analogue was also achieved by reacting $[PPN][OCH_3]$ with $PPh_3Mo(CO)_5$ for 17 hours at room temperature.

Cp type metalloesters ($CpMo(CO)_2(PPh_3)COOCH_3$ and $CpMo(CO)_2(PPh_3)COOCH_2CH_3$ derivatives) were successfully synthesized and characterized but found to be thermally unstable. Their solubility in organic solvents improved e.g CH_2Cl_2 & MeOH, but no crystals could be grown.

Another method for the synthesis of molybdenum alkoxycarbonyl complexes ($Mo(CO)_5(COOR)^-$) was developed by using methoxide, ethoxide and isopropoxide as nucleophiles in respective alcoholic solvents. Reaction of molybdenum hexacarbonyl with nucleophiles RO^- [R= CH_3, CH_2CH_3, $CH(CH_3)_2$)] under refluxing conditions gave alkoxycarbonyl complexes. Relative to the free CO, metal coordinated carbon monoxide was strongly activated by the alkoxides. The solvent polarity did not influence the rate of reaction under reflux. During the synthesis of alkoxycarbonyl complexes, a molybdenum alkoxide complex, $[Mo(CO)_5(OCH(CH_3)_2)]^-$, was formed through a direct substitution of CO by isopropoxide which competed with the nucleophilic attack to form the alkoxycarbonyl complex. This was also observed with ethoxide. Addition of excess isopropoxide ($[Ph_4As][OCH(CH_3)_2]$ to $Mo(CO)_6$ solution resulted in the formation of a *bis*(isopropoxycarbonyl) complex. All mono substituted alkoxycarbonyl complexes ($Mo(CO)_5(COOR)^-$, R= Me, Et and ^{i}Pr), on standing under a CO atmosphere, decarbonylate to molybdenum alkoxide complexes $(Mo(CO)_5OR)^-$.

The mono substituted isopropoxycarbonyl complex ($Mo(CO)_5(COO^iPr)^-$) slowly decarbonylates on standing in solution to form the molybdenum isopropoxide complex ($Mo(CO)_5O^iPr)^-$ even under CO atmosphere. The molybdenum isopropoxide complex in solution further decarbonylates to form the stable molybdenum oxo cluster, $[PPN]_2[Mo_6O_{19}]$, when exposed to ambient light. A tetraethylammonium pentacarbonyl molybdenum methoxycarbonylato derivative, $[Et_4N][Mo(CO)_5(COOCH_3)]$, also decomposed in solution to form an oxo cluster compound, $[Et_4N]_2[Mo_4O_{13}]$. However, this cluster does not have a centered oxygen atom.

There is a significant role played by the methoxycarbonyl intermediate ($Mo(CO)_5(COOCH_3)^-$) in the production of methyl formate from $Mo(CO)_6$ and $KOCH_3$. Addition of potassium methoxide to a methanolic solution of ($[PPN][Mo(CO)_5(COOCH_3)]$) under syngas increased the conversion of syngas from 6% to 32 % and the amount of methyl formate produced. HPIR studies of $[PPN][Mo(CO)_5(COOCH_3)]$ under syngas suggest a decomposition of the metalloester with the formation of $Mo(CO)_6$. A possible mechanism for the formation of methyl formate from $[PPN][Mo(CO)_5(COOCH_3)]$ involves the breakdown of the metalloester through protonation by methanol to eliminate the $Mo(CO)_5$ intermediate (**Scheme 6.1**). The $Mo(CO)_5$ intermediate is then carbonylated to form $Mo(CO)_6$.

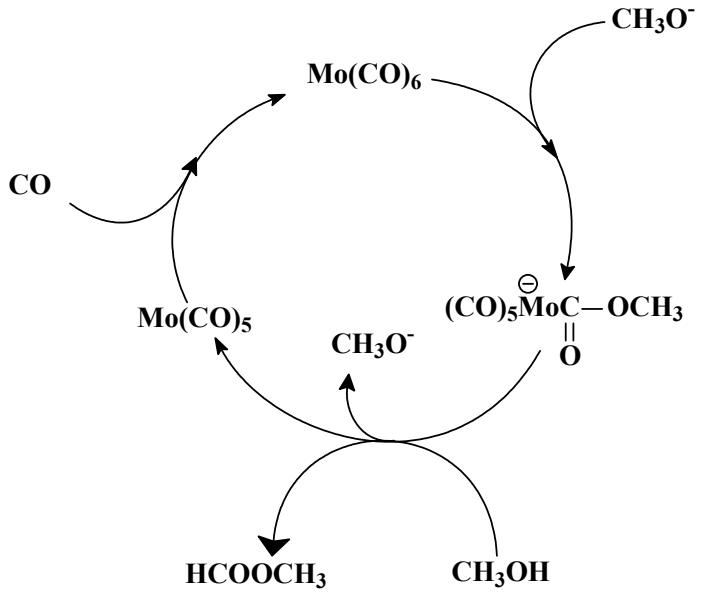

Scheme 6.1: Mechanistic formation of methyl formate from $Mo(CO)_6/KOCH_3$ under syngas *via* $[PPN][Mo(CO)_5(COOCH_3)]$ intermediate.

7. APPENDICES

Appendix 1

Crystal structure data pattern for chapter 3

Crystal data and structure refinement for $[CpMo(CO)_2(P(CH_3)_3)_2][CF_3SO_3]$

$[Mo(C_5H_5)(CO)_2(C_3H_9P)_2][CF_3SO_3]$	$F000 = 1048$
$Mr = 518.26$	$Dx = 1.677$ Mg m^{-3}
Monoclinic, $P21/n$	Mo $K\alpha$ radiation
	$\lambda = 0.71073$ Å
Hall symbol: -P 2yn	Cell parameters from 6234 reflections
$a = 10.8919$ (5) Å	$\theta = 1.8–28.0^o$
$b = 8.0864$ (3) Å	$\mu = 0.94$ mm−1
$c = 23.4132$ (10) Å	$T = 296$ (2) K
$\beta = 95.464$ (1)º	Block, yellow
$V = 2052.78$ (15) Å^3	0.48 × 0.23 × 0.16 mm
$Z = 4$	

Data collection

Bruker SMART CCD area-detector diffractometer	4960 independent reflections
Radiation source: fine-focus sealed tube	4542 reflections with $I > 2\sigma(I)$
Monochromator: graphite	Rint = 0.042
$T = 296(2)$ K	$\theta_{max} = 28.0^o$
φ and ω scans	$\theta_{min} = 1.8^o$
Absorption correction: integration (SADABS; Bruker, 2005)	$h = -14\rightarrow14$
Tmin = 0.660, Tmax = 0.864	$k = -10\rightarrow10$
20835 measured reflections	$l = -29\rightarrow30$
Refinement	
Refinement on $F2$	Secondary atom site location: difference Fourier map

Least-squares matrix: full	Hydrogen site location: inferred from neighbourin sites
$R[F2 > 2\sigma(F2)] = 0.024$	H-atom parameters constrained
$wR(F2) = 0.05$	$w = 1/[\sigma2(Fo^2) + (0.0157P)^2 + 1.38P]$ where $P = (Fo^2 + 2Fc^2)/3$
$S = 1.09$	$(\Delta/\sigma)max = 0.003$
4960 reflections	$\Delta\rho max = 0.43$ e Å−3
241 parameters	$\Delta\rho min = -0.48$ e Å−3
Primary atom site location: structure-invariant direct methods	Extinction correction: none

Table 1: Bond lengths [Å] for $[CpMo(CO)_2(P(CH_3)_3)_2][CF_3SO_3]$

Bond	Length (Å)	Bond	Length (Å)
Mo1—C17	1.9581 (19)	C14—H14	0.9500
Mo1—C16	1.9683 (19)	C12—C13	1.400 (3)
Mo1—C13	2.3123 (19)	C12—C11	1.407 (3)
Mo1—C14	2.314 (2)	C12—H12	0.9500
Mo1—C15	2.3346 (19)	C21—H21A	0.9800
Mo1—C12	2.3348 (19)	C21—H21B	0.9800
Mo1—C11	2.362 (2)	C21—H21C	0.9800
Mo1—P12	2.4729 (5)	C31—H31A	0.9800
Mo1—P13	2.4751 (5)	C31—H31B	0.9800
S4—O42	1.4379 (14)	C31—H31C	0.9800
S4—O41	1.4384 (15)	C11—C15	1.406 (3)
S4—O43	1.4408 (15)	C11—H11	0.9500
S4—C41	1.826 (2)	C15—H15	0.9500
P12—C21	1.804 (2)	C32—H32A	0.9800
P12—C22	1.814 (2)	C32—H32B	0.9800
P12—C23	1.815 (2)	C32—H32C	0.9800
P13—C31	1.812 (2)	C22—H22A	0.9800
P13—C32	1.8122 (19)	C22—H22B	0.9800
P13—C33	1.815 (2)	C22—H22C	0.9800
O11—C16	1.152 (2)	C33—H33A	0.9800
O12—C17	1.150 (2)	C33—H33B	0.9800
F42—C41	1.323 (3)	C33—H33C	0.9800
F43—C41	1.341 (3)	C13—H13	0.9500
F41—C41	1.321 (3)	C23—H23A	0.9800
C14—C13	1.399 (3)	C23—H23B	0.9800
C14—C15	1.403 (3)	C23—H23C	0.9800

Table 2: Bond angles [degrees] for $[CpMo(CO)_2(P(CH_3)_3)_2][CF_3SO_3]$

Bonds	Angles (degrees)	Bonds	Angles (degrees)
C17—Mo1—C16	108.55 (8)	C11—C12—H12	125.9
C17—Mo1—C13	99.54 (8)	Mo1—C12—H12	120.6
C16—Mo1—C13	145.16 (8)	P12—C21—H21A	109.5
C17—Mo1—C14	95.73 (8)	P12—C21—H21B	109.5
C16—Mo1—C14	151.85 (8)	H21A—C21—H21B	109.5
C13—Mo1—C14	35.22 (8)	P12—C21—H21C	109.5
C17—Mo1—C15	123.82 (9)	H21A—C21—H21C	109.5
C16—Mo1—C15	116.75 (8)	H21B—C21—H21C	109.5
C13—Mo1—C15	58.33 (7)	P13—C31—H31A	109.5
C14—Mo1—C15	35.14 (9)	P13—C31—H31B	109.5
C17—Mo1—C12	131.26 (8)	H31A—C31—H31B	109.5
C16—Mo1—C12	110.69 (8)	P13—C31—H31C	109.5
C13—Mo1—C12	35.06 (8)	H31A—C31—H31C	109.5
C14—Mo1—C12	58.41 (8)	H31B—C31—H31C	109.5
C15—Mo1—C12	58.10 (7)	C15—C11—C12	107.4 (2)
C17—Mo1—C11	153.87 (8)	C15—C11—Mo1	71.51 (11)
C16—Mo1—C11	97.31 (8)	C12—C11—Mo1	71.51 (11)
C13—Mo1—C11	58.21 (8)	C15—C11—H11	126.3
C14—Mo1—C11	58.30 (9)	C12—C11—H11	126.3
C15—Mo1—C11	34.84 (9)	Mo1—C11—H11	122.4
C12—Mo1—C11	34.86 (7)	F41—C41—F42	107.85 (19)
C17—Mo1—P12	75.35 (5)	F41—C41—F43	107.34 (19)
C16—Mo1—P12	75.84 (5)	F42—C41—F43	107.02 (19)
C13—Mo1—P12	92.28 (5)	F41—C41—S4	111.54 (16)
C14—Mo1—P12	125.47 (6)	F42—C41—S4	111.43 (15)
C15—Mo1—P12	145.32 (5)	F43—C41—S4	111.42 (15)
C12—Mo1—P12	87.35 (5)	C14—C15—C11	108.34 (19)
C11—Mo1—P12	115.83 (6)	C14—C15—Mo1	71.62 (11)
C17—Mo1—P13	76.49 (5)	C11—C15—Mo1	73.65 (11)
C16—Mo1—P13	75.55 (5)	C14—C15—H15	125.8
C13—Mo1—P13	132.34 (6)	C11—C15—H15	125.8
C14—Mo1—P13	97.26 (6)	Mo1—C15—H15	120.6
C15—Mo1—P13	84.17 (5)	O12—C17—Mo1	176.13 (18)
C12—Mo1—P13	140.93 (5)	P13—C32—H32A	109.5
C11—Mo1—P13	107.38 (6)	P13—C32—H32B	109.5
P12—Mo1—P13	130.342 (16)	H32A—C32—H32B	109.5
O42—S4—O41	115.43 (10)	P13—C32—H32C	109.5
O42—S4—O43	115.41 (9)	H32A—C32—H32C	109.5
O41—S4—O43	114.49 (10)	H32B—C32—H32C	109.5
O42—S4—C41	102.81 (10)	O11—C16—Mo1	177.79 (17)
O41—S4—C41	103.07 (10)	P12—C22—H22A	109.5
O43—S4—C41	103.04 (10)	P12—C22—H22B	109.5
C21—P12—C22	104.03 (11)	H22A—C22—H22B	109.5
C21—P12—C23	103.48 (11)	P12—C22—H22C	109.5
C22—P12—C23	101.91 (10)	H22A—C22—H22C	109.5
C21—P12—Mo1	112.96 (7)	H22B—C22—H22C	109.5

Table 2: Bond lengths [Å] for $[CpMo(CO)_2(P(CH_3)_3)_2][CF_3SO_3]$ continues

Bonds	Angles (degrees)	Bonds	Angles (degrees)
C22—P12—Mo1	116.01 (7)	P13—C33—H33A	109.5
C23—P12—Mo1	116.75 (8)	P13—C33—H33B	109.5
C31—P13—C32	103.58 (10)	H33A—C33—H33B	109.5
C31—P13—C33	103.56 (11)	P13—C33—H33C	109.5
C32—P13—C33	103.05 (10)	H33A—C33—H33C	109.5
C31—P13—Mo1	113.33 (7)	H33B—C33—H33C	109.5
C32—P13—Mo1	116.40 (7)	C14—C13—C12	108.3 (2)
C33—P13—Mo1	115.32 (8)	C14—C13—Mo1	72.45 (12)
C13—C14—C15	107.8 (2)	C12—C13—Mo1	73.35 (11)
C13—C14—Mo1	72.33 (11)	C14—C13—H13	125.9
C15—C14—Mo1	73.24 (12)	C12—C13—H13	125.9
C13—C14—H14	126.1	Mo1—C13—H13	120.1
C15—C14—H14	126.1	P12—C23—H23A	109.5
Mo1—C14—H14	120.2	P12—C23—H23B	109.5
C13—C12—C11	108.2 (2)	H23A—C23—H23B	109.5
C13—C12—Mo1	71.59 (11)	P12—C23—H23C	109.5
C11—C12—Mo1	73.63 (11)	H23A—C23—H23C	109.5
C13—C12—H12	125.9	H23B—C23—H23C	109.5

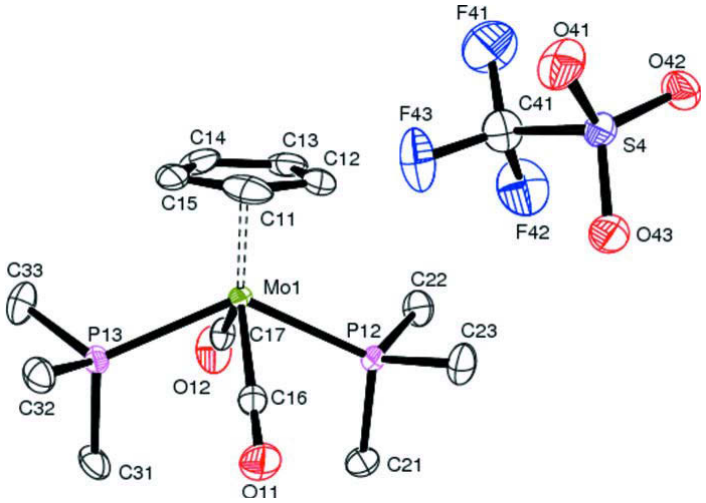

Appendix 2

Crystal structure data pattern for chapter 4

Crystal data and structure refinement for $[PPN]_2[Mo_6O_{19}]$

Identification code	$[PPN]_2[Mo_6O_{19}]$
Empirical formula	$C_{72}H_{60}Mo_6N_2O_{19}P_4$
Formula weight	1956.74
Temperature	173(2) K
Wavelength	0.71073 A
Crystal system, space group	Triclinic, P-1
Unit cell dimensions	a = 11.3053(3) Å α = 61.4760(10) deg.
	b = 13.4241(3) Å β = 84.5490(10) deg.
	c = 13.4928(3) Å γ = 87.8120(10) deg.
Volume	1790.96(7) A^3
Z, Calculated density	1, 1.814 Mg/m^3
Absorption coefficient	1.182 mm^{-1}
F(000)	970
Crystal size	0.53 x 0.45 x 0.17 mm
ϕ range for data collection	1.72 to 28.34 deg.
Limiting indices	$-13 \leq h \leq 15$, $-17 \leq k \leq 17$, $-17 \leq l \leq 17$
Reflections collected / unique	15084 / 8918 [R(int) = 0.0378]
Completeness to theta =	28.34 99.8 %
Absorption correction	Integration
Max. and min. transmission	0.8208 and 0.5737
Refinement method	Full-matrix least-squares on F^2
Data / restraints / parameters	8918 / 0 / 466
Goodness-of-fit on F^2	1.005
Final R indices [I>2sigma(I)]	R1 = 0.0295, wR2 = 0.0764
R indices (all data)	R1 = 0.0388, wR2 = 0.0925
Largest diff. peak and hole	0.526 and -0.781 $e.A^{-3}$

Table 3: Bond lengths [Å] for $[PPN]_2[Mo_6O_{19}]$

Bond	Length (Å)
C(1)-C(6)	1.386(4)
C(1)-C(2)	1.395(4)
C(1)-P(1)	1.791(3)
C(2)-C(3)	1.384(4)
C(2)-H(2)	0.9500
C(3)-C(4)	1.392(4)
C(3)-H(3)	0.9500
C(4)-C(5)	1.363(5)
C(4)-H(4)	0.9500
C(5)-C(6)	1.394(4)
C(5)-H(5)	0.9500
C(6)-H(6)	0.9500
C(7)-C(12)	1.391(4)
C(7)-C(8)	1.397(4)

Table 3: Bond lengths [Å] for $[PPN]_2[Mo_6O_{19}]$ continues

Bond	Length (Å)
C(7)-P(1)	1.797(3)
C(8)-C(9)	1.395(4)
C(8)-H(8)	0.9500
C(9)-C(10)	1.383(5)
C(9)-H(9)	0.9500
C(10)-C(11)	1.379(5)
C(10)-H(10)	0.9500
C(11)-C(12)	1.388(4)
C(11)-H(11)	0.9500
C(12)-H(12)	0.9500
C(13)-C(18)	1.389(4)
C(13)-C(14)	1.396(4)
C(13)-P(1)	1.803(3)

Table 3: Bond lengths [Å] for $[PPN]_2[Mo_6O_{19}]$ continues

Bond	Length (Å)
C(14)-C(15)	1.387(4)
C(14)-H(14)	0.9500
C(15)-C(16)	1.391(5)
C(15)-H(15)	0.9500
C(16)-C(17)	1.375(4)
C(16)-H(16)	0.9500
C(17)-C(18)	1.388(4)
C(17)-H(17)	0.9500
C(18)-H(18)	0.9500
C(19)-C(24)	1.400(4)
C(19)-C(20)	1.395(4)
C(19)-P(2)	1.790(3)
C(20)-C(21)	1.376(4)

Table 3: Bond lengths [Å] for $[PPN]_2[Mo_6O_{19}]$ continues

Bond	Length (Å)
C(20)-H(20)	0.9500
C(21)-C(22)	1.377(5)
C(21)-H(21)	0.9500
C(22)-C(23)	1.382(5
C(22)-H(22)	0.9500
C(23)-C(24)	1.379(5)
C(23)-H(23)	0.9500
C(24)-H(24)	0.9500
C(25)-C(26)	1.386(4)
C(25)-C(30)	1.398(4)
C(25)-P(2)	1.793(3)
C(26)-C(27)	1.385(4)
C(26)-H(26)	0.9500
C(27)-C(28)	1.382(5)

Table 3: Bond lengths [Å] for $[PPN]_2[Mo_6O_{19}]$ continues

Bond	Length (Å)
C(27)-H(27)	0.9500
C(28)-C(29)	1.375(4)
C(28)-H(28)	0.9500
C(29)-C(30)	1.389(4)
C(29)-H(29)	0.9500
C(30)-H(30)	0.9500
C(31)-C(32)	1.378(4)
C(31)-C(36)	1.398(4)
C(31)-P(2)	1.795(3)
C(32)-C(33)	1.404(4)
C(32)-H(32)	0.9500

Table 3: Bond lengths [Å] for $[PPN]_2[Mo_6O_{19}]$ continues

Bond	Length (Å)
C(33)-C(34)	1.365(5)
C(33)-H(33)	0.9500
C(34)-C(35)	1.368(5)
C(34)-H(34)	0.9500
C(35)-C(36)	1.390(5)
C(36)-H(36)	0.9500
C(35)-H(35)	0.9500
N(1)-P(1)	1.571(2)
N(1)-P(2)	1.566(2)
O(1)-Mo(2)	1.883(2)
O(1)-Mo(1)	1.966(2)

Table 3: Bond lengths [Å] for $[PPN]_2[Mo_6O_{19}]$ continues

Bond	Length (Å)
O(2)-Mo(1)	1.684(2)
O(3)-Mo(1)	1.875(2)
O(3)-Mo(2)1	1.956(2)
O(4)-Mo(2)1	2.2994(2)
O(4)-Mo(2)	2.2994(2)
O(4)-Mo(3)1	2.3255(2)
O(4)-Mo(3)	2.3255(2)
O(4)-Mo(1)1	2.3281(2)
O(4)-Mo(1)	2.3281(2)
O(5)-Mo(2)	1.679(2)
O(6)-Mo(1)	1.878(2)

Table 3: Bond lengths [Å] for $[PPN]_2[Mo_6O_{19}]$ continues

Bond	Length (Å)
O(6)-Mo(3)	1.990(2)
O(7)-Mo(3)	1.861(2)
O(7)-Mo(2)	2.006(2)
O(8)-Mo(3)	1.8694(19)
O(8)-Mo(1)1	1.986(2)
O(9)-Mo(2)1	1.858(2)
O(9)-Mo(3)	1.994(2)
O(10)-Mo(3)	1.690(2)
Mo(1)-O(8)1	1.986(2)
Mo(2)-O(9)1	1.858(2)
Mo(2)-O(3)1	1.956(2)

Table 4: Bond angles for $[PPN]_2[Mo_6O_{19}]$ in degrees

Bonds	Angle (degrees)
C(6)-C(1)-C(2)	119.9(3)
C(6)-C(1)-P(1)	119.1(2)
C(2)-C(1)-P(1)	121.0(2)
C(3)-C(2)-C(1)	120.0(3)
C(3)-C(2)-H(2)	120.0
C(1)-C(2)-H(2)	120.0
C(2)-C(3)-C(4)	119.5(3)
C(2)-C(3)-H(3)	120.2
C(4)-C(3)-H(3)	120.2
C(5)-C(4)-C(3)	120.5(3)
C(5)-C(4)-H(4)	119.8
C(3)-C(4)-H(4)	119.8
C(4)-C(5)-C(6)	120.6(3)
C(4)-C(5)-H(5)	119.7
C(6)-C(5)-H(5)	119.7
C(1)-C(6)-C(5)	119.4(3)
C(1)-C(6)-H(6)	120.3
C(5)-C(6)-H(6)	120.3

Table 4: Bond angles for $[PPN]_2[Mo_6O_{19}]$ in degrees

Bonds	Angle (degrees)
C(12)-C(7)-C(8)	119.6(3)
C(12)-C(7)-P(1)	122.5(2)
C(8)-C(7)-P(1)	117.9(2)
C(7)-C(8)-C(9)	119.4(3)
C(7)-C(8)-H(8)	120.3
C(9)-C(8)-H(8)	120.3
C(10)-C(9)-C(8)	120.2(3)
C(10)-C(9)-H(9)	119.9
C(8)-C(9)-H(9)	119.9
C(9)-C(10)-C(11)	120.6(3)
C(9)-C(10)-H(10)	119.7
C(11)-C(10)-H(10)	119.7
C(10)-C(11)-C(12)	119.6(3)
C(10)-C(11)-H(11)	120.2
C(12)-C(11)-H(11)	120.2
C(7)-C(12)-C(11)	120.5(3)
C(7)-C(12)-H(12)	119.7
C(11)-C(12)-H(12)	119.7

Table 4: Bond angles for $[PPN]_2[Mo_6O_{19}]$ in degrees continues

Bonds	Angle (degrees)
C(18)-C(13)-C(14)	119.6(3)
C(18)-C(13)-P(1)	121.0(2)
C(14)-C(13)-P(1)	119.5(2)
C(15)-C(14)-C(13)	120.0(3)
C(15)-C(14)-H(14)	120.0
C(13)-C(14)-H(14)	120.0
C(14)-C(15)-C(16)	120.0(3)
C(14)-C(15)-H(15)	120.0
C(16)-C(15)-H(15)	120.0
C(17)-C(16)-C(15)	119.8(3)
C(17)-C(16)-H(16)	120.1
C(15)-C(16)-H(16)	120.1
C(16)-C(17)-C(18)	120.7(3)
C(16)-C(17)-H(17)	119.6
C(18)-C(17)-H(17)	119.6
C(13)-C(18)-C(17)	119.9(3)
C(13)-C(18)-H(18)	120.1
C(17)-C(18)-H(18)	120.1

Table 4: Bond angles for $[PPN]_2[Mo_6O_{19}]$ in degrees continues

Bonds	Angle (degrees)
C(24)-C(19)-C(20)	119.0(3)
C(24)-C(19)-P(2)	118.8(2)
C(20)-C(19)-P(2)	122.1(2)
C(21)-C(20)-C(19)	120.0(3)
C(21)-C(20)-H(20)	120.0
C(19)-C(20)-H(20)	120.0
C(22)-C(21)-C(20)	120.4(3)
C(22)-C(21)-H(21)	119.8
C(20)-C(21)-H(21)	119.8
C(21)-C(22)-C(23)	120.4(3)
C(21)-C(22)-H(22)	119.8
C(23)-C(22)-H(22)	119.8
C(24)-C(23)-C(22)	119.8(3)
C(24)-C(23)-H(23)	120.1
C(22)-C(23)-H(23)	120.1
C(23)-C(24)-C(19)	120.2(3)
C(23)-C(24)-H(24)	119.9
C(19)-C(24)-H(24)	119.9

Table 4: Bond angles for $[PPN]_2[Mo_6O_{19}]$ in degrees continues

Bonds	Angle (degrees)
C(26)-C(25)-C(30)	119.6(3)
C(26)-C(25)-P(2)	118.1(2)
C(30)-C(25)-P(2)	122.3(2)
C(27)-C(26)-C(25)	119.7(3)
C(27)-C(26)-H(26)	120.1
C(25)-C(26)-H(26)	120.1
C(26)-C(27)-C(28)	120.3(3)
C(26)-C(27)-H(27)	119.8
C(28)-C(27)-H(27)	119.8
C(29)-C(28)-C(27)	120.5(3)
C(29)-C(28)-H(28)	119.7
C(27)-C(28)-H(28)	119.7
C(28)-C(29)-C(30)	119.7(3)
C(28)-C(29)-H(29)	120.2
C(30)-C(29)-H(29)	120.2
C(29)-C(30)-C(25)	120.1(3)
C(29)-C(30)-H(30)	120.0
C(25)-C(30)-H(30)	120.0

Table 4: Bond angles for $[PPN]_2[Mo_6O_{19}]$ in degrees continues

Bonds	Angle (degrees)
C(32)-C(31)-C(36)	119.7(3)
C(32)-C(31)-P(2)	118.9(2)
C(36)-C(31)-P(2)	121.4(2)
C(31)-C(32)-C(33)	120.4(3)
C(31)-C(32)-H(32)	119.8
C(33)-C(32)-H(32)	119.8
C(34)-C(33)-C(32)	119.2(3)
C(34)-C(33)-H(33)	120.4
C(32)-C(33)-H(33)	120.4
C(33)-C(34)-C(35)	120.8(3)
C(33)-C(34)-H(34)	119.6
C(35)-C(34)-H(34)	119.6
C(34)-C(35)-C(36)	120.8(3)
C(34)-C(35)-H(35)	119.6
C(36)-C(35)-H(35)	119.6
C(31)-C(36)-C(35)	119.0(3)
C(31)-C(36)-H(36)	120.5
C(35)-C(36)-H(36)	120.5

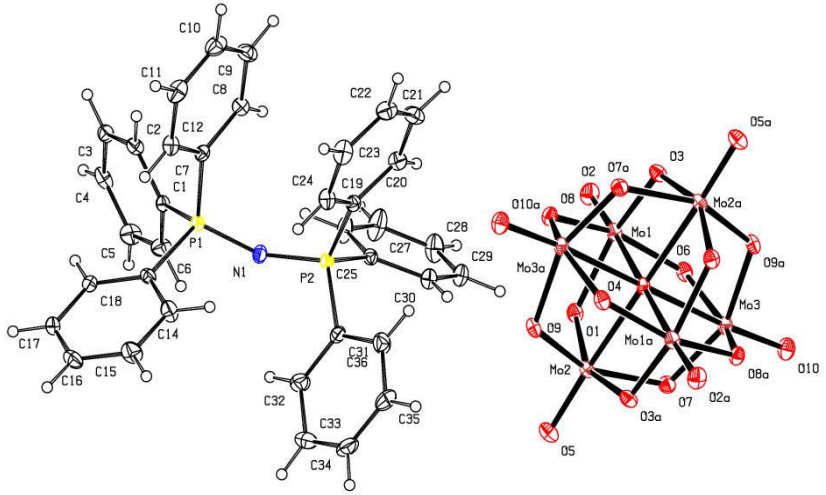
C10
C9
C11
C8
C22
C21
C2
C12
C23
C3
C7
C1
C24
C19
C20
C4
P1
C28
C5
C6
N1
P2
C25
C27
C29
C18
C30
C14
C17
C31
C36
C16
C15
C32
C35
C33
C34
O5a
O3
O2
O7a
O10a
O8
Mo2a
Mo1
O6
O9a
Mo3a
O4
Mo3
O9
O1
Mo1a
O10
Mo2
O8a
O7
O2a
O3a
O5

Appendix 3

Crystal data and structure refinement for $[Et_4N]_2[Mo_4O_{13}]$.

Identification code	$[Et_4N]_2[Mo_4O_{13}]$
Empirical formula	$C_{16}H_{40}Mo_4N_2O_{13}$
Formula weight	852.26
Temperature	293(2) K
Wavelength	0.71073 A
Crystal system, space group	$P2_1/n$
Unit cell dimensions	a = 11.884(5) A α = 90.000(5) deg.
	b = 20.066(5) A β = 105.182(5) deg.
	c = 12.096(5) A λ = 90.000(5) deg.
Volume	2783.8(18) A^3
Z, Calculated density	4, 2.033 Mg/m^3
Absorption coefficient	1.821 mm^{-1}
F(000)	1687
Crystal size	? x ? x ? mm
Theta range for data collection	2.68 to 32.12 deg.
Limiting indices	-17<=h<=16, -29<=k<=29, -16<=l<=17
Reflections collected / unique	27081 / 9002 [R(int) = 0.0392]
Completeness to theta = 32.12	92.2 %
Absorption correction	None
Refinement method	Full-matrix least-squares on F^2
Data / restraints / parameters	9002 / 0 / 304
Goodness-of-fit on F^2	1.098
Final R indices [I>2sigma(I)]	R1 = 0.0498, wR2 = 0.1253
R indices (all data)	R1 = 0.0697, wR2 = 0.1392
Largest diff. peak and hole	0.988 and -1.719 $e.A^{-3}$

Table 5: Bond lengths [Å] for $[Et_4N]_2[Mo_4O_{13}]$

Bonds	Length (Å)
O(11)-Mo(1)	1.703(4)
O(14)-Mo(1)	1.703(4)
O(1)-Mo(3)	1.915(4)
O(1)-Mo(1)	1.917(4)
O(12)-Mo(3)	1.707(4)
O(15)-Mo(3)	1.708(4)
O(8)-Mo(3)	1.912(4)
O(8)-Mo(4)1	1.923(4)
C(7)-C(8)	1.503(9)
C(7)-H(7A)	0.9600
C(7)-H(7B)	0.9600
C(7)-H(7C)	0.9600
C(8)-N(1)	1.527(8)
C(8)-H(8A)	0.9700
C(8)-H(8B)	0.9700

Table 5: Bond lengths [Å] for $[Et_4N]_2[Mo_4O_{13}]$

Bonds	Length (Å)
O(3)-Mo(2)	1.787(4)
O(3)-Mo(4)1	2.431(4)
O(3)-Mo(3)	2.445(4)
O(7)-Mo(2)	1.789(3)
O(7)-Mo(1)	2.416(3)
O(7)-Mo(4)	2.433(3)
O(13)-Mo(2)	1.722(3)
O(2)-Mo(2)1	1.791(4)
O(2)-Mo(3)	2.421(4)
O(2)-Mo(1)	2.461(4)
O(4)-Mo(1)	1.918(4)
O(4)-Mo(4)	1.919(4)
O(18)-Mo(4)	1.707(4)
O(16)-Mo(4)	1.701(4)
C(21)-N(1)	1.488(9)

Table 5: Bond lengths [Å] for $[Et_4N]_2[Mo_4O_{13}]$

Bonds	Length (Å)
C(21)-C(22)	1.493(14)
C(21)-H(21A)	0.9700
C(21)-H(21B)	0.9700
C(22)-H(22A)	0.9600
C(22)-H(22B)	0.9600
C(22)-H(22C)	0.9600
C(23)-C(24)	1.473(12)
C(23)-N(1)	1.541(10)
C(23)-H(23A)	0.9700
C(23)-H(23B)	0.9700
C(24)-H(24A)	0.9600
C(24)-H(24B)	0.9600
C(24)-H(24C)	0.9600
C(25)-N(1)	1.513(8)
C(25)-C(26)	1.515(9)
C(25)-H(25A)	0.9700

Table 5: Bond lengths [Å] for $[Et_4N]_2[Mo_4O_{13}]$

Bonds	Length (Å)
C(25)-H(25B)	0.9700
C(26)-H(26A)	0.9600
C(26)-H(26B)	0.9600
C(26)-H(26C)	0.9600
C(40)-N(2)	1.517(8)
C(40)-C(41)	1.525(10)
C(40)-H(40A)	0.9700
C(40)-H(40B)	0.9700
C(41)-H(41A)	0.9600
C(41)-H(41B)	0.9600
C(41)-H(41C)	0.9600
C(42)-C(43)	1.492(10)
C(42)-N(2)	1.518(7)
C(42)-H(42A)	0.9700
C(42)-H(42B)	0.9700
C(43)-H(43A)	0.9600

Table 5: Bond lengths [Å] for $[Et_4N]_2[Mo_4O_{13}]$ continues.

Bonds	Length (Å)
C(43)-H(43B)	0.9600
C(43)-H(43C)	0.9600
N(2)-C(250)	1.517(9)
N(2)-C(253)	1.518(9)
Mo(2)-O(2)1	1.791(4)
Mo(4)-O(8)1	1.923(4)
Mo(4)-O(3)1	2.431(4)
C(253)-C(254)	1.508(11)
C(253)-H(25C)	0.9700

Table 5: Bond lengths [Å] for $[Et_4N]_2[Mo_4O_{13}]$ continues.

Bonds	Length (Å)
C(253)-H(25D)	0.9700
C(250)-C(251)	1.523(13)
C(250)-H(25E)	0.9700
C(250)-H(25F)	0.9700
C(254)-H(25G)	0.9600
C(254)-H(25H)	0.9600
C(254)-H(25I)	0.9600
C(251)-H(25J)	0.9600
C(251)-H(25K)	0.9600
C(251)-H(25L)	0.9600

Table 6: Bond angles [deg] for $[Et_4N]_2[Mo_4O_{13}]$

Bonds	Angle (degrees)
Mo(3)-O(1)-Mo(1)	124.24(19)
Mo(3)-O(8)-Mo(4)1	124.0(2)
C(8)-C(7)-H(7A)	109.5
C(8)-C(7)-H(7B)	109.5
H(7A)-C(7)-H(7B)	109.5
C(8)-C(7)-H(7C)	109.5
H(7A)-C(7)-H(7C)	109.5
H(7B)-C(7)-H(7C)	109.5
C(7)-C(8)-N(1)	116.1(5)
C(7)-C(8)-H(8A)	108.3
N(1)-C(8)-H(8A)	108.3
C(7)-C(8)-H(8B)	108.3
N(1)-C(8)-H(8B)	108.3
H(8A)-C(8)-H(8B)	107.4
Mo(2)-O(3)-Mo(4)1	130.26(18)
Mo(2)-O(3)-Mo(3)	129.97(17)
Mo(4)1-O(3)-Mo(3)	87.92(12)
Mo(2)-O(7)-Mo(1)	130.94(18)
Mo(2)-O(7)-Mo(4)	131.59(18)

Table 6: Bond angles [deg] for $[Et_4N]_2[Mo_4O_{13}]$

Bonds	Angle (degrees)
Mo(1)-O(7)-Mo(4)	87.70(11)
Mo(2)1-O(2)-Mo(3)	129.92(18)
Mo(2)1-O(2)-Mo(1)	129.96(18)
Mo(3)-O(2)-Mo(1)	87.88(12)
Mo(1)-O(4)-Mo(4)	122.22(19)
N(1)-C(21)-C(22)	113.2(7)
N(1)-C(21)-H(21A)	108.9
C(22)-C(21)-H(21A)	108.9
N(1)-C(21)-H(21B)	108.9
C(22)-C(21)-H(21B)	108.9
H(21A)-C(21)-H(21B)	107.7
C(21)-C(22)-H(22A)	109.5
C(21)-C(22)-H(22B)	109.5
H(22A)-C(22)-H(22B)	109.5
C(21)-C(22)-H(22C)	109.5
H(22A)-C(22)-H(22C)	109.5
H(22B)-C(22)-H(22C)	109.5
C(24)-C(23)-N(1)	117.5(8)
C(25)-C(26)-H(26A)	109.5

Table 6: Bond angles [deg] for $[Et_4N]_2[Mo_4O_{13}]$ continues

Bonds	Angle (degrees)
C(26)-C(25)-H(25B)	108.2
H(25A)-C(25)-H(25B)	107.4
C(25)-C(26)-H(26B)	109.5
C(24)-C(23)-H(23A)	107.9
N(1)-C(23)-H(23A)	107.9
C(24)-C(23)-H(23B)	107.9
N(1)-C(23)-H(23B)	107.9
H(23A)-C(23)-H(23B)	107.2
C(23)-C(24)-H(24A)	109.5
C(23)-C(24)-H(24B)	109.5
H(24A)-C(24)-H(24B)	109.5
C(23)-C(24)-H(24C)	109.5
H(24A)-C(24)-H(24C)	109.5
H(24B)-C(24)-H(24C)	109.5
N(1)-C(25)-C(26)	116.2(5)
N(1)-C(25)-H(25A)	108.2
C(26)-C(25)-H(25A)	108.2
N(1)-C(25)-H(25B)	108.2

Table 6: Bond angles [deg] for $[Et_4N]_2[Mo_4O_{13}]$ continues

Bonds	Angle (degrees)
H(26A)-C(26)-H(26B)	109.5
C(25)-C(26)-H(26C)	109.5
H(26A)-C(26)-H(26C)	109.5
H(26B)-C(26)-H(26C)	109.5
N(2)-C(40)-C(41)	115.6(5)
N(2)-C(40)-H(40A)	108.4
C(41)-C(40)-H(40A)	108.4
N(2)-C(40)-H(40B)	108.4
C(41)-C(40)-H(40B)	108.4
H(40A)-C(40)-H(40B)	107.5
C(40)-C(41)-H(41A)	109.5
C(40)-C(41)-H(41B)	109.5
H(41A)-C(41)-H(41B)	109.5
C(40)-C(41)-H(41C)	109.5
H(41A)-C(41)-H(41C)	109.5
H(41B)-C(41)-H(41C)	109.5
C(43)-C(42)-N(2)	114.7(5)
C(43)-C(42)-H(42A)	108.6
N(2)-C(42)-H(42A)	108.6

Table 6: Bond angles [deg] for $[Et_4N]_2[Mo_4O_{13}]$ continues

Bonds	Angle (degrees)
C(43)-C(42)-H(42B)	108.6
N(2)-C(42)-H(42B)	108.6
H(42A)-C(42)-H(42B)	107.6
C(42)-C(43)-H(43A)	109.5
C(42)-C(43)-H(43B)	109.5
H(43A)-C(43)-H(43B)	109.5
C(42)-C(43)-H(43C)	109.5
H(43A)-C(43)-H(43C)	109.5
H(43B)-C(43)-H(43C)	109.5
C(21)-N(1)-C(25)	111.8(5)
C(21)-N(1)-C(8)	108.8(5)
C(25)-N(1)-C(8)	109.6(5)
C(21)-N(1)-C(23)	111.2(6)
C(25)-N(1)-C(23)	105.5(5)
C(8)-N(1)-C(23)	109.8(5)
C(40)-N(2)-C(250)	105.4(5)
C(40)-N(2)-C(253)	111.3(5)
C(250)-N(2)-C(253)	110.4(5)
C(40)-N(2)-C(42)	110.5(5)

Table 6: Bond angles [deg] for $[Et_4N]_2[Mo_4O_{13}]$ continues

Bonds	Angle (degrees)
C(250)-N(2)-C(42)	112.8(5)
C(253)-N(2)-C(42)	106.5(5)
O(14)-Mo(1)-O(11)	104.6(2)
O(14)-Mo(1)-O(1)	100.10(18)
O(11)-Mo(1)-O(1)	101.5(2)
O(14)-Mo(1)-O(4)	103.06(19)
O(11)-Mo(1)-O(4)	100.5(2)
O(1)-Mo(1)-O(4)	142.70(15)
O(14)-Mo(1)-O(7)	88.38(17)
O(11)-Mo(1)-O(7)	166.58(18)
O(1)-Mo(1)-O(7)	79.15(14)
O(4)-Mo(1)-O(7)	72.74(13)
O(14)-Mo(1)-O(2)	163.06(17)
O(11)-Mo(1)-O(2)	91.58(18)
O(1)-Mo(1)-O(2)	71.20(13)
O(4)-Mo(1)-O(2)	78.42(14)
O(7)-Mo(1)-O(2)	75.84(12)
O(13)-Mo(2)-O(3)	109.56(18)
O(13)-Mo(2)-O(7)	109.01(17)

Table 6: Bond angles [deg] for $[Et_4N]_2[Mo_4O_{13}]$ continues

Bonds	Angle (degrees)
O(3)-Mo(2)-O(7)	109.67(16)
O(13)-Mo(2)-O(2)1	109.58(17)
O(3)-Mo(2)-O(2)1	109.78(16)
O(7)-Mo(2)-O(2)1	109.23(16)
O(12)-Mo(3)-O(15)	104.2(2)
O(12)-Mo(3)-O(8)	101.3(2)
O(15)-Mo(3)-O(8)	102.04(19)
O(12)-Mo(3)-O(1)	102.00(19)
O(15)-Mo(3)-O(1)	99.64(19)
O(8)-Mo(3)-O(1)	142.96(15)
O(12)-Mo(3)-O(2)	88.78(18)
O(15)-Mo(3)-O(2)	166.05(18)
O(8)-Mo(3)-O(2)	79.99(14)
O(1)-Mo(3)-O(2)	72.18(14)
O(12)-Mo(3)-O(3)	165.06(18)
O(15)-Mo(3)-O(3)	90.38(17)
O(8)-Mo(3)-O(3)	71.87(14)
O(1)-Mo(3)-O(3)	78.35(14)
O(2)-Mo(3)-O(3)	77.05(12)

Table 6: Bond angles [deg] for $[Et_4N]_2[Mo_4O_{13}]$ continues

Bonds	Angle (degrees)
O(16)-Mo(4)-O(18)	104.1(2)
O(16)-Mo(4)-O(4)	101.08(19)
O(18)-Mo(4)-O(4)	100.66(19)
O(16)-Mo(4)-O(8)1	100.74(19)
O(18)-Mo(4)-O(8)1	102.2(2)
O(4)-Mo(4)-O(8)1	143.31(15)
O(16)-Mo(4)-O(3)1	165.31(17)
O(18)-Mo(4)-O(3)1	90.09(18)
O(4)-Mo(4)-O(3)1	79.60(14)
O(8)1-Mo(4)-O(3)1	72.05(14)
O(16)-Mo(4)-O(7)	90.42(17)
O(18)-Mo(4)-O(7)	164.99(18)
O(4)-Mo(4)-O(7)	72.31(13)
O(8)1-Mo(4)-O(7)	78.40(14)
O(3)1-Mo(4)-O(7)	75.73(12)
C(254)-C(253)-N(2)	115.6(6)
C(254)-C(253)-H(25C)	108.4
N(2)-C(253)-H(25C)	108.4
C(254)-C(253)-H(25D)	108.4

Table 6: Bond angles [deg] for $[Et_4N]_2[Mo_4O_{13}]$ continues

Bonds	Angle (degrees)
N(2)-C(253)-H(25D)	108.4
H(25C)-C(253)-H(25D)	107.4
N(2)-C(250)-C(251)	114.4(7)
N(2)-C(250)-H(25E)	108.7
C(251)-C(250)-H(25E)	108.7
N(2)-C(250)-H(25F)	108.7
C(251)-C(250)-H(25F)	108.7
H(25E)-C(250)-H(25F)	107.6
C(253)-C(254)-H(25G)	109.5
C(253)-C(254)-H(25H)	109.5

Table 6: Bond angles [deg] for $[Et_4N]_2[Mo_4O_{13}]$ continues

Bonds	Angle (degrees)
H(25G)-C(254)-H(25H)	109.5
C(253)-C(254)-H(25I)	109.5
H(25G)-C(254)-H(25I)	109.5
H(25H)-C(254)-H(25I)	109.5
C(250)-C(251)-H(25J)	109.5
C(250)-C(251)-H(25K)	109.5
H(25J)-C(251)-H(25K)	109.5
C(250)-C(251)-H(25L)	109.5
H(25J)-C(251)-H(25L)	109.5
H(25K)-C(251)-H(25L)	109.5

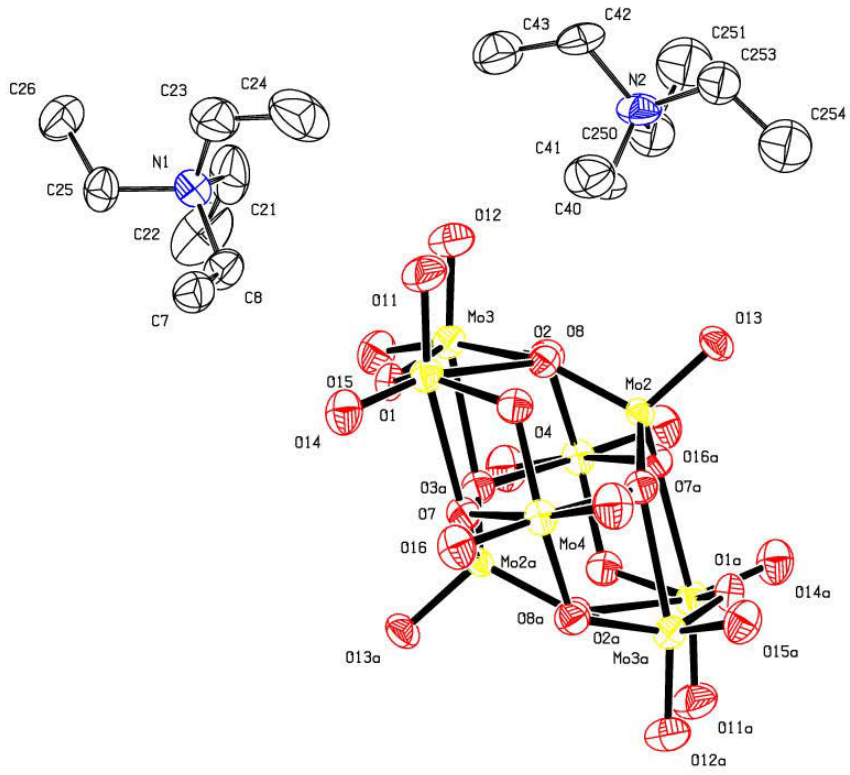
C43
C42
C251
C253
N2
C254
C41
C250
C40
C26
C23
C24
N1
C25
C21
C22
C8
C7
O12
O11
Mo3
O2
O8
O13
O15
Mo2
O1
O14
O4
O16a
O3a
O7a
O7
Mo4
O16
Mo2a
O1a
O14a
O8a
O2a
O15a
O13a
Mo3a
O11a
O12a